

***Republic of Iraq  
Ministry of Higher Education  
And Scientific Research  
University of Babylon  
Mechanical Engineering Department***



# ***Improving of Fatigue Behaviour and Mechanical Properties of Low-Carbon Steel 17100***

***A Thesis***

***Submitted to the Collage of Engineering / University of  
Babylon in Partial Fulfillment of the Requirement for the  
Degree of Master in Engineering/Mechanical  
Engineering / Applied mechanics***

***Presented By***

***Sajjad Hassan Nasser Eidan***

***B.SC. (2018)***

***Supervised By***

***Prof. Dr. Qasim H. Bader***

***2023 A.D***

***1443 A.H***

بِسْمِ اللَّهِ الرَّحْمَنِ الرَّحِيمِ

﴿ قَالُوا سُبْحَنَكَ لَا عِلْمَ لَنَا إِلَّا مَا عَلَّمْتَنَا

إِنَّكَ أَنْتَ الْعَلِيمُ الْحَكِيمُ ﴾

صَدَقَ اللَّهُ الْعَلِيِّ الْعَظِيمِ

سورة البقرة، الآية (٣٢)

## **Supervisor Certification**

I certify that this thesis (*Improving of Fatigue Behaviour and Mechanical Properties of Low-Carbon Steel17100*) and submitted by student ( **Sajjad Hassan Nasser**) prepared under my supervision at the department of Mechanical Engineering/ college of Engineering /University of Babylon as part of the requirements for a master degree Mechanical Engineering Sciences/Applied Mechanics. We recommend that this thesis be forwarded for examination in accordance with the regulation of the University of Babylon.

**Signature:**

**Prof. Dr. Qasim Hassen Bader**

**Date:**     /     / 2023

I certify that this thesis mention above has been completed in mechanical Engineering in college of Engineering / University of Babylon

**Signature:**

**Head of department: Prof. Dr. Sammer Mohamad.**

**Date:**     /     /2023

## **Examination Committee Certification**

We certify that we have read the thesis entitled " *Improve Fatigue Behavior and Mechanical Properties of Low Carbon Steel DIN 17100* " and as examining committee, examined the student " **Sajjad Hassan Nasser** " in its content and what is related to it, and that in our opinion it meets the standard of a thesis for the degree of Master in applied mechanics / Mechanical Engineering Science.

**Signature:**

**Name:** prof. Dr. Abdulmohsin naji almuhasen

**Chairman**

**Date:**     /     / 2023

**Signature:**

**Name:** prof. Dr. Hatem Hadi Obeid

**Member**

**Date:**     /     / 2023

**Signature:**

**Name:** Prof. Dr. Basim A. Abass

**Member**

**Date:**     /     / 2023

**Signature:**

**Name:** prof. Dr. Qasim H. Bader

**Supervisor**

**Date:**     /     / 2023

**Signature:**

**Name:** Prof. Dr. Sammer Mohamad.

**Approval of Head Department**

**Date:**     /     / 2023

**Signature:**

**Name:** Prof. Dr. Hatem Hadi Obeid

**Approval of the Dean of the College**

**Date:**     /     / 2023

## **Acknowledgement**

"In The Name of ALLAH, The Gracious, The Merciful"

First, I would like to confirm that this work not to be finished without the help of Allah, greater of all creations and the Merciful Prophet Mohammad and his Ahl-Albait (Peace up on them).

I would like to express my sincere thanks and profound gratitude to my supervisor Prof. Dr. Qasim Hassen Bader for his kindness, patience, guidance and encouragement throughout this work.

Also I would like to express my thankful and grateful to the staff of Heat treatments labs in Engineering of Materials College of Babylon University for support this work.

Also, my sincere thanks goes to Dean of College of Engineering Prof. Dr. Hatem H. Obeid and Head of Mechanical Engineering Department Prof. Dr. Sammer Mohamad.

My sincere thanks and great appreciation are also expressed to Mr. Karar Saad , Mrs. Zainab H. Kadthim for their great help in this work.

My sincere thanks and great appreciation are also expressed to Mr. Hussain for their great help in this work.

I wish to extend my gratitude to my family; my father and brothers for all the patience and support given during the time I spent doing all this work. Special thanks to my friends who stood with me and supported me throughout the work.

***Sajjad Hassan Nasser***

## **Dedication**

To my father .....

The Everlasting Support and lasting giving

To the soul of my mother and brother

To my Brothers.....

To my friends .....

A beautiful greeting to all of you

***Sajjad Hassan Nasser***

## ABSTRACT

This work focuses on the experimental investigation of the influence type of surface hardening, soaking time and depth of hardening on high cycle fatigue behavior for low carbon steel beam 17100, this study was done on both plane and v-notched beam with a depth of 1 mm and an angle of 45°.

The experimental works includes, mechanical tests, surface hardening, fatigue test, inspection of sodium cyanide balls by using a device X-Ray diffraction, also examine the microstructure using optical microscope device was done.

Two types of surface hardening, namely pack carburizing and carbonitriding have been performed.

In the first method, carbonate medium is prepared from wood charcoal and converted into a powder by grinding, and mixed it with 10% of barium carbonate to be used during the pack carburizing process. The beam samples are hardening with three different soaking times, 2, 4 and 6 hours at temperature 925°C followed by cooling in water and tempering operations at temperature 180°C for 2 hours.

In the second method, molten salt bath is prepared by dissolving sodium cyanide balls by heating inside furnace. The time of immersion of the samples through the carbonitriding is 0.5, 1 and 1.5 hours at constant temperature 800°C then quenching directly in water followed by tempering.

Rotating-bending fatigue test was performed using. The results of an experimental fatigue test indicate that various behaviors depend on hardening method and time of hardening.

The results indicate that carbonitriding method has a greater effect on fatigue strength and lifetime than pack carburizing. In addition, the increase in soaking time leads to an increase in the fatigue life of both types increased by 20.2% and 15.9% for carbonitriding and pack carburizing.

The obtained result show that the hardening using the carbonitriding method achieved a higher surface hardness 1644.28HV. where the hardness increased by 461% relative to unhardened samples. While hardening using the pack carburizing process where increased by 270%.

The test of Cross-sectional area of the broken sample which is hardened by pack carburizing and carbonitriding was to have two zones, surface layer and core. It can be noticed that the surface layer rich by carbon, or carbon and nitrogen together, while the core region has no change. It was also noticed that soaking time causes an increasing the depth of the hardening depth towards the core.

The improvement percentage of fatigue strength at the standard fatigue life of ( $10^6$ ) cycles in comparison with the un-treated specimens are obtained for both types of hardening process. The maximum improvement percentage of fatigue strength of (44.56%) and (61.87%) for pack carburizing and carbonitriding respectively, for V-notched beam.

While the improvement percentage of fatigue strength for un-notched samples (plane) are 31.92% and 38.46% respectively at soaking time 2 and 0.5 hours.

## Contents

Section No.	Subject	Page No.
	Abstract	I
	List of content	III
	List of figure	V
	List of table	VII
	Nomenclatures	VIII
	Greek symbols	IX
	Abbreviation	IX
<b>Chapter one : introduction</b>		<b>1-13</b>
1.1	General Overview	1
1.2	The S-N Curve	2
1.3	Mechanism of Fatigue Failure	3
1.3.1	Fatigue Crack Initiation	3
1.3.2	Fatigue Crack Propagation	4
1.3.3	Fatigue Crack Fracture	4
1.4	Surface Hardening Effect	5
1.4.1	Diffusion methods	6
1.5	Carburizing	7
1.5.1	Solid Carburizing	8
1.6	Cyaniding	9
1.7	Application	11
1.8	Carbon steel	11
1.8.1	Low-carbon steels (LCS)	12
1.9	Objectives of the Present Work	13
<b>Chapter Two: Literature Review</b>		<b>14-24</b>
2.1	Overview	14
2.2	Fatigue Literature Review	14
2.3	Pack Carburizing Effect	20
2.4	Carbonitriding Effect	22
2.5	Concluding remarks	24
<b>Chapter three : Experimental Work</b>		<b>25-47</b>
3.1	Introduction	25
3.2	Material Selection and Chemical Composition	28
3.3	Mechanical Tests	29
3.3.1	Tensile Test	29
3.3.2	Hardness Test	31
3.3.3	Impact Test	32
3.4	Preparation of Fatigue Specimens	33
3.5	Surface Heat Treatments	34

3.6	Pack (solid) Carburizing	35
3.7	Quenching (hardening)	37
3.8	Tempering	38
3.9	X-ray powder diffraction (XRD)	39
3.10	Carbonitriding (cyaniding)	40
3.11	Calculate case hardness (depth of hardness).	41
3.12	Microscopic examination:	42
3.13	Fatigue Testing Machine	43
3.13.1	Reversed Bending Machine	44
<b>Chapter Four :Results and Discussion</b>		<b>48-73</b>
4.1	Introduction	48
4.2	Mechanical Test Results	48
4.2.1	Tensile Test Results	48
4.2.2	Hardness Test	49
4.2.3	Case Depth (Depth of Hardness)	50
4.2.4	Impact Test	52
4.3	Experimental Results Of Fatigue Test Under Constant Amplitude Stress for V-Notch Low Carbon Steel After Surface Hardness	53
4.3.1	Fatigue Strength and S-N Equation	56
4.4	Effect of Case Hardened Treatments on the Fatigue Properties for V-Notch Low Carbon Steel.	59
4.4.1	Fatigue Strength Improvement Factor (FSIF)	62
4.4.2	Fatigue Life Improvement Factor (FLIF)	63
4.5	Experimental Results for Un-Notched St44-DIN17100 Before and After Surface Heat Treatment	65
4.5.1	Fatigue Strength Improvement Factor (FSIF) for plain steel	66
4.5.2	Fatigue Life Improvement Factor (FLIF) for plain steel	67
4.6	Validation	68
4.7	Result of Microstructural	69
4.8	Inspection of the sodium cyanide	74
<b>Chapter five: Conclusions And Recommendations</b>		<b>75-76</b>
5.1	Conclusions	75
5.2	Recommendations for the Future Works	76
<b>References</b>		<b>77-82</b>
<b>Appendices</b>		<b>A1-E1</b>
A	Chemical Composition Analysis	A1
B	Type Of Material	B1

C	Life Evolution Due To Constant Amplitude Loading	C1
D	The Coefficient Of Determination	D1
E	Iron –Carbon Phase Diagram	E1
F	Published Paper	F1

## Figures

Figure No.	Subject	Page No.
1.1	S-N diagram for steel	2
1.2	Schematic of the fracture surface of a steel shaft that failed in fatigue	5
1.3	Methods for surface hardening of steels	6
1.4	Carbon diffusion process in carburizing and quenching	7
1.5	Mechanical parts	11
1.6	Classification of steels on basis of chemical composition and range of Carbon percentage for each type of steels	12
3.1	Scheme of experimental work	26
3.2	Average Specimens distribution of mechanical tests and fatigue test	27
3.3	Spectrometer test device.	28
3.4	Tensile test machine	30
3.5	Samples of specimens used for tensile test	30
3.6	Schematic of tensile test specimen according to the specification of (ASTM-A 370).	31
3.7	Hardness test: (a) device Vickers. (b) Dimensions of specimen.	31
3.8	Impact test device and specimen dimension.	32
3.9	Schematic diagram for fatigue test specimens	33
3.10	Dimensions of V shape notch specimens	34
3.11	Notched Specimens	34
3.12	Pack Carburizing Process :( a) barium carbonate. (b) Powder carbon. (c) Carburizing Box. ( d) Electric Furnace	36
3.13	Specimens after pack carburizing	37
3.14	Specimen After quenching	38
3.15	Heat treatment (pack carburizing).	39
3.16	X-ray Diffractometer Lab XRD-6000	39

3.17	Cyaniding Process	40
3.18	Heat treatments(cyaniding) for low carbon steel	41
3.19	Schematic for hardness sample.	42
3.20	Optical microscope device	43
3.21	(a) Machine of rotating bending fatigue test. (b)Components of test machine	46
3.22	Comparison between the present work device and the device (GUNT HAMBURG WP 140)	47
3.23	(a) fatigue test device.(b) Components of test machine	47
4.1	Relationship between surface hardness and soaking time.	50
4.2a	The relationship between hardness of specimens carburized and the distance from surface to core	51
4.2b	The relationship between hardness of specimen's carbonitrid and the distance from surface to core	51
4.3	Relationship between depth of hardness and soaking time	52
4.4	Comparison of S.N curve between pack carburizing with un-treated samples at different time.	54
4.5	Comparison of S.N curve between carbonitriding with un-treated samples at different time	55
4.6	Variation in fatigue strength with time	58
4.7	Variation in fatigue strength with Depth of hardness	59
4.8	Comparison S-N curve of specimen on carbonitriding at temperature 800°C and soaking time 0.5 hour with pack carburizing at different time	60
4.9	Comparison S-N curve of specimen on carbonitriding at temperature 800°C and soaking time 1 hour with pack carburizing at different time.	61
4.10	Comparison S-N curve of specimen on carbonitriding at temperature 800°C and soaking time 1.5 hour with pack carburizing at different time	61
4.11	Comparison S-N curve between carbonitrid (1.5h) with pack carburizing (6h).	61
4.12	Fatigue Strength Improvement Factor for different time for carburizing and carbonitrid	63

4.13	Fatigue life Improvement Factor for different time for carburizing and carbonitrid	64
4.14	Comparison surface hardening by carburizing and carbonitriding with untreated for plain specimens	66
4.15	A comparison S.N curve between present results with researcher's results for plain low carbon steel without treated	68
4.16	Microstructure of the raw material	70
4.17	Microstructure of low carbon steel after carburizing :(a) specimen at time 2 hour.(b) specimen at time 4 hour.(c) specimen at time 6hour. Magnification 100x)	71
4.18	Microstructure of low carbon steel after carbonitriding: (a) specimen at time 0.5 hour. (b) Specimen at time 1 hour. (c) Specimen at time 1.5 hour. Magnification 100x).	72
4.19	Fracture surface of a specimen: (a) with carbonitriding. (b) With pack carburizing followed by quenching. (c) With pack carburizing without quenching. (d) Specimen without treatment.	73
4.20	XRD pattern of sodium cyanide ball.	74

## Tables

Table No.	Subject	Page No.
3.1	Chemical composition for Low carbon steel material (wt %)	29
4.1	Tensile test results for low carbon steel specimens	48
4.2	Tensile test results after surface treatments.	49
4.3	Hardness test results of low carbon steel.	50
4.4	Impact test result.	53
4.5	Results of fatigue stresses with life of specimens experimentally for carburizing at time 4h and 6h.	55
4.6	Results of fatigue stresses with life of specimens experimentally for carbonitriding at time 1h and 1.5h.	55
4.7	Results of fatigue stresses with life of specimens experimentally for carbonitriding and Pack Carburizing at time 0.5h and 2h respectively.	56

4.8	Results S-N curve equation, and fatigue strength $\sigma_e$ at $10^6$ cycles function to (Pack carburizing) at temp $925^\circ\text{C}$ .	57
4.9	Results S-N curve equation and fatigue strength $\sigma_e$ at $10^6$ cycles function to (carbonitriding).	58
4.10	Percentage of Fatigue Strength Improvement Factor (FSIF %) for pack carburizing and carbonitriding at different time.	62
4.11	Percentage of Fatigue life Improvement Factor (FLIF %) for pack carburizing and carbonitriding at different time.	64
4.12	Experimental S-N curve equation and fatigue strength $\sigma_e$ at $10^6$ cycles function for carburizing and carbonitriding.	66
4.13	Percentage of Fatigue Strength Improvement Factor (FSIF %) For Carburizing and Carbonitriding at Time 2, 0.5 hr.	67
4.14	Percentage of Fatigue Life Improvement Factor (FLIF %) for For Carburizing and Carbonitriding at Time 2, 0.5 hr.	67
4.15	Basquin's equations compared with available fatigue data at room temperature for the current study.	69

## Nomenclatures

Symbol	Meaning	Unit
A	Cross section area	$\text{mm}^2$
a,b	Curve fitting parameters	----
C%	Carbon percentage	----
D	Cross sectional diameter of the specimen	mm
E	Elastic modulus of material	GPa
E <sub>i</sub>	initial pendulum energy	Joule
E <sub>r</sub>	remaining pendulum energy	Joule
F	Applied load	Newton
G	Gauge length	mm
$G_c$	Impact strength of material	$\text{Joule/m}^2$
h	depth of notch	mm
j	Section modulus of the sample	$\text{mm}^3$
L	Bending arm	mm
M	Bending moment	N.mm

N	Number of cycles	Cycle
R	Radius of fillet	mm
R <sup>2</sup>	Correlation coefficient	----
S	Stress	MPa
U <sub>s</sub>	Impact energy absorbed for the specimen rapture	Joule

## Greek Symbols

Symbol	Meaning	Unit
$\sigma$	Alternating stress	MPa
$\sigma_e$	Fatigue strength	MPa
$\sigma_Y$	Yield stress	MPa
$\sigma_{ult}$	Ultimate stress	MPa

## Abbreviations

Symbol	Description
ASTM	American Society for Testing and Material
AISI	American Iron and Steel Institute
Al <sub>2</sub> O <sub>3</sub>	Aluminum oxide
NaCl	Sodium chloride
ANN	Artificial Neural Network
C	Carbon Element
Ca	Calcium Element
C.N	Cyanide or Carbonitrid
B <sub>4</sub> C	Boron Carbide
CO	Carbon Monoxide
CO <sub>2</sub>	Carbon Dioxide
CH <sub>4</sub>	Methane
FEM	Finite Element Method
FeB	Iron Boride
Fe <sub>3</sub> C	Iron carbide
Fe <sub>4</sub> N	Iron Nitride
HVOF	High Velocity Oxy-Fuel
HCF	High Cycle Fatigue
HV	Hardness Vickers
H <sub>2</sub>	Hydrogen
LCS	Low Carbon Steel
LCF	Low Cycle Fatigue

MCS	Medium Carbon Steel
HCS	High Carbon Steel
BaCO <sub>3</sub>	Barium Carbonate
CaCO <sub>3</sub>	Calcium Carbonate
NaCO <sub>3</sub>	Sodium Carbonate
NaCN	Sodium Cyanide
K <sub>2</sub> CO <sub>3</sub>	Potassium carbonate
KCL	Chloride Potassium
NaBF <sub>4</sub>	Sodium Tetrafluoroborate
MTS	Make Torque-Testing Machine
OM	Optical Microscopy
P.C	Pack Carburizing
PCL	Pomacea Canalikulata Lamarck
PMSP	Pinctada Maxima Shell Powder
RCF	Rolling Contact Fatigue
S-N	Stress Number of Cycle
SiC	Silicon Carbide
SEM	Scanning Electron Microscopy
TPB	Three Point Bending
TWC	Teak Wood Charcoal
UNSM	Ultrasonic Nanocrystal Surface Modification
WC-CoCr	Tungsten Carbide-Cobalt-Chrome
XRD	X-Ray Diffraction
ZnO	Zinc Oxide
SS <sub>reg</sub>	Regression sum of squares
SS <sub>res</sub>	Residual sum of squares
SS <sub>tot</sub>	Total sum of squares

# ***Chapter One***

## ***Introduction***

## 1.1. General Overview

As technology has advanced, particularly in the field of industry. There are more structural sections and components that are subject to fatigue failure as a result of the applied of high dynamic stresses [1]. Fatigue is a problem that can affect any part or component that moves, it is a process of degradation of a material's mechanical properties defined by the slow growth of one or more cracks under dynamic stress, ultimately leading to fracture. Fatigue failures can occur in land-based turbines, nuclear reactors, aircraft wings and fuselages, ships at sea, and automobiles on highways. Fatigue failure is one of the most serious types of failure for steel structures and can result in considerable casualties and economic loss [2-4]. That is why it was highly demanded to increase the life of structures and machinery. To achieve this matter, many different surface engineering techniques are becoming increasingly necessary as they provide additional properties such as thermal barrier, high strength, wear resistance and corrosion. The low carbon /mild steel is relatively soft, weak, low tensile strength, and easy to form. Therefore, it is important to use surface treatment to enhance those properties[5] .There are several ways to modify the fatigue behavior of low carbon steel like, laser, shot peening, induction hardening, coating and flame hardening...etc. In addition to these ways, a carbonitriding and carburizing technology long used in the industry, these technologies increase the surface hardness and fatigue resistance of steel products, while maintaining the hardness of the core. LCS are exposed to a carbon-rich atmosphere at temperatures between 850 and 950°C for a suitable period of time ‘during modern carburizing processes, which improves the surface's carbon content while maintaining the sample's original chemical composition. Finally, the carburized metal is quenched in a cooling medium to ensure that the phase transformation to martensite

occurs. A successful carburizing process and providing of necessary mechanical properties for the part depend on careful management of the surface carbon content [6].

## 1.2 The S-N Curve:

The method S-N is the study of fatigue stress to number of cycles to failure approach. It is essential to describe the relationship so that fatigue life may be expected. This curve is one of the earliest techniques for describing this relationship. 'S' indicates for the range of cyclic stress, while N stands for the number of cycles until failure. A number of samples are tested till failure at various stress ranges to improve the curve. The resulting lives are plotted versus the corresponding stress range [7]. S-N curve or as called with "Wohler curve" was investigated by scientist "August Wohler".

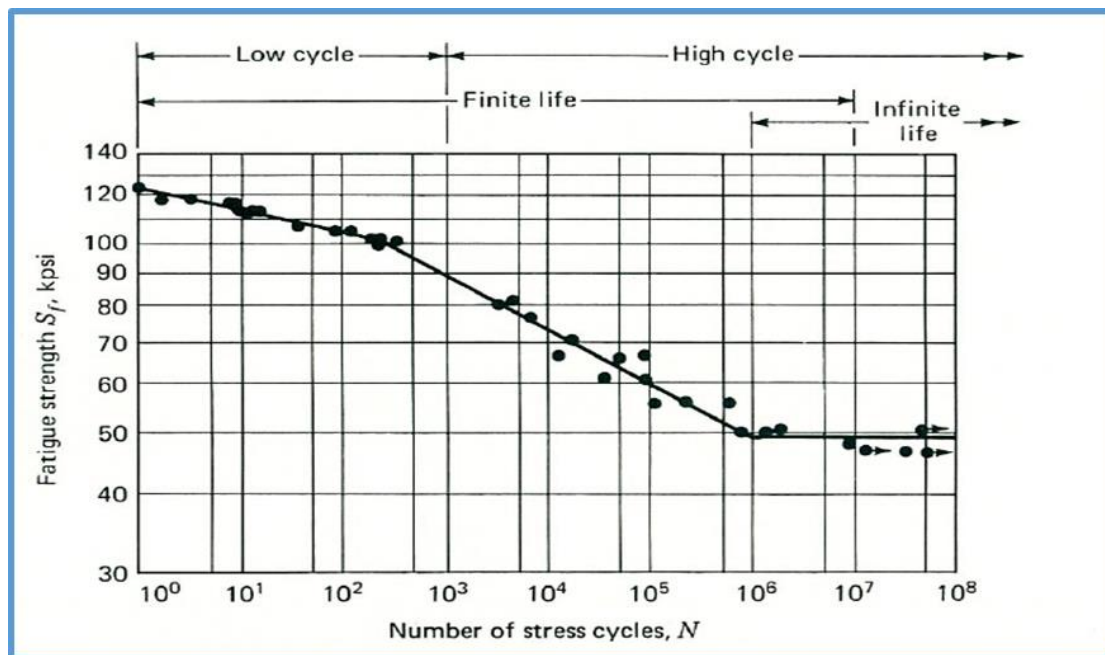


Figure (1.1): S-N diagram for steel.

The scientist proved that when a structural component is subjected to a single loads, applications under the static strength of the structures didn't

make any damages to the part, and if the same load was repeated for many times can cause a fully failures. Fatigue failure generally classified to low cycle fatigue with less than ( $N < 10^3$ ) cycles, and high-cycle fatigue with greater than ( $N > 10^3$ ) cycles, as illustrated in figure (1.1) [8].

### **1.3 Mechanism of Fatigue Failure**

Fatigue cracking is one of the critical failure mechanisms of structural components. Under cyclic loading conditions, a material often fails at a stress level below its nominal strength. The fatigue life of a component is presented as the number of loading cycles required to initiate a fatigue crack and to propagate the crack to a critical size. Therefore, fatigue failure occurs in three stages, crack initiation, crack propagation and fracture, as shown in figure (1.2) [9]. Fatigue cracks initiate from surface defects or regions of high-stress concentration, surface roughening generated due to vibrations or high repetitive stress amplitudes, and internal defects or material in homogeneities.

#### **1.3.1 Fatigue Crack Initiation**

Tiny crack initiates or nucleates often at a time well after loading begins. Normally, crack initiates sites are located at or near the surface, where the stress is at a maximum, and include surface defects such as scratches or pits, sharp corners due to poor design or manufacture, inclusions, grain boundaries, or dislocation concentrations. Surface roughness is important to avoid or delay this initiation. The process of fatigue crack initiation depends greatly on the plastic strain amplitude, the temperature, the deformation characteristics of the material (dislocation mobility, dislocation substructure etc.) and the material microstructure

(degree of inhomogeneity) [10-11]. Crack initiation stage fatigue is a material surface phenomenon [12].

### **1.3.2 Fatigue Crack Propagation**

The initiation stage finished with the formation of micro cracks which are usually located along the activated slip planes. Propagation or growth of those cracks occur through two distinct stage leading to a complete failure. The 1<sup>st</sup> stage of the crack propagation is the extension of micro cracks along their habit planes and it is usually grow through a few grain diameters before it deviate to 2<sup>nd</sup> stage. The 1<sup>st</sup> stage of crack propagation region is crystallographic in nature while the 2<sup>nd</sup> stage is typically non-crystallographic stage and the crack propagated in the directions perpendicular to the applied load direction. As increasing in the levels of the stresses are lead to propagations process of the crack across the grain or along the boundaries of the grain, slowly increases the cracks-size. As the crack size increase, the cross section areas that have resistance to applied load decreases and growing to the critical size at this it is insufficient to have resisted the applied stress [13].

### **1.3.3 Fatigue Crack Fracture**

After crack initiated and propagated. The area becomes too insufficient to carry the load anymore a sudden fracture results in the component. The third stage sudden fracture is instantaneous in time.

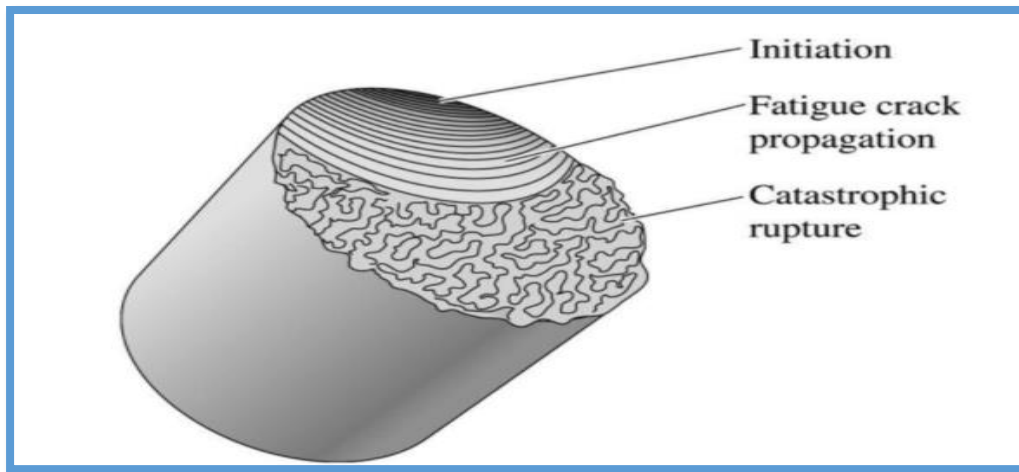


Figure (1.2): Schematic of the fracture surface of a steel shaft that failed in fatigue.

## 1.4 Surface Hardening Effect

It is preferred that steel used in engineering applications have a hardened surface to prevent wear, corrosion, impact resistance and improve fatigue behavior[14]. Carbon steel can be treated with heat or mechanically to increase its surface hardness while tough its interior [15]. Surface hardening is a process that includes a wide variety of techniques as shown in figure (1.3). Combination of hard surface and resistance to breakage on impact is useful in parts such as a camshaft or ring gear that must have a very hard surface to resist wear, along with a tough interior to resist the impact that occurs during operation. Most surface treatments result in compressive residual stresses at the surface that reduce the probability of crack initiation and help arrest crack propagation at the case-core interface. In addition, surface hardening of steel has advantage over through hardening, because less expensive low carbon steels can be surface hardened without the problems of distortion and cracking associated with through hardening of thick sections [16].

There are three distinctly approaches to different surface hardening methods: diffusion methods, selective-hardening methods and coating and surface modification.

### 1.4.1 Diffusion Methods

Thermochemical diffusion methods are those, which modify the chemical composition of the surface with hardening species such as carbon and nitrogen. Diffusion methods allow effective hardening of the entire surface of a part and are generally used when a large number of parts are to be surface hardened there are several types of hardening by diffusion, such (Carburizing and carbonitriding...etc) as shown in figure(1.3) [16-17].

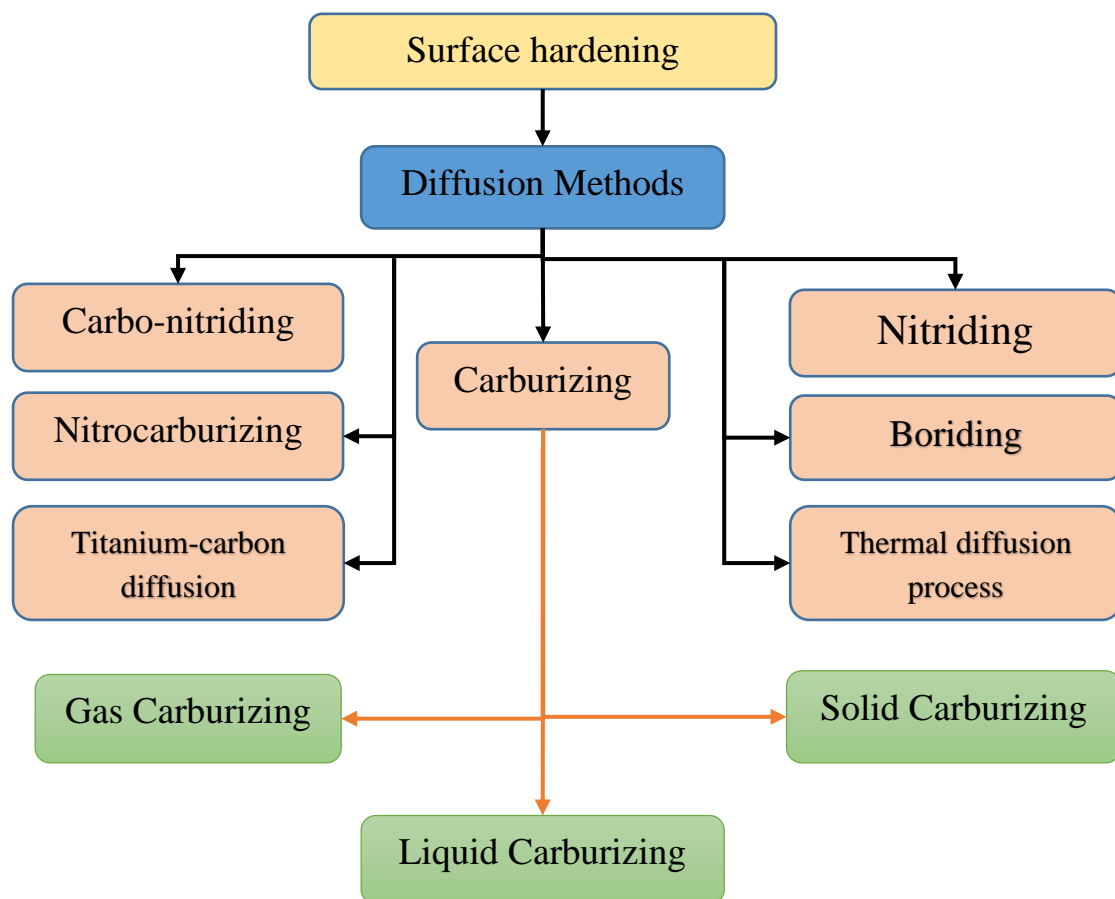


Figure (1.3): Methods for surface hardening of steels.

## 1.5 Carburizing

Carburizing is one of the most popular surface hardening processes for steel, due to the excellent combinations of mechanical properties it may provide [18]. To create a surface made of high carbon, the procedure entails diffusing carbon into an alloy of low carbon steel. Low carbon steels subjected to the process of carburization, which involves adding carbon to their surface, with temperature ranging from 850 to 950°C, at which austenite, with a high solubility of carbon, is the stable crystal structure [19]. Due to its excellent carburizing response and good hardenability for most section sizes, carburizing steel is frequently used as a material for machines, differential ring gears, springs, automobiles, camshafts, and transmission gears. Martensite is created when the next high-carbon surface layer is quenched, hardening is achieved, resulting in the superposition of a hard, With good wear and fatigue resistance, the low carbon steel core is encased in a high carbon martensitic casing, as shown in figure (1.4) [20]. Carbonation includes three types, (Solid Carburizing, Liquid Carburizing and Gas Carburizing). Solid Carburizing was adopted in this work.

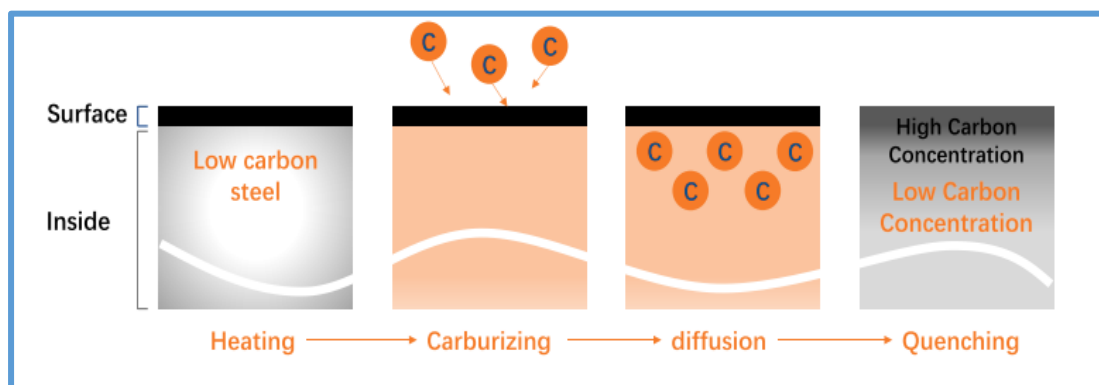


Figure (1.4): Carbon diffusion process in carburizing and quenching.

### 1.5.1 Solid Carburizing

Also called Pack carburizing is the process of increasing the carbon percentage (C) to the surface of the material, for increasing the hardness number of the surface. The carbon element is obtained from materials containing carbon charcoal. To speed up the process barium carbonate ( $\text{BaCO}_3$ ) calcium carbonate ( $\text{CaCO}_3$ ) or sodium carbonate ( $\text{NaCO}_3$ ) was added energizers. The charcoal, energizer and specimen are inserted into the carburizing box then heated in the electric furnace. On pack carburizing use of charcoal mixed with 10% - 40%  $\text{NaCO}_3$ ,  $\text{BaCO}_3$ , steel is incorporated into this mixture, placed in a carburizing box and then heated at  $850^\circ\text{C}$  -  $950^\circ\text{C}$ . After holding time, the process is continued by hardening with quenching to achieve high hardness, and tempering to reduce excessive brittle and residual stress [21]. Pack carburizing, produces a relatively thick layer on the part surface, ranging from around (0.6 to 4 mm) [18]. There are two types of gas, namely  $\text{CO}_2$  and  $\text{CO}$  that are produced during heating.



The oxygen of the entrapped air (in the carburizing box) initially reacts with the carbon of the carburizing medium as follows:



With higher temperatures the reaction equilibrium is more likely to the right, more  $\text{CO}$ . On the steel surface  $\text{CO}$  will decompose



The C element formed in the form of carbon atom, which actively enters diffuses into the austenite phase of the steel. With the energizer the process will be easier because even the air trapped in the box is very small, but the energizer provides the CO that will immediately begin activating the next reactions. The decomposition reaction of BaCO<sub>3</sub>:



So, the formed CO<sub>2</sub> carbon dioxide gas is created by reaction with the carburizer's carbon. BaCO<sub>3</sub> is known as an energizer because it releases CO<sub>2</sub> early in the carburization process. 925°C is the ideal carburizing temperature. In the state pack carburization, Canister depth is difficult to accurately control because of the many factors that affect it, such as reactivity carburizer, the density of the air amount inside the box and so on. Similar effects will occur when employing the energizer calcium carbonate (CaCO<sub>3</sub>):



## 1.6 Cyaniding (Carbonitriding)

It is used to give a hard outer case. In a surface-hardening process known as cyanide, the surface of low and medium carbon steels treated by adding both C and N<sub>2</sub> atoms of the cyanide salt. The hardening media might be used an either potassium cyanide or sodium cyanide. The specimens that need to be case-hardened are submerged in a sodium cyanide salt bath that is heated to between 760 and 870°C. Then, the specimen is cooled in a water or with bath. This method was used effectively to increasing the fatigue limit of medium and small sized parts

such as gears, spindle, shaft etc. Cyaniding process gives bright finishing on the product. Distortion can be easily avoided and fatigue limit can be increased. But the main disadvantage of this process is that it is costly and highly toxic process in comparison to other process of case hardening. Cyaniding is generally applied to the low carbon steel parts of automobiles (sleeves, speed gears box, drive worm screws, oil pump gears etc), motor cycle parts (gears, shaft, pins etc.) and agriculture machinery. Molten cyanide decomposes in the presence of air at the surface of the bath to produce sodium cyanate, which in turn decomposes in accordance with the following chemical reactions: [22].



This process requires 30–90 minutes for completion.

Cyaniding salts are fatally poisonous if ingested and violently poisonous if allow to come in contact with scratches or wounds. The work area should be well ventilated, and cyaniding baths should have a hood for venting the gases created during heating. Never allow molten cyanide to come into touch with sodium or potassium nitrates, which are frequently used as tempering baths, as the resulting mixture is explosive. [23].

## 1.7 Application

In general, many of structural components and machine parts in services subjected to a varying loads at the same time. These varying loads influence the fatigue properties (fatigue life, fatigue strength). Components like's blades and disks on the turbines, and turbine shafts, aircraft parts, are subjected to a High Cycle Fatigue (HCF) as well as to a temperature variation. Most of the moving components in the automotive engines likes springs and exhaust valves, crank shaft, cam shaft, and connecting rod, and spindle. Figure (1.5) shows application of mechanical parts.



Figure (1.5): Mechanical parts.

## 1.8 Carbon steel

Carbon steel is a steel with carbon content from about 0.03 up to 2 percent by weight and small percentage of alloying elements. Alloying elements such as (Si, Mn, Al, p, Cr, Ni, S, etc.), and each element has an effect on the mechanical and physical properties of steel. All steel types, however, contains small amounts of carbon and manganese. In fact, there

are three types of carbon steel, low, medium, and high carbon, low carbon steels have been used in this work [24]. Figure (1.6) presents types of carbon steel.

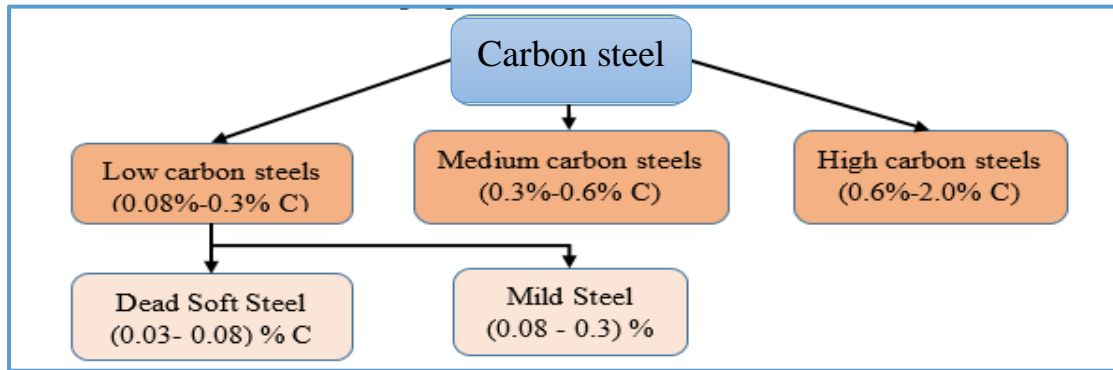


Figure (1.6): Classification of steels on basis of chemical composition and range of Carbon percentage for each type of steels [25]

### 1.8.1 Low-Carbon Steels (LCS):

Low carbon steel, also known as mild steel, is steel that contains carbon of range 0.08-0.3 percent. This low percentage of carbon making it malleable and ductile, so it is often called mild steel. Mild steel or low carbon steel has a relatively low strength and hardness compared with other types of carbon steel and can improve it by one of method surface hardening process. It consists of ferrite and pearlite and some impurities and some manganese to neutralize the effect of any sulphur content left over from the extraction process. Low carbon steel is the most common type of steel because it's low price while it provides material properties that are acceptable for many applications. The application of this type are in nails, rivets, bolts and nuts, chains, automobile body, beams such as I beam and channel and other many applications. There are many examples of low carbon steel according to international standards such as AISI 1008, 1020, 1030, ASTM A510, SAE 1020, etc. [25].

### **1.9 Objectives of the Present Work:**

1. Study the surface hardening effect the improvement percentage of fatigue strength.
2. Study the surface hardening effect the improvement percentage of fatigue life.
3. Study the soaking time affects the fatigue behavior of cantilever steel beam.
4. Study the surface hardening affect the fatigue property specimens.

***Chapter Two***

***Literature***

***Review***

## 2.1 Overview:

Fatigue failure is a predominant type of failure in many engineering and construction applications. The degree of fatigue effect depends on the severity or frequency of the applied stress has something to do with eradicating small cracks or creating new, larger ones. An easy way to speed up fatigue failure is for metal surfaces to have already corroded [26].

## 2.2 Fatigue Literature Review:

In this part, attention is turned to a review of past works that studied the fatigue in metals and focused on the main criteria of this work represented by surface hardening effect on the fatigue behavior. Many researches have studied this subject:

**Gangaraj, et al.,(2013)** investigated how a low-alloy steel fatigue limit responds to the combination of severe shot peening and nitriding. Severe shot peening is done under certain processing conditions to create ultra-fine/nano-structured surface layers. On single and hybrid surface treated specimens, including nitrided, severely shot peened, nitrided plus severely shot peened, and severely shot peened plus nitrided specimens, microstructural observation, microhardness, surface roughness, and X-ray diffraction (XRD) measurement of residual stress were performed. The fatigue limit is determined experimentally for all surface-treated samples and compared to the received samples. The fatigue limit is increased by 11.6% and 51.3%, respectively, by severe shot peening and nitriding [27].

**Xie, et al.,(2014)** studied the effect of surface hardening by using three methods “Vacuum carburizing, induction hardening, and atmosphere carburizing” at different case depths on steel rods (AISI 8620, 9310 and 4140) investigated the rolling contact fatigue (RCF) resistance. A rolling contact fatigue test apparatus with three balls on rod is used to measure the

RCF life of the rods. The surfaces of the rods were examined using scanning electron microscopy (SEM). Investigations were done on the connections between case depth, RCF life, and surface hardness. The longest life of AISI 9310 samples was observed by vacuum carburizing treatment, while the shortest life was observed for AISI 4140 inductively hardened samples [28].

**Fragoudakis ,et al.,(2014)** Studied the manufacturing process parameters(quenching in oil at 850°C and tempering at 500C° for 30 min) to convert the primary microstructure of 56SiCr7 Spring Steel into tempered martensite, and increasing surface hardness and fatigue resistance after heat treatment. Shot peening is used to create compressive residual stresses on the steel's surface. As a result, its surface hardness increases, as does the number of cycles to failure. The results indicate a significant improvement in surface steel hardness as well as a fatigue limit. S-N curves calculated experimentally at 4-point cyclic bending characterize the specific influence of the applied shot peening and heat treatment on fatigue life [29].

**Chang, S ., (2016)** used ultrasonic nanocrystal surface modification (UNSM) to reinforce the surface of standard railways. After UNSM treatment, there are a few changes in surface attributes in terms of hardness and compressive residual stress. In rolling contact fatigue testing, rails with UNSM-hardened surfaces and heat-treated rails are used. The material of the surface hardened rail shows improved rolling contact fatigue properties [30].

**Abdulrazzaq,(2016)** studied the flame hardening method (oxy acetylene torch) at various speeds, followed by fatigue testing using a rotating bending fatigue test apparatus to determine the influence of hardening on the hardening strength of medium carbon steel. The first

sample (as received), the second sample (3.5 mm/s), the third sample (1.75 mm/s), and the fourth sample (1.165 mm/s) are all measured. It was concluded that the fatigue strength of the material reduces as the flame speed rises [31].

**Poursaiedi and Salarvand,(2016)** studied the influence of surface quality on fatigue performance in air and 3.5% NaCl solution on a custom 450 stainless steel substrate coated with nanoparticles (Ti, Cr) via cathodic physical vapor deposition. The findings indicated that the measured in plane residual stress is compressive and has a value of  $-2.8 \pm 0.4$  GPa. The results show that compressive residual stress is measured in plane. The surface roughness of the coating ( $R_a$  from 0.35 to 0.07  $\mu\text{m}$ ) is decreased by chemical mechanical polishing. This greatly decreases the area of high stress concentration and delays the occurrence of microscopic cracks in the coating during the fatigue test. According to the findings, coated samples with polished surfaces have fatigue strengths that are 10.6% higher in air and 26.7% higher in NaCl solution than coated samples with unpolished surfaces [32].

**Maleki and Kashyzadeh., (2017)** effects of the hardened nickel coating on the fatigue behavior CK45 steel with two different thicknesses experimentally. The specimens has been tested under cantilever type rotating bending fatigue machine. The High-Cycle-Fatigue (HCF) characteristics of the coated samples with various thicknesses are determined using the fatigue test. The capability of the two different approaches of finite element method (FEM) and artificial neural network (ANN) in modeling the fatigue life of the coated specimens was compared. The achieved results of the accomplished simulations represent that both simulations are acceptable and have good agreement with the experimental

results. Results of FEM and ANN have the average relative errors of 9.60 and 0.55 %, respectively, and that the ANN model has a better performance than FEM. The fatigue life was reduced by increasing the thickness, which has detrimental effects [33].

**Guarino, S., (2017)** analyzed the effects of the laser treatment on surface of steel and the interaction between laser radiation and steel surface, where the analysis is done by fatigue test. In order to extend the fatigue life of AISI 1040 low carbon steel, a high-power diode laser is used. The tests are conducted using a revolving bending machine with four points. Results show that the best thermal treatment conditions are using laser power of 200W with a 20 mm/s scan rate, also note that life cycles increasing with increase of scan speed. Inferred from a study of the experimental data, Wohler curves demonstrated that laser therapy may greatly lengthen the fatigue life of irradiated components, demonstrating the applicability of this technique for industrial uses [34].

**Barkat. A, et al., (2017)** examined how boriding treatment in a solid media affected the cyclic fatigue resistance of C20 carbon steel. Specimens of C20 steel coating by boriding in a solid medium consisting of 5% B<sub>4</sub>C, 5% NaBF<sub>4</sub> and 90% SiC are subjected to rotating-bending fatigue. The findings indicated that the boriding treatment on C20 steel does not significantly improve fatigue resistance. This is explained by the presence of FeB boride in addition to Fe<sub>2</sub>B boride, which leads to surface cracking [35].

**Zhang, et al., (2017)** studied how fatigue cracks grow in the surface-enhanced material's gradient microstructure layer. It is used surface induction treatment is used for material a train axle steel. Fatigue experiments are carried out to collect data on fatigue using three-point

bending (TPB) fracture propagation along the specimen's gradient microstructure layer. The results show that the fatigue crack growth rate decelerated first and subsequently accelerated as crack length increases within the gradient layer. The fatigue crack in the gradient layer is stopped by an increase in the threshold value for crack growth within the region of 3 mm from the surface under relatively low stress amplitude [36].

**Vackel.,(2017)** studied the effect thermal spray deposited coating by using (WC-CoCr) a DJ-2600 High Velocity Oxy-Fuel (HVOF) torch on 1018 steel. Rotating bending fatigue studies examine the impact of both torch operation settings (particle states) and deposition conditions (particularly substrate temperature). The findings show a significant influence of process variables on relative fatigue life. The findings show that compressive residual stress and acceptable load bearing capability of the coating (both regulated by torch and deposition settings) postpone the beginning of substrate deterioration, allowing the coated component to be fatigued [37].

**Ali. M.,(2019)** studied the effect coating of nanomaterial type and its thickness on the fatigue behavior for plain LCS beam, and this effect on the V-notch low carbon steel with a depth of 1mm and an angle of 45°. The nanomaterial used are ZnO, Al<sub>2</sub>O<sub>3</sub>, and a mixture of both ZnO and Al<sub>2</sub>O<sub>3</sub>. The results show that Al<sub>2</sub>O<sub>3</sub> (aluminum oxide) has more effect on the fatigue stress and fatigue life compared to the specimen coated ZnO (zinc oxide) and Mixed of both them. While coating with mixed gives improvement to fatigue performance than ZnO. In addition, as the thickness of the coating material increases, the fatigue life increases for all types of coating material [38].

**Dunchev,et al.,(2019)** examined of the 35HGS low-alloy steel nitriding sample' fatigue behavior. The effect of the hardening process,

along with the grinding process and the ion nitriding process compared. All samples tested under rotational bending fatigue test. Fatigue specimens test performed on a MUI6000 cyclic bending test machine. Five different groupings of specimens have been produced. The first group of samples is hardened at 860°C, then tempered at 550 °C, and lastly grounded. At a constant temperature of 520 °C, the other four sets of specimens underwent ion nitriding for a different process time of 4, 8, or 16 hours, respectively. Results revealed that, in the area of high-cycle fatigue, the ion nitriding process has a more beneficial influence on fatigue life than hardened at 860°C procedure followed by grinding [39].

**Selva,et al., (2021)** investigated how shot peening affected fatigue life, by changing shot peening process variables like peening distance and pressure with amachrome as shots, surface hardness and corrosion properties of SAE 4140 low carbon alloy steel are examined at room temperature. The experimental finding indicates that the two most important variables in the shot peening process are pressure and distance (distance between nozzle and work piece). The results illustrate that the average pressure of 7 bar and distance of 100 mm improves fatigue life by 1.5% of unpeened material under 20 Hz frequency while corrosion resistance improves by 4% with unpeening of the low carbon alloy steel by using amachrome as a shot [40].

**Ramesh ,et al.,(2021)** studied the effect of surface hardness by vacuum carburizing then followed by tempering on the torsional fatigue behavior Of 20MnCr5 Steel. The fatigue tests are performed out in an MTS machine torque testing with bi-directional torsional cyclic loading. The power train shaft's fatigue performance has not been much improved by surface retained austenite, while the fatigue performance is greatly improved from

12,000 to 35,000 cycles on a 3100 N. m torque load due to the presence of a marten site with a low austenite proportion [41].

### 2.3 Pack Carburizing Effect

**Priyadarshini, et al., (2014)** found that quenching and tempering do not work on low carbon steel that contains 0.15 to 0.3% carbon, and quenching virtually ever results in martensitic transformation. Thus, carburizing treatment is used to improve surface hardness, in which the surface composition of low carbon steel changes due to carbon diffusion, resulting in a hard outer shell with high wear resistance. The low carbon steel is carburized a temperature of 900°C for 5 hours. Following carburizing, treatments such as annealing, normalizing, hardening, and tempering were carried out [42].

**abdul motalleb (2014)** used heat treatment to improve the mechanical properties of locally available low carbon steel used to replace the spindle of a Sacolowel ring twisting machine. The specimen is initially made out of low carbon steel that is readily available locally, which was heat treated by pack carburizing, quenching, and tempering to enhance the mechanical properties. Additionally, the characteristics of the specimens before and after heat treatment have been investigated. Water and oil have both been utilized as quenching mediums for these materials. Oil-quenched spindles were found in sound condition while water-quenched spindles are found bent. According to the results of this experiment, the heat-treated specimen's hardness, tensile strength, and compressive strength have all significantly increased in comparison to the unheated specimen [43].

**Negara, et al., (2015)** studied effect carburizing on mild steel to enhance the mechanical properties. It was observed that the hardness was transferred from the surface to the core at a lower hardness level. The best

energizer in the study was clearly energizer (20% BaCO<sub>3</sub> + 80% bamboo charcoal) based on the surface hardness, core hardness, and effective case depth attained. In the meantime, the surfaces' original microstructure, which is composed of ferrite and pearlite, transforms into a hard marten site component following carburization [44].

**Widodo, et al., (2018)** explained the effect of various carburizer media on the mild steel's fatigue strength. Wood charcoal and Pomacea Canalikulata Lamarck (PCL) shell powder are utilized as the carburizer media. The (PCL) shell powder's weight percentages are 10, 20, and 30. Carburizing is performed out at 950°C for 5 hours, then the metal is tempered at 250°C, 300°C, and 350°C before being quenched in salt solution (30% NaCl + water). Following the Rotating Bending Test, the specimens' fatigue strength and microstructure are examined using a SEM (scanning electron microscope). Finally, after pack carburizing, the fatigue strength can be increased by tempering and quenching in 30% NaCl solution [45].

**Darmo, 2019)** studding the effect of different carburetor media on SS400 low carbon steel to discuss fatigue strength. Pinctada maxima shell powder (PMSP) is composed of 10, 20 and 30 (wt%) while teak charcoal is composed of 90, 80 and 70 (wt%). At temperatures between 800 and 950 degrees Celsius, the process of carbonizing the package lasts for five hours. After the rotating bending test, SEM observations were performed to determine the samples' microstructure and fatigue strength. Finding out that surface hardness of SS400 low carbon steel can be increased while the amount of fatigue cycles is reduced by using a compound media carburetor with 30% PMSP and 70% TWC compared with 10 and 20% PMSP. Fatigue strength test using a rotating bending machine to fracture under different minimum stress levels (275-390 MPa) [46].

**Diyar, et al., (2020)** examined how the carburizing procedure affected the mechanical properties of low carbon steel, AISI 1011. (80% wood charcoal, 10% BaCO<sub>3</sub>, 9% CaCO<sub>3</sub>, 1% Na<sub>2</sub>CO<sub>3</sub>). Discovered that the alloy's hardness rises for samples subjected to a five-hour carburizing treatment at 950°C, rising to 431.65 HV compared to 169.65 HV of untreated specimens. The samples have been quenched in the oil. Additionally, the metal's surface roughness rise for specimens subjected to the carburizing procedure and increases to 1.98 µm [47].

**Qin,S ,et al.,(2022)** studied high cycle fatigue performance of carburized and un-carburized 18CrNiMo7-6 gear steel, and carried out various carburizing operations on steel. Four types of case depth specimens with 0 mm, 0.3 mm, 0.8 mm, and 1.9 mm are generated. At room temperature, the rotating bending fatigue test was conducted using a four-point force method, a frequency of 50 Hz, and a stress ratio of 1. The performance of steel under rotary bending fatigue is greatly improved by carburizing treatment, according to the results. The fatigue limit of carburized specimens is 1108 MPa as opposed to the non-carburized specimens' 680 MPa, an increase of 62.9% [48].

## 2.4 Carbonitriding Effect

**Ayodeji, et al., (2011)** investigated the effect of cyanide salt bath heat treatment process on four types of steels, namely, LCS MCS, LAS and HAS . The steels, after heated quickly quenched in different media including air, oil and brine. The heat treatment time was varied from 30minutes to 120 minutes. The surface hardness are measured by using Rockwell hardness tester. [49]. The results carbonitriding collected lead to the following conclusions.

- Cyaniding is a useful technique for making steels' surfaces harder.
- The cooling medium affects the surface hardness of cyanide steel.
- The surface hardness of the steels increases with temperature rise within the heat treatment temperature range of 790°C to 920°C.
- LCS surface hardness increases with heat treatment time.

**Aziz, et al., (2020)** performed Chemical heat treatment (liquid nitriding) by using mixture from (sodium cyanide, potassium carbonate and chloride potassium) at temperatures 500 °C and 560 °C and followed by Nd:YAG laser surface treatment. Cycle of laser surface treatment is melting the layer surface, soaking time and cooling in air medium. Microstructures, molted cross sections, and heat impacted zones have all been studied using optical microscopy (OM) and scanning electron microscopy (SEM), respectively. The results shown that increasing in laser energy lead to increase in the area of melted and heat affected zones of nitriding steel. Also increasing in laser energy lead to increase micro hardness about 61%, while wear rate decrease about 40 % and increased depth of molted zone [50].

**Alza.,(2020)** studied the effect of cyanide in a salt bath to improve mechanical properties ( hardness and wear) of ASTM A-517 medium carbon steel. Samples were prepared according to ASTM G-65 standard. The CN treatment was carried out, at high temperatures: 800 – 850 – 900 – 950 °C. It is found that when cyanide is applied to ASTM A-517 steel, the hardness and wear characteristics are raised to optimal values if the cyanide treatment (CN) is carried out at 850°C [51].

**Ghanem. A, and Mohamedali. T (2022)** experimentally studied three-point fatigue flexion examined the impact of gas-carbonitriding time on fatigue limit improvement of low alloy steel specimens. In order to simultaneously diffuse nitrogen and carbon into the tested steel, the

specimens are carbonitrided at 870°C for 7 and 8 hours in an atmosphere of endothermic gas comprising a high volume of methanol gas and ammonia gas combination. They are then tempered for one hour at 200°C after being quenched in oil at a temperature of 60°C. Utilizing optical, scanning electron, and metallographic methods, micro-Vickers hardness tests are conducted. The fatigue resistance improved, according to the results. Comparing carbonitrided specimens to their untreated counterparts, the fatigue life is enhanced by 16% to 32% [52].

## 2.5 Concluding remarks

Treatments by pack carburizing and carbonitriding are important for improving mechanical properties, in particular fatigue resulting from repeated stresses over time on moving parts or components. The literature survey on the performance of surface hardening done in the present work shows that different types of surface hardening particular (pack carburizing and carbonitriding) were used to investigate effect diffusion carbon and nitrogen on mechanical properties of low carbon steel. The same procedure was used to prepare carbon medium and ratio of energizer by **Darmo,(2019)**. The same procedure also was used to prepare molten salt bath (carbonitriding) by **Aziz, et al., (2020)**. The details of the v notched specimens have been prepared according to **Ali mohamed, (2019)** in this master thesis. The fatigue behavior of notched and un-notched beam 17100 steel with surface hardening by carbonitriding and pack carburizing together not discussed in the previous work, which is the main goal of the present work.

***Chapter Three***  
***Experimental***  
***Work***

### 3.1 Introduction

In this chapter the effect of two types of surface hardening (pack carburizing and carbonitriding at various soaking times) with V notch at angle  $45^\circ$  and depth 1mm and without notch (plain) on the fatigue life in steel beam made of carbon steel have been studied. Fatigue life of notched specimens measured by applying a fully reversed cyclic load. The experimental work involves Sixth parts. The first part is the analysis of chemical compositions of the specimen material, which is used, in the current work. The mechanical specimens preparation and tested in the second section using the tensile, hardness, and impact tests. The third part is the specimen's preparation of the fatigue. The specimens divided into two groups, first group contain notched beam and second group un-notch beam. The specimens is prepared according to the ASTM 606-80. The fourth part includes surface hardening by both pack carburizing and carbonitriding. The fifth part includes the fatigue test. Sixth part has Microstructure examination. All machines and tools used in this study are calibrated before use. Figures (3.1) and (3.2) show the scheme of experimental work and the distribution of specimens.

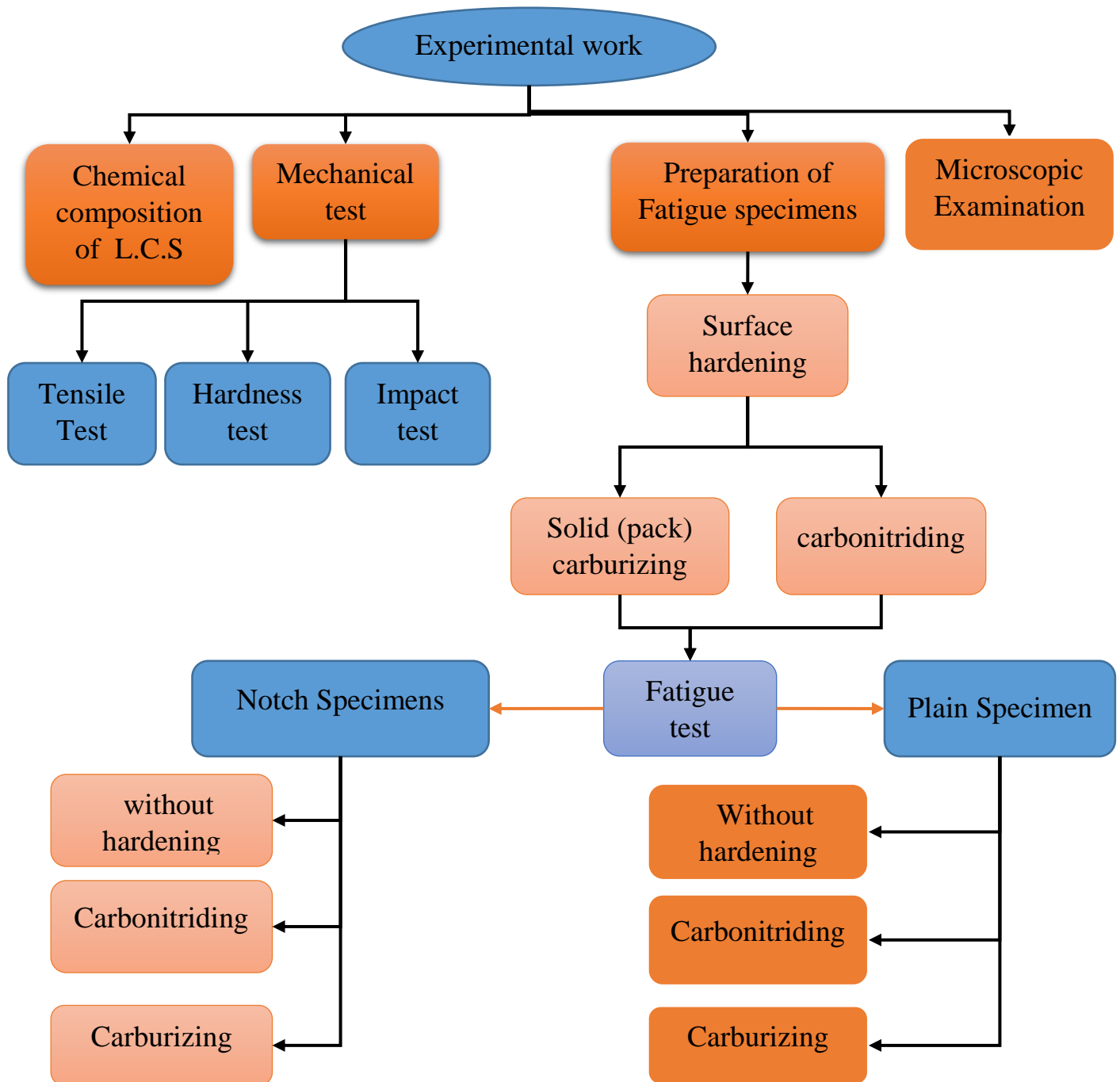


Figure (3.1): Scheme of experimental work.

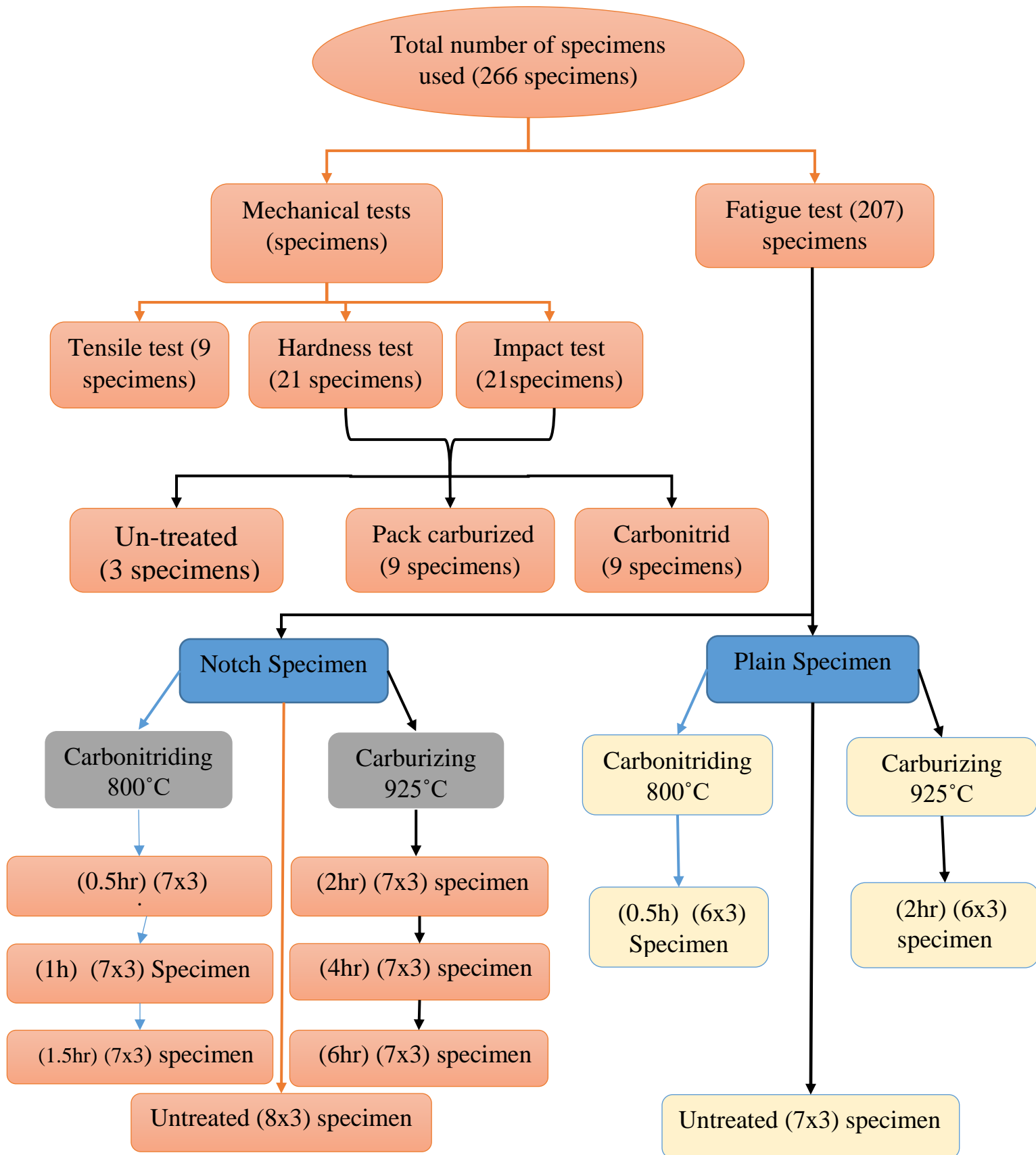


Figure (3.2): Average Specimens distribution of mechanical tests and fatigue test.

### 3.2 Material Selection and Chemical Composition

The material selected in this work is low carbon steel alloy (DIN 17100) was bought from Iraqi Ministry of Industry and Minerals Kufa cement plant. This type of steel alloy has a wide application in industry. The chemical analysis of this alloy is carried out using a spectrometer device in state Company for inspection and Engineering Rehabilitation (SIER) as shown in figure (3.3). The purpose of the chemical composition analysis is to classify the material by knowing the percentage of carbon and finding out the percentage of each element added to the material. Low carbon Steel generally contains many elements; the most important element is carbon and can be up to 2%. All the alloying elements added to the low carbon alloy have an effect on the mechanical properties of the steel so it is necessary to know the percentage of each element. The results obtained are illustrated in Table (3.1). According to results obtained the international code for alloy selected for the certificate of the test achieved, see (DIN17100-St44-2).

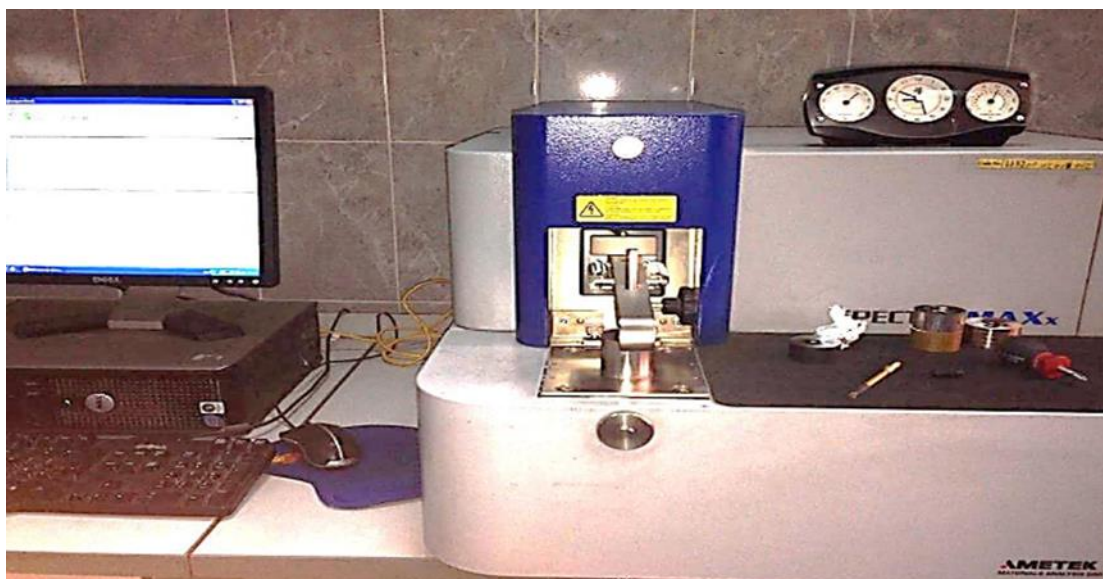


Figure (3.3): Spectrometer test device.

**Table (3.1):** Chemical composition for Low carbon steel material (wt %)

Elem	LCS (measured)	LCS(standard) [25]	Uex
C %	0.221	0.17-0.23	$\pm 0.013$
Si%	0.136	-----	$\pm 0.007$
Mn%	0.499	0.3-0.6	$\pm 0.039$
P%	0.0193	$\leq 0.04$	$\pm 0.002$
S%	0.0727	$\leq 0.05$	$\pm 0.057$
Cr%	0.138	-----	$\pm 0.002$
Mo %	0.023	-----	$\pm 0.02$
Ni%	0.147	-----	$\pm 0.008$
Al %	0.0099	-----	$\pm 0.009$
Cu%	0.394	-----	$\pm 0.005$
Fe %	Ball.	99.08-99.53	$\pm$ ----

### 3.3 Mechanical Tests

Mechanical tests are a standard and essential part of any design and manufacturing process. Whether it is characterizing the properties of materials or providing validation for final products, ensuring safety is the primary mission of all-mechanical testing. Testing also plays a crucial role in ensuring a cost-effective design as well as technological evolution and superiority. The mechanical tests including tensile, hardness and impact.

#### 3.3.1 Tensile Test

Tensile tests are performed for several reasons. The results of tensile tests are used in illustrate the mechanical properties. Tensile properties frequently are included in material specifications to ensure quality. Tensile properties often are measured during development of new materials and processes, so that different materials and processes can be compared [53]. The tensile test is conducted using the universal testing machine type (WAW-200 - 180KN) with a speed rate of 2 mm/min as it is shown in figure (3.4), where the test was carried out in the lab of Materials

Engineering Department of College of Engineering / University of Babylon. The specimens for tensile test are manufactured according to the specification of ASTM-A 370 (Gauge length (G) of 35 mm, diameter (D) of 8.75 mm, length of reduce section (A) is 45 mm and Radius of fillet (R) 6mm) [54], as shown figures (3.5) and (3.6). Average value of three readings for low carbon steel material type has been recorded to satisfy an additional accuracy.

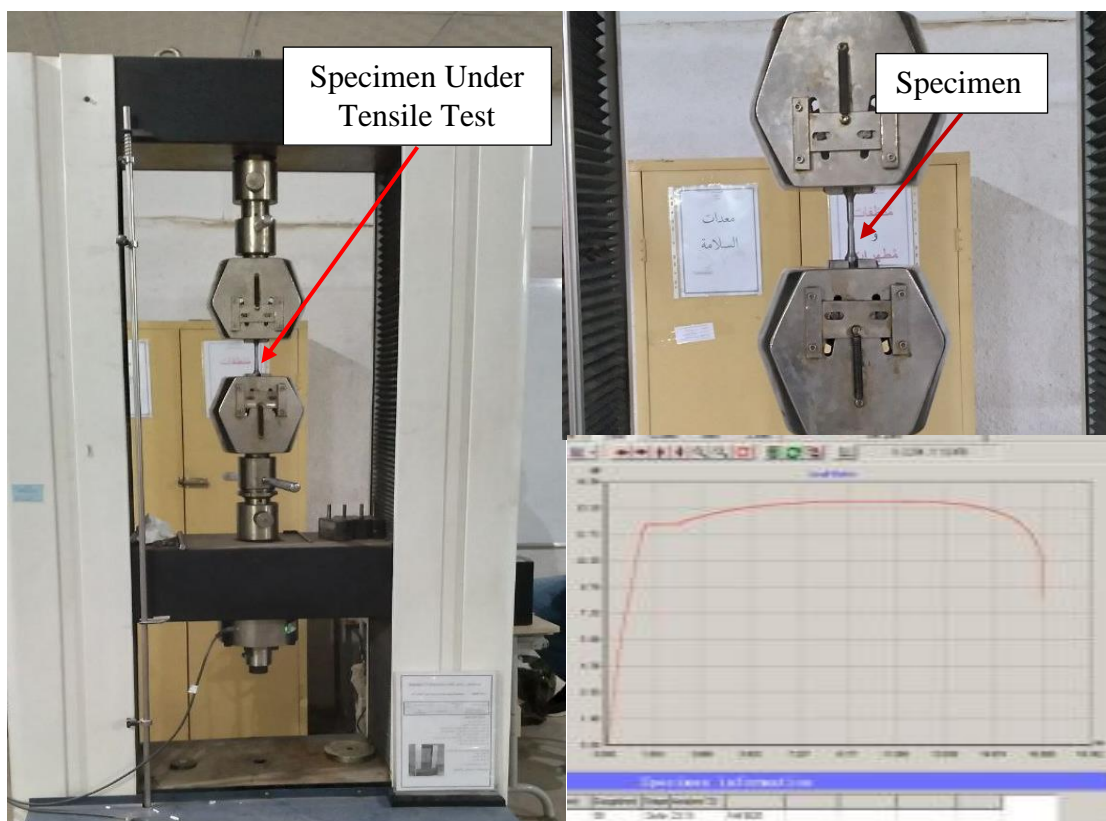


Figure (3.4): Tensile test machine.



Figure (3.5): Samples of specimens used for tensile test.

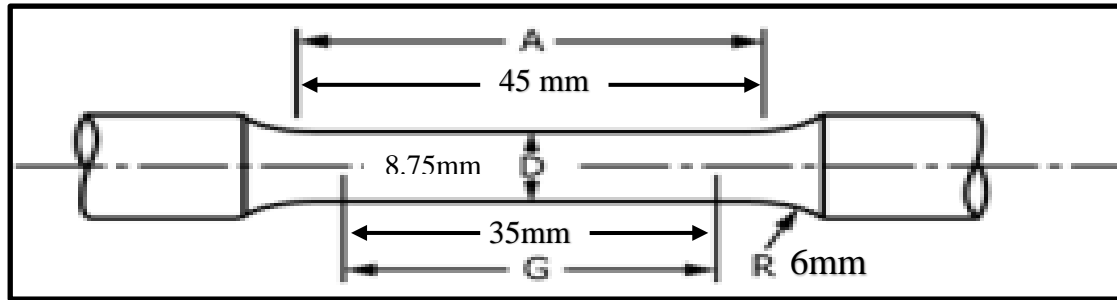


Figure (3.6): Schematic of tensile test specimen according to the specification of (ASTM-A 370).

### 3.3.2 Hardness Test

Hardness is defined as the resistance of a material to penetration, scratching, and erosion. It is an important property when judging the quality and possible applications of a material. It can also give indications concerning the tensile strength, ductility, or wear resistance of the material [55]. There are various techniques for evaluating hardness such as Brinell hardness test, Rockwell hardness test and Vickers hardness test. The dimensions of specimen were diameter 10mm and 10mm height according to [50].

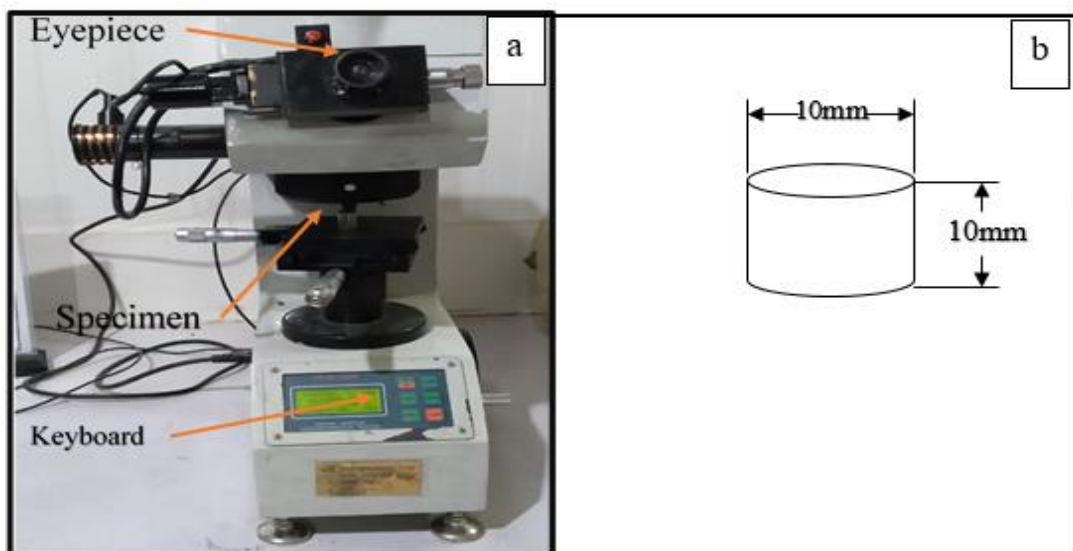


Figure (3.7): Hardness test: (a) device Vickers. (b) Dimensions of specimen.

The hardness test of low carbon steel sample is tested by the Vickers method with the type of device (HVS-1000), of (100 g) applied load as shown in figure (3.7). The specimen hardness is measured before and after heat treatment. This test is carried out in the Laboratory of Engineering of Materials College of Babylon University.

### 3.3.3 Impact Test

Impact testing of metals performed to determine the impact resistance or toughness of materials by calculating the amount of energy absorbed during fracture. There are two method of impact test, one first is Izod method and another is charpy method. Impact test is achieved for the selected material using Izod method by using the impact-testing machine of type (Brooks AME 01-19) according to ISO A 370. This test performed in the Laboratory of Engineering of Materials College of Babylon University shown figure (3.8).

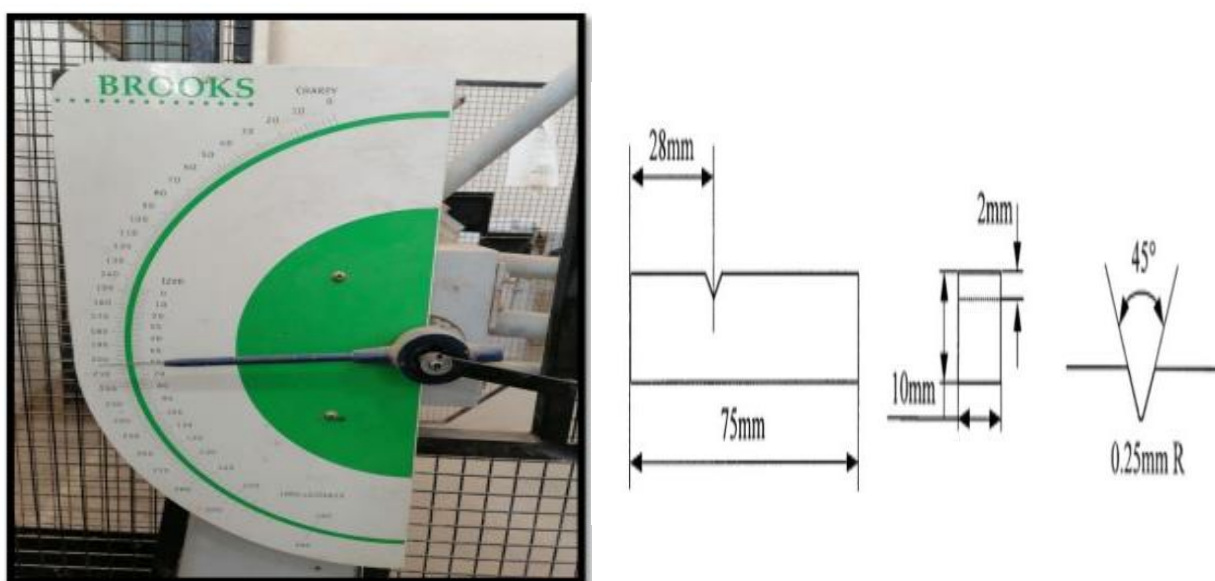


Figure (3.8): Impact test device and specimen dimension.

Impact strength is calculated from the following equation [56]: -

$$G_c = \frac{U_s}{A} \quad \dots (3.1)$$

Where:

$G_c$ : Impact strength of material (J/m<sup>2</sup>).

$U_s$ : Impact energy absorbed for the specimen rapture (J).

$A$ : cross sectional area of specimen (m<sup>2</sup>).

$$U_s = E_i - E_r \quad \dots (3.2)$$

$E_i$  : initial pendulum energy (J).

$E_r$  : remaining pendulum energy (J)

### 3.4 Preparation of Fatigue Specimens

Fatigue specimens in this work are manufactured according to the ASTM606-80 standard (cantilever rotating bending model) specifications as shown in figure (3.9) by using CNC machine. Fatigue specimens worked with dimensions that suitable for the requirements of the device test for specimens with cylinder-shape. During the manufacture of the Specimens, careful observation taken to produce smooth surface and to reduce the residual stresses. The specimens are divided into two groups, first group contain notched beam and second group un-notch beam. The notches are V shape with angle ( $\alpha = 45^\circ$ ) to a depth ( $h = 1$  mm) [57]. Figure (3.10) show the fatigue specimens with dimensions. Figure (3.11) present details v-notch samples.

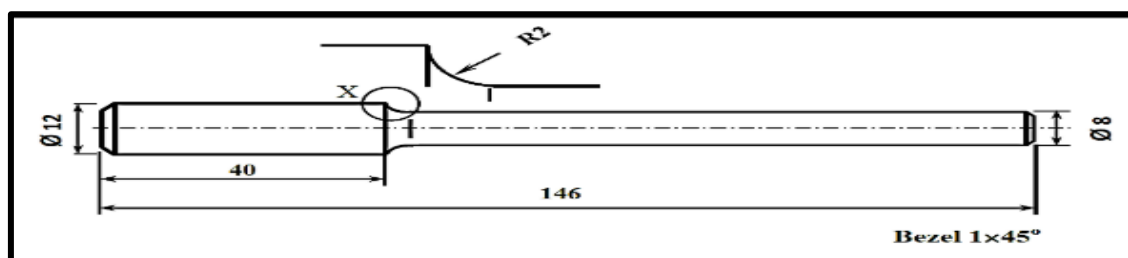


Figure (3.9): Schematic diagram for fatigue test specimens.

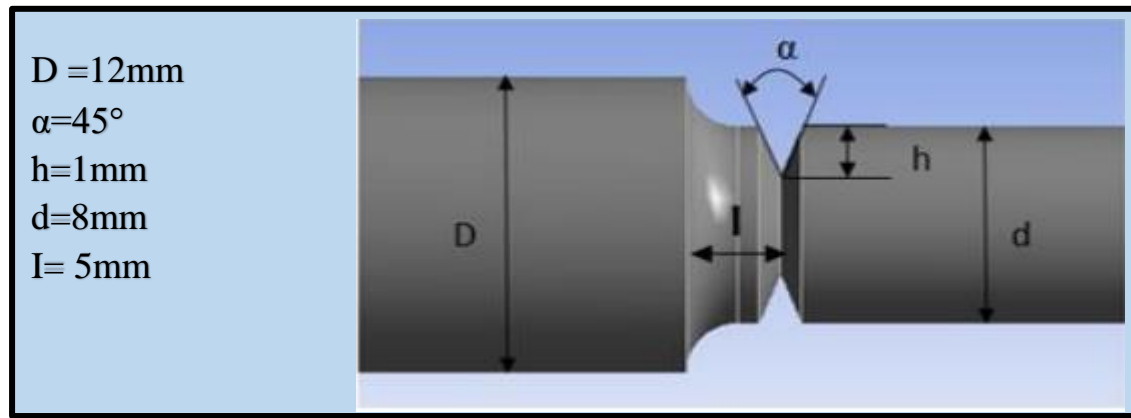


Figure (3.10): Dimensions of V shape notch specimens [38].



Figure (3.11): Notched Specimens.

### 3.5 Surface Heat Treatments:-

Two types of surface Heat treatments are used that aim to harden the steel surface only, and these treatments are:

- Pack (solid) carburizing
- Carbonitriding (Cyaniding)

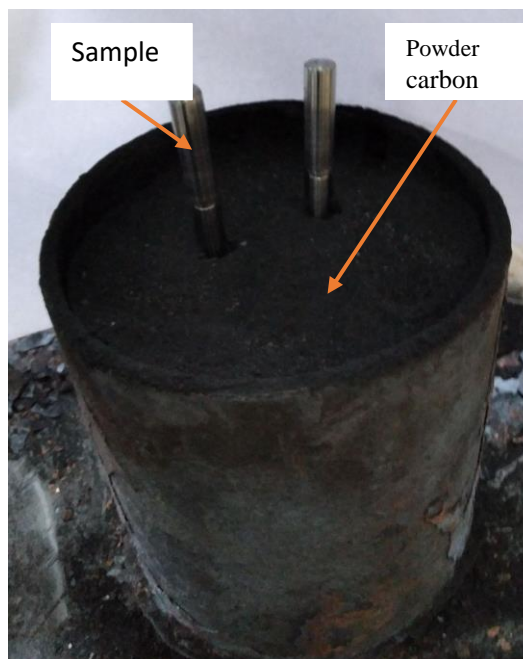
### 3.6 Pack (sold) Carburizing

Carburizing media used is the wood charcoal and Barium Carbonate ( $\text{BaCO}_3$ ). 10% barium carbonate and 90% carbon powder were used and mixed together, placed into container (box) made from low carbon steel thickness (8mm) and height (160 mm) diameter (100 mm). Specimens and media carburizer (Powder carbon mixed with  $\text{BaCO}_3$ ) are inserted into the carburizing box and the box was closed tightly. Then the box was heated to ( 925 °C) in electric furnace (nabertherm more than 30-3000 °C) made in Germany for (2 hr,4hr and 6hr) as shown in figure (3.12). As a result of a chemical reaction, carbon dioxide is released, which, in turn, combines with other carbon atoms to generate carbon monoxide gas. The resulting carbon monoxide liberates carbon atoms on the surface of the hot steel, which spread across the surface of the metal at a certain depth in the direction of the core of the metal. The surface carburizing process works to enrich the surface with carbon, which reacts with iron to form the precipitated iron carbide ( $\text{Fe}_3\text{C}$ ), and this free cementite leads to the steel gaining high brittleness and the risk of scaling at the crystalline boundaries when the steel slowly cooled from the carburizing temperature. So the solidification process must be carried out (hardening) in order to obtain martensite and then thermal tempering process is carried out to improve the properties mechanical [58]. The temperature of 850°C was also tested at the beginning, but it showed a slight improvement due to the depth of the small surface layer formed at this temperature. Therefore, the temperature was raised to 925 °C, which was used in this study. Figure (3.13) show specimens after pack carburizing. Where the test is carried out in the lab of Materials Engineering Department / College of Engineering / University of Babylon.



(a)

(b)



(c)



(d)

Figure (3.12): Pack Carburizing Process. (a) Barium carbonate. (b) Carbon powder. (c) Carburizing Box. (d) Electric Furnace.



Figure (3.13): Specimens after pack carburizing.

### 3.7 Quenching (hardening)

Quenching is important among the heat treatment techniques. Quenching is a technique of forming a martensitic structure by heating the steel to austenitic temperature and then using a coolant such as water, oil, polymer solution [21]. Water is used when a faster cooling rate is desired. The transition from start of martensite formation to the finish is higher and this increases the likelihood of cracking but it gives a high hardness compared to other cooling media like (oil and polymer solution). Water also are intermediate quenching media and they are ideal for quenching steels. Quenching operation is usually done to room temperature [43]. This quenching media produces highest cooling rate the quenching has been done following the below procedure –

1. The specimen is heated to the temperature of  $850^{\circ}\text{C}$  and was allowed to homogenize at that temp for 16 minutes.
2. After 16 minutes, the specimen is taken out from the furnace and directly quenched in water for rapid cooling using the quenching medium water.
3. The samples are again placed in the electric Furnace until the temperature reached  $760^{\circ}\text{C}$ , and then be cooled in water.

Specimen After quenching bath is shown in figure (3.14). Test condition (18°C, 30%).

The holding time of quenching is selected on basis of the diameter of the specimen as per 2 minute per 1 mm of diameter [59].

A temperature of 800°C is also used, but there is no improvement in fatigue life. Due to the fact that the grains of the metal core remained rough in contrast to the use of the temperature of 850 °C, which improved the mechanical properties of the metal and the fatigue test.



Figure (3.14): Specimen After quenching.

### 3.8 Tempering

Tempering is a necessary process to modify the microstructure to improve the mechanical properties and the remove the residual stress in quenched steel specimen. With the development of technology and equipment, and the advancement of automation for heat treatment industry, the tempering time effect. The variation of the strength and hardness of quenched steel with the tempering time during tempering, is a necessarily considered factor in the formulation of heat treatment for hardened steel. The tempering temperature of low carbon steel ranges from 150 to 200 °C [59].

- The specimen is heated to 180°C for 2 hours to reduce the internal stress. After the tempering, specimens are air cooled in the furnace

[60]. Time and temperature for heat treatment after carburizing shown in figure (3.15).

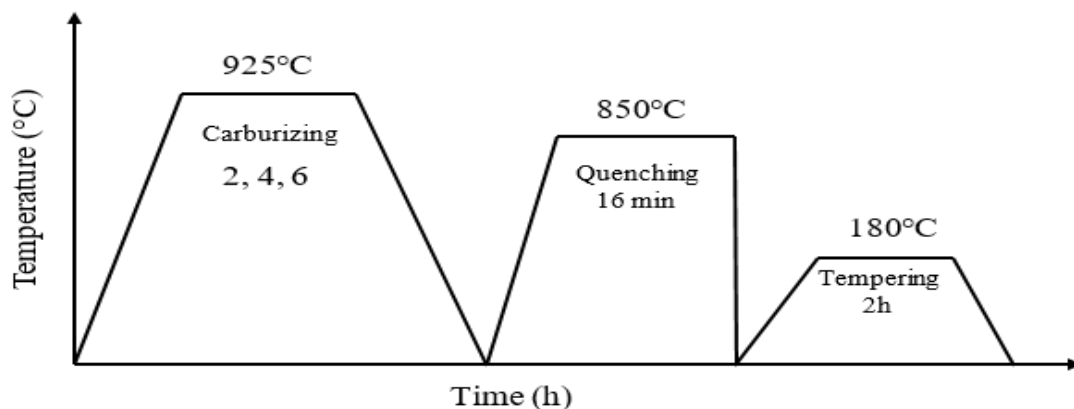


Figure (3.15): Heat treatment (pack carburizing) [58].

### 3.9 X-ray powder diffraction (XRD)

The chemical composition of the ball cyaniding used in this study is investigated by using an X-ray Diffractometer modal type a Lab XRD-6000, as shown in figure (3.16). To know XRD composition pattern of ball cyaniding.



Figure (3.16): X-ray Diffractometer Lab XRD-6000.

The diffraction meter is prepared for measurement in progressive scan mode over a range of  $2\theta$  ( $10^\circ$ - $90^\circ$ ). The field is selected because it appeared on all the prominent diffraction peaks for the crystal structures. A sample step size or sampling pitch of  $0.2^\circ$  and a scan speed of  $10^\circ / \text{min}$  are used.

### 3.10 Carbonitriding(cyaniding):

Sodium cyanide balls of German origin have been used with the following composition (61% NACN +24% KCL + 15%  $\text{K}_2\text{CO}_3$ ) according to standard [61]. They are placed in tank (box) made from stainless steel, and then placed inside electric furnace (same furnace mentioned above) until they are completely melted at a temperature of  $800^\circ\text{C}$ .

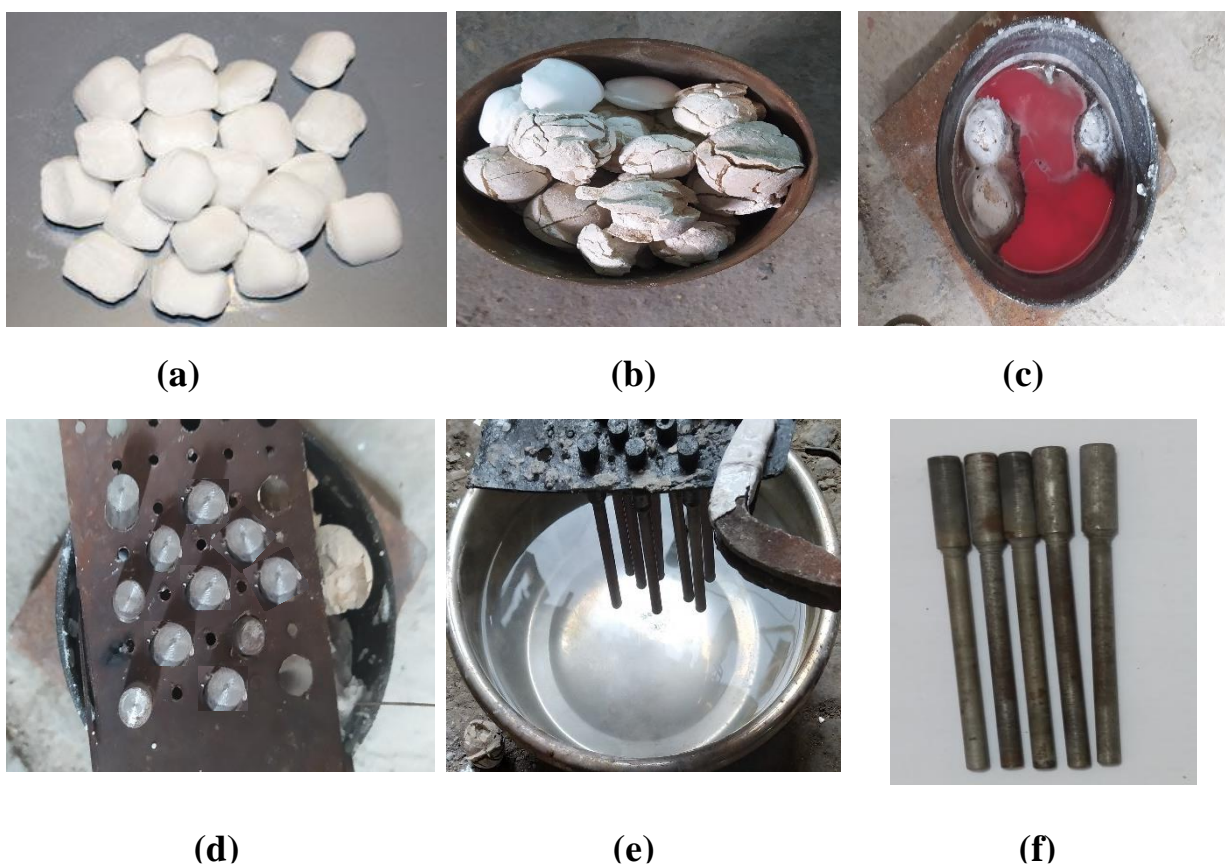


Figure (3.17): Cyaniding Process: (a) Sodium cyanide. (b) Box cyaniding. (c) Melton bath of cyaniding. (d) Holder and spacers inside box. (e) Specimens during quenching. (f) Spacers after quenching.

After that, the molten is taken out of the furnace and the samples are placed on the holder. Then the holder and samples are put inside the molten and returned it to the furnace at a temperature of  $800^{\circ}\text{C}$  for (0.5 h, 1h and 1.5 h). Then the specimen is taken out from the molten and directly quenched for rapid cooling using the water as quenching medium, as shown in the figure (3.17), where the test is carried out in the lab of Materials Engineering Department / College of Engineering / University of Babylon. Figure (3.18) shows surface heat treatment for low carbon steel by using liquid carbonitriding.

After quenching in water followed by tempering, where the specimens are heated to  $180^{\circ}\text{C}$  for 2 hours to reduce the internal stress. After the tempering, specimens are air cooled inside the furnace.

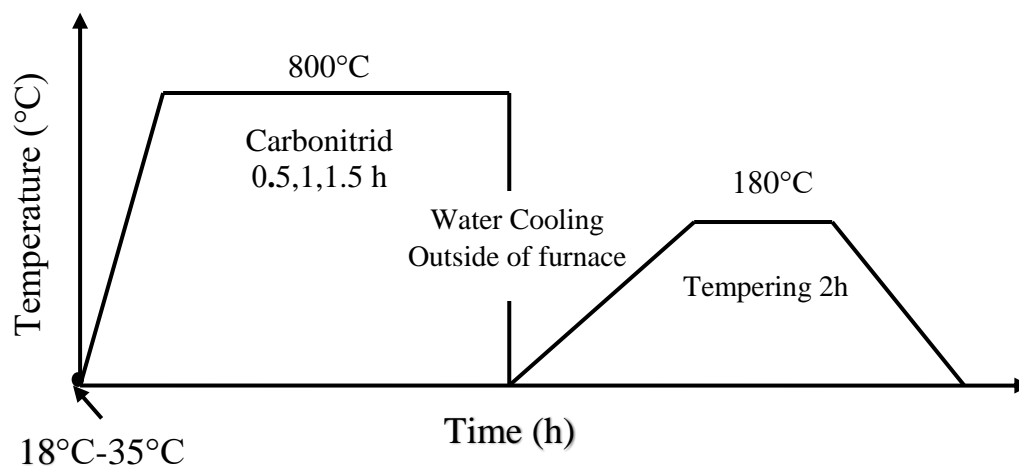


Figure (3.18): Heat treatments (cyaniding) for low carbon steel [58].

### 3.11 Calculate the Depth of Hardness

It refers to the hardened layer (depth of hardness) of a piece of material. Due to surface treatment by one of the hardening methods, where the depth of the hard layer reaches the same hardness as the received metal, and the area that follows the depth of the hardened layer is called the metal core.

By using a Vickers device the hardening layer from the surface towards the core is measured as showing in the figure (3.19). Specimens of hardness cut from the middle after hardened treatment to get the dimensions diameter is 10 mm and length 5mm [50]. The hardness values were taken from surface to the center at distance 0.05mm for each reading.

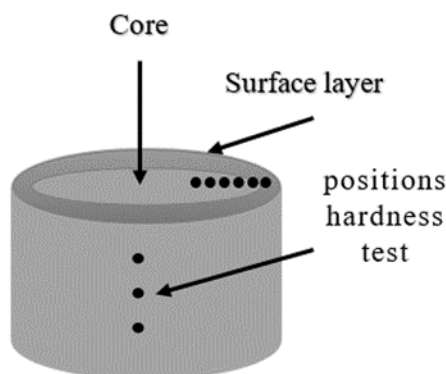


Figure (3.19): schematic for hardness sample.

### 3.12 Microscopic examination

Low carbon steel samples with a surface treatment were prepared for the purpose of microscopic examination using an optical microscope ‘ as shown in the figure(3.20) which included grinding and smoothing operations using silicon carbide (sic)sandpaper in degrees (220 ,400 ,800, 1000, 2000, 3000) . Then electrical polishing with gradient granular size diamond paste ( $3\mu$ ) until they have a surface that resembles, this is followed by the process of showing (Etching) using a solution of Nital (which consists of the following ratios: 2% nitric acid and 98% methyl alcohol). To identify surface hardening region and core of metal, the specimens are studied using a computerized optical at a 100x magnification with a digital camera and computer attached. After etching the snapped pictures of microstructures of the optical are taken and downloaded to the computer. The purpose of conducting the Microscopic examination is the

knowledge of the change in the surface layer and the proof of the penetration of carbon and nitrogen atoms. Show the two regions first region is depth layer of hardening and second region is core for the treated samples by pack carburizing and carbonitriding.

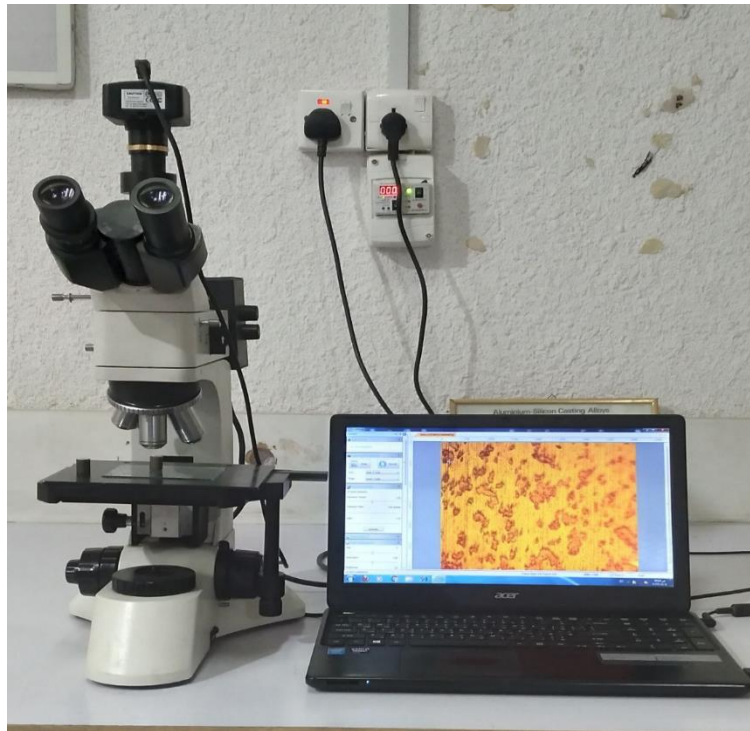


Figure (3.20): Optical microscope device.

### 3.13 Fatigue Testing Machine

There are many types of fatigue testing machines generally can be divided into:

- Axial Machine
- Torsion Machine
- Universal Machine
- Rotating Bending Machine
- Reversed Bending Machine (This type was used in this work)

### 3.13.1 Reversed Bending Machine

It is available at the labs of Department of Mechanical Engineering - college of Engineering at University of Babylon. The machine type is (WP 140) cantilever rotating bending model with a constant amplitude (fully reversed bending), with this machine, it is possible to demonstrate the basic principles of fatigue strength testing, including the production of (stress and number of cycle failure) curve. The number of failure cycles is displayed by a digital counter. A rotating sample is clamped which on one side is loaded with a concentrated force with a maximum capacity of (0.5 KN) with constant frequency of (50Hz). A sinusoidal cyclic load with a stress ratio  $R = -1$  (minimum load/maximum load) is applied throughout the experiment. As a result, an alternating bending stress is created in the cylindrical sample after a certain number of loading cycles; the sample failure results from material fatigue. The tests are carried out at room temperature (18-30C°), and environmental humidity comprised between (30-45%). The load  $F$  is applied on the opposite side in order to obtain the rotating bending fatigue conditions. Once the specimen is broken, the shutdown sensor stopped the machine automatically. The number of cycle to failure is then counted and displayed on the digital control. Bending moment values are used to determine the alternating bending stress, which can be determined directly from equation (3.7). Fatigue testing machine and components diagram of this machine is shown in figure (3.21 (a). (b)).

The bending moment is calculated with the load and the lever arm as follows [62].

$$M = F \cdot L \quad \dots (3.3)$$

By using the section modulus of the sample, it is possible to calculate the alternating stress amplitude.

$$\sigma_f = \frac{M}{j} \quad \dots(3.4)$$

$$j = \frac{\pi d^3}{32} \quad \dots(3.5)$$

$$\sigma_f = \frac{32FL}{\pi d^3} \quad \dots(3.6)$$

$$\sigma_f \approx 2F \quad \dots (3.7)$$

**Where:**

$\sigma_f$  : Maximum alternating stress (MPa)

F : Applied load (N)

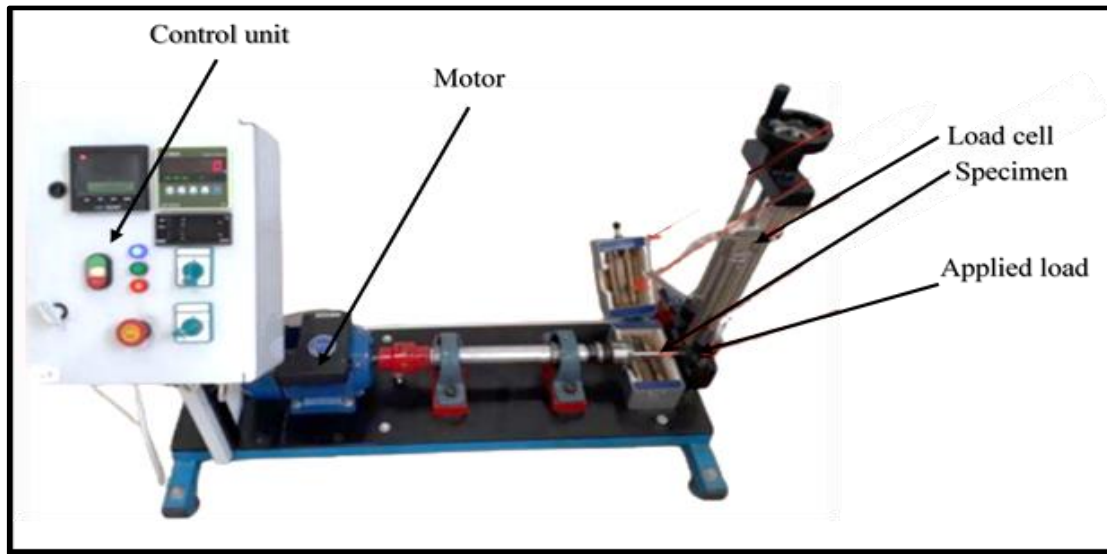
L : Bending arm =  $106 \pm 0.1$  mm

d : Diameter of the specimen =  $8 \pm 0.1$  mm

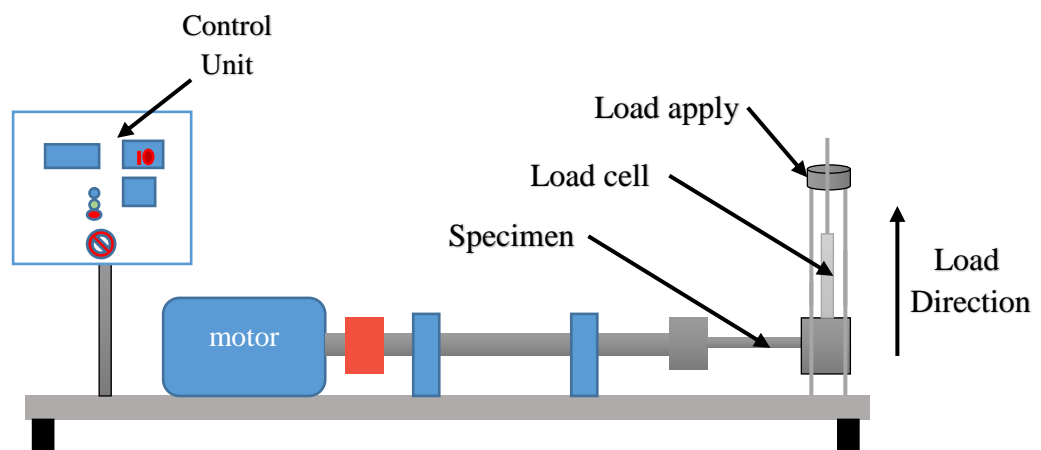
M : Bending moment (N.mm)

j: = Section modulus of the sample

Figure (3.22) show the comparison of the device on which the current work is carried out with the device (GUNT HUMBURG WP 140) made by (G.U.N.T Gerätebau GmbH company, Germany) as shown in figure (3.23). It is available at the labs of Department of Mechanical Engineering - college of Engineering at University of Kufa. The aim is to calibrate the device and know the error ratio. The maximum overall average error is 5.7%. This percentage is due to several reasons Machine accuracy, vibration generated during operation and load cell (S-type (SS 300 model).



(a)



(b)

Figure (3.21): (a) Machine of rotating bending fatigue test.  
(b) Components of test machine.

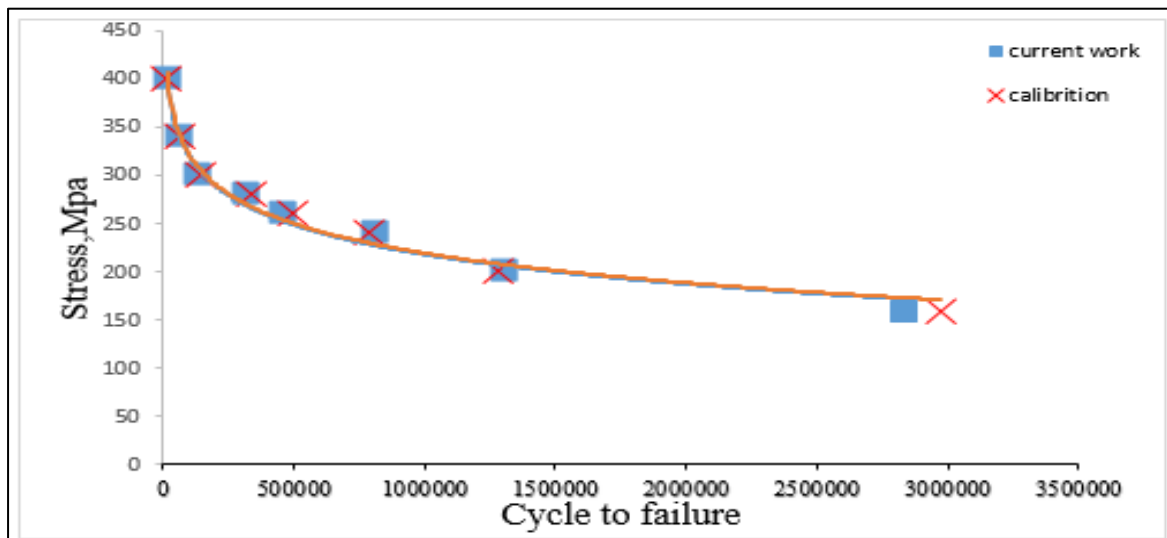
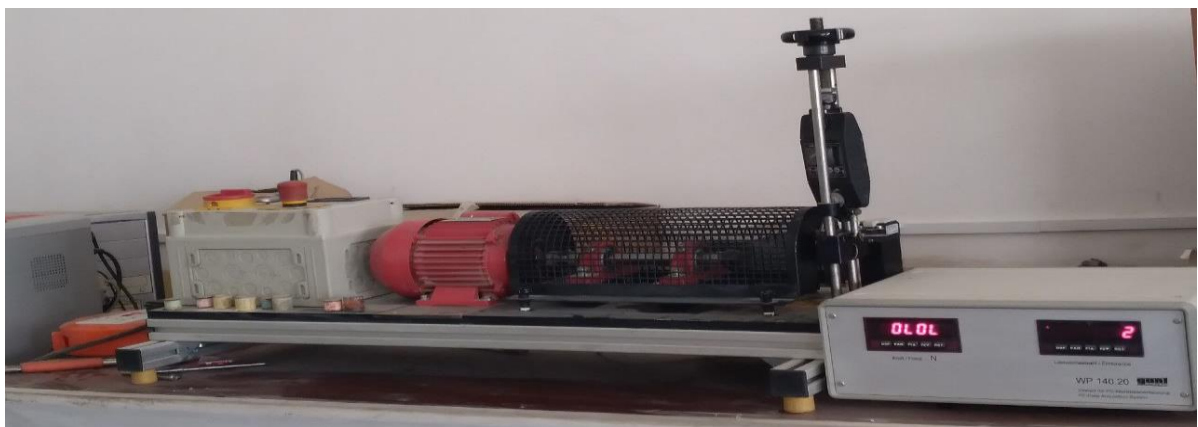
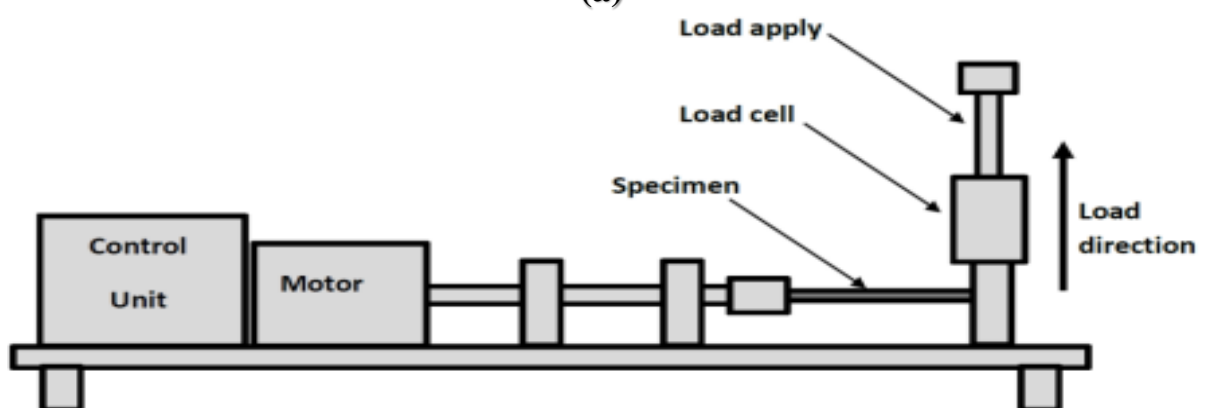


Figure (3.22): Comparison between the present work device and the device (GUNT HAMBURG WP 140).



(a)



(b)

Figure (3.23): (a) fatigue test device. (b) Components of test machine.

# ***Chapter Four***

## ***Results and***

## ***Discussions***

## 4.1 Introduction

This chapter contains the results of experimental work related to the effect of surface heat treatments, soaking time and notch on the fatigue properties of low carbon steel, in addition to microstructure examination.

The experimental results include the results of mechanical test (tensile, hardness and impact tests) and S-N curves of rotating bending fatigue tests for the different types of specimens, at room temperature.

The S-N diagrams are plotted and discussed for each type of specimens to investigate the fatigue behavior.

## 4.2 Mechanical Test Results

The results presented in this section illustrate the tensile, hardness, and impact tests, all of which are performed at room temperature.

### 4.2.1 Tensile Test Results

Mechanical parameters obtained from a tensile test at room temperature are presented in Table (4.1), with the average value of the three readings recorded for each property. Three specimens are tested for raw material.

Table (4.1): Tensile test results for low carbon steel specimens before treatment.

Material	Property	Specimen No.			Average Value
		1	2	3	
LCS	Yield Strength (MPa)	383	387	385	385
	Ultimate Strength (MPa)	528	530	532	530
	Percentage Elongation	21	22	20	21

Table (4.2) presents results of tensile test after treatment by carburizing and carbonitriding. The values which recorded after hardening increased due to increase hardness of outer surface and keeps the core as received.

Table (4.2): Tensile test results after surface treatments.

Surface treatment	Time (h)	Yield Strength (MPa)	Ultimate Strength (MPa)	Percentage Elongation	Improve Yield Strength%	improve Ultimate Strength%
As received	---	385	530	21	-----	-----
Carburizing	2	634	801	16.12	64	51
	4	907	1166	14.6	135	120
	6	1044	1211	11.09	171	128
Carbonitrid	0.5	702	875	17.15	82	65
	1	896	1032	15	132	94
	1.5	991	1390	13.2	157	162

#### 4.2.2 Hardness Test

Table (4.3) shows the results of hardness test for St44-2 DIN 17100 after and before surface treatment.

It is observed that the hardness of the samples was increases by the heat treatment process. The hardness increases due to formation of martensite phase after quenching (quick cooling) from austenite phase because carbon atoms which impeds into the surface do not have time to diffuse out of the crystal structure [63]. Surface heat treatments temperature and time are also affect the hardness of specimen. An increase in the surface hardness of both solid carburizing and carbonitrided is observed with increasing time due to the chemical reaction, where the diffusion of carbon atoms in the surface towards the core occurs forming iron carbide during the carbonization process. As for carbonitriding, both carbon and nitrogen diffuse in the surface towards the core, forming iron nitride and iron carbide on the surface to a certain depth. Figure (4.1) presents the relation between surface hardness and immersion time for each hardening process.

Highest hardness value achieved 1082.68 HV and 1644.62 HV during pack carburizing and carbonitriding, respectively at time 6 and 1.5 hours. Table (4.3) shows the effect of surface heat treatment by pack (solid) carburizing and carbonitrid at different soaking time. It is concluded that in pack carburizing process, surface hardness improves about 239% , 254% and 270% for 2h,4h and 6h respectively while in cyaniding process, it improves about 420%,429% and461% with time 0.5h,1h and 1.5h.

Table (4.3): Hardness test results of low carbon steel.

Surface treatments	Time/h	No. specimens			Average Value	Improve hardness %
		Vickers ,HV				
		1	2	3		
As received	---	291	293	295	293	----
carburizing	2	992.21	996.1	997.51	995.27	239
	4	1027.9	1034.23	1039.65	1033.92	254
	6	1079.02	1083.87	1085.15	1082.68	270
carbonitriding	0.5	1511	1529.33	1533.25	1524.52	420
	1	1543.34	1547.61	1551.11	1547.35	429
	1.5	1610.9	1655.7	1667.28	1644.62	461

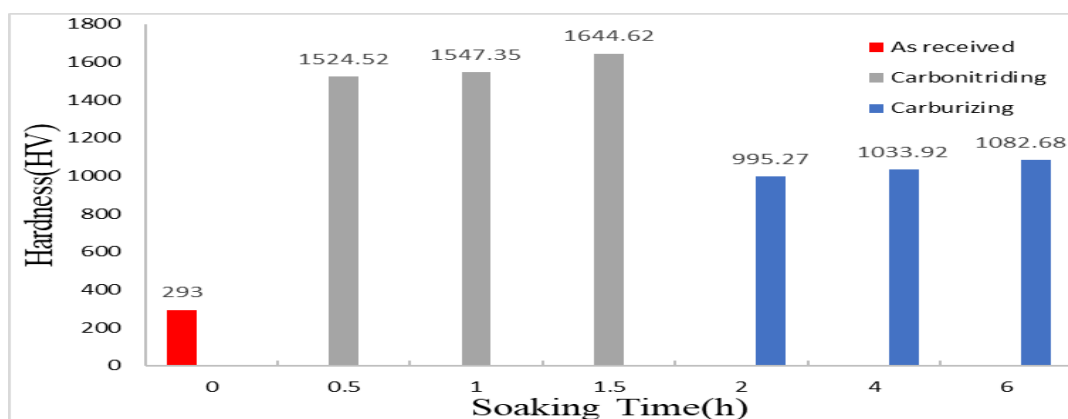


Figure (4.1): Relationship between surface hardness and soaking time.

#### 4.2.3 Case Depth (Depth of Hardness)

The hardening layer was measured using a Vickers hardness tester from the surface of the metal towards the core, at each point being measured, three readings are taken on the same line and the final average of the

readings is taken to obtain the accuracy. During the pack carburizing (P.C) process, at a temperature of 925 °C and a time (2, 4 and 6) hours, the depth of penetration of carbon atoms into the steel surface is (0.77mm, 1.25mm and 1.58mm) respectively. While the carbonitriding process (C.N) achieved a depth of hardness (0.33mm, 0.59mm and 0.84mm) at temperature of 800°C during a time of (0.5, 1, and 1.5) hour. Figures (4.2(a&b)) illustrate the relationship between hardness and the distance from the surface to the core after hardening operations. Figure (4.3) show the relationship between depth of hardened layer with soaking time for St44-2 DIN 17100.

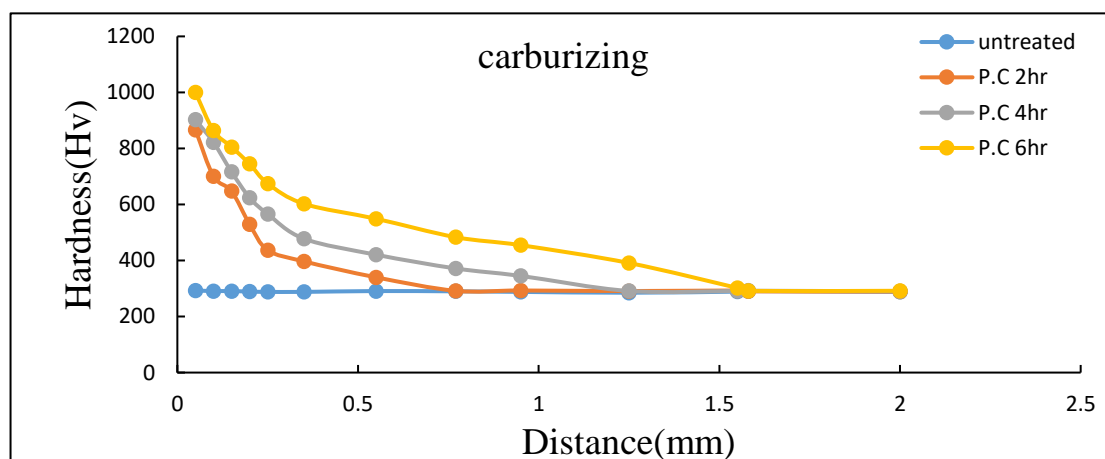


Figure (4.2 (a)): The relationship between hardness of specimens carburized and the distance from surface to core.

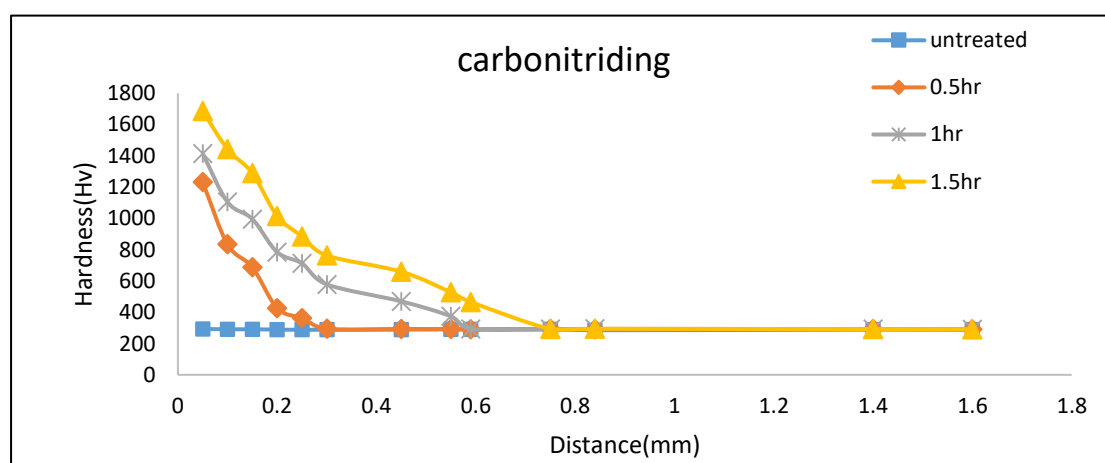


Figure (4.2 (b)): The relationship between hardness of specimen's carbonitrid and the distance from surface to core.

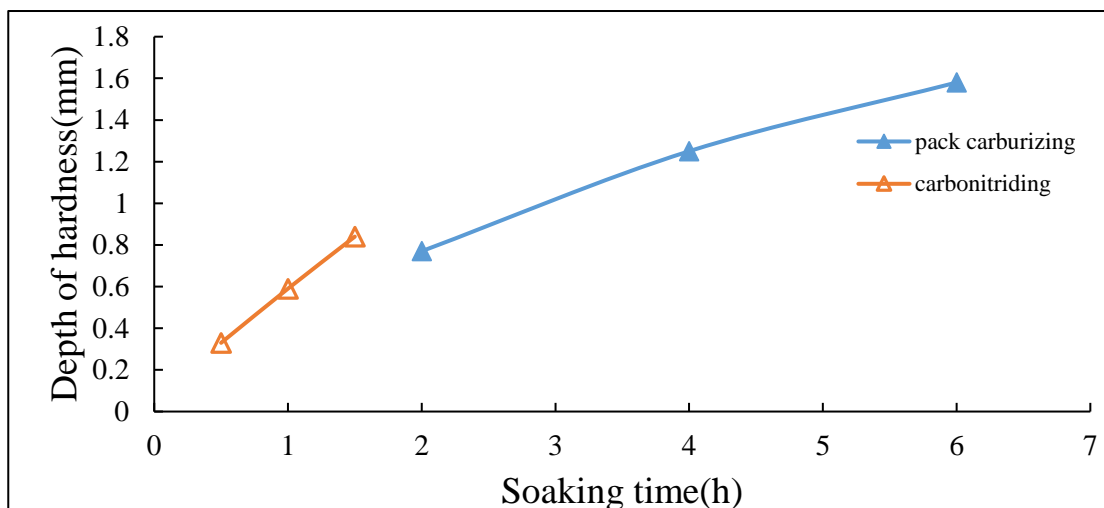


Figure (4.3): Relationship between depth of hardness and soaking time.

#### 4.2.4 Impact Test

In this test, izod method is used. Table (4.4) shows the results of the impact test at room temperature for material Untreated and treated, three specimens are tested each case. In this table, the energy is absorbed which is resulted directly from the test increase with increasing soaking time. This improvement is due to surface treatment by carburizing and carbonitriding. Maximum value for energy absorbed is 39J for St44-2 DIN 17100 choosing at the treatment by using cyanide salt bath due to diffusing carbon and nitrogen, while maximum value at carburizing is 37.3J due to diffusing only atoms of carbon. Best enhancement for energy absorbed was at carbonitred increased by 42% at time 1.5 hour while at pack carburizing achieved percentage improvement 36% at time 6 hours .

**Table (4.4):** Impact test result.

Surface treatment	Time (h)	Energy absorbed U <sub>s</sub> (Joule)				Impact Strength G <sub>c</sub> (KJ/m <sup>2</sup> )	improve Energy absorbed%
		Specimen No			Average value		
		1	2	3			
As received	---	27	29	26	27.33	273.3	-----
Carburizing	2	28	33	32	31	310	13
	4	34	36	35	35	350	28
	6	37	38	37	37.3	373	36
Carbonitriding (cyaniding)	0.5	35	33	37	35	350	28
	1	37	38	35	36.6	366	33
	1.5	39	40	38	39	390	42

### 4.3 Experimental Results of Fatigue Test under Constant Amplitude Stress for V-Notch Low Carbon Steel after Surface Hardness

This section deals with the results of the group that represents specimens that have v-notch with a depth of 1mm and an angle of 45° degrees have been treated by surface heat treatments (pack carburizing (P.C) and carbonitriding (C.N)). Fatigue tests are performed for all specimens that treated. Twenty one specimens are used for each soaking time in this section. The results are graphically recorded in the form of S-N, curves. These curves are constructed by curve fitting of the experimental data of fatigue tests.

Figures (4.4) and (4.5) show the S-N curves of carburizing and carbonitriding respectively. These figures show that fatigue behavior after surface thermal treatments and the effect of soaking time. It can be noted that, a significant change in fatigue behavior after surface hardening with pack carburizing and carbonitriding has been observed. It is observed that the increase in soaking time (Samples retention time in the carbon medium inside the furnace at high temperatures) leads to an improvement in the

fatigue performance of each hardening process, whether by the method of pack carburizing or carbonitriding. The improvement in fatigue performance (life and strength) of the surface-hardened samples comes by using surface heat treatments that create a protective layer (hardened layer). This layer resulted from diffusions of carbon or carbon and nitrogen atoms together inside the metal surface due to the difference in concentrations from of high concentrations (carbon medium) towards low concentrations (Steel surface that low carbon content) [59], where the surface of the steel becomes smoother and has a higher hardness, which leads to delay crack initiation and growth.

Tables (4.5) , (4.6) , and (4.7) present the experimental results of bending fatigue load at different level of the testing surface heat treatments, where the specimen life is taken from the average value of three repeated test.

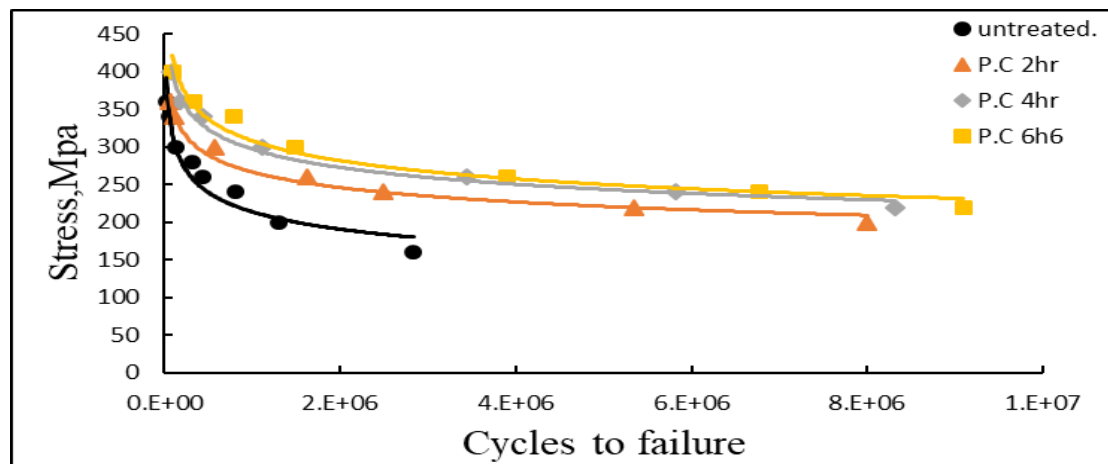


Figure (4.4): Comparison of S.N curve between pack carburizing with untreated samples at different time.

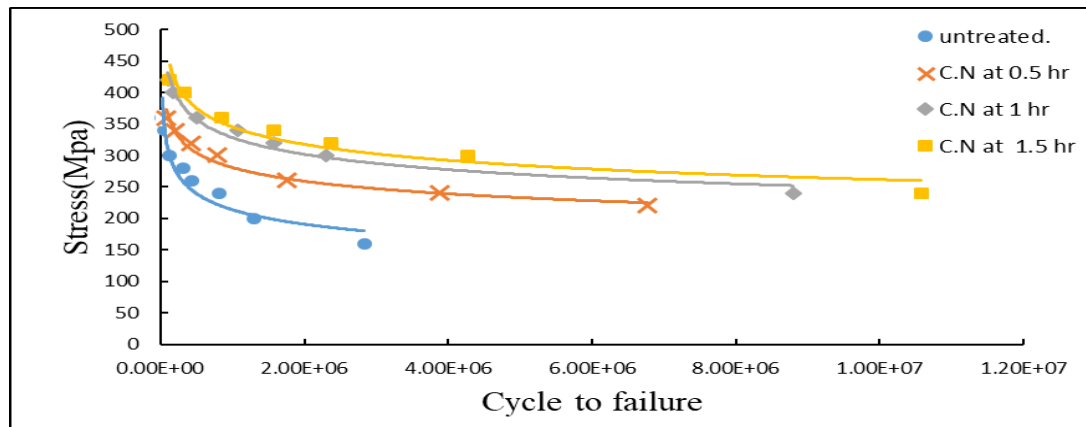


Figure (4.5): Comparison of S.N curve between carbonitriding with untreated samples at different time.

**Table (4.5):** Results of fatigue stresses with life of specimens experimentally for carburizing at time 4h and 6h.

Stress(Mpa)	Life of Specimens (Cycles)	
	Time(h)	
	4h	6h
400	77321	89318
360	183038	323604
340	434562	789532
300	1119472	1494698
260	3445652	3907925
240	5814921	6778768
220	8318225	9095845

**Table (4.6):** Results of fatigue stresses with life of specimens experimentally for carbonitriding at time 1h and 1.5h.

Stress(Mpa)	Life of Specimens (Cycles)	
	Time(h)	
	1h	1.5h
420	105879	132359
400	175968	324796
360	505487	852715
340	1067562	1582471
320	1584314	2775724
300	3304556	4279637
240	8799378	10173851

**Table (4.7):** Results of fatigue stresses with life of specimens experimentally for carbonitriding and Pack Carburizing at time 1h and 1.5h respectively.

Stress(Mpa)	Life of Specimens (Cycles)	
	Carbonitrid	Pack Carburizing
	Time(h)	Time(h)
	0.5h	2h
360	86746	61318
340	197433	110635
320	426785	275927
300	785543	568328
260	1694657	1431895
240	3878576	2398344
220	6764086	5510451

### 4.3.1 Fatigue Strength and S-N Equation

Tables (4.8) and (4.9) represent the experimental fatigue strength (fatigue limit) and the experimental S-N equations (Basquin's equations) for Pack carburizing and carbonitriding (cyaniding) respectively. The Basquin's equation is a power law regression and can be given by equation 4.1 [64].

$$\sigma = a N^b \quad \dots (4.1)$$

Observe that these equations have reasonably high correlation coefficients, indicating that the power law formula (Basquin's formula) adequately explains the experimental results. Since the correlation coefficient is a hand measure of the goodness of fit [58].

It is noted that the maximum fatigue strength at  $10^6$  cycles is 310.436MPa and 347.594MPa for Pack carburizing at temperature (925°C) and carbonitriding (cyaniding) respectively with time (6 and 1.5 hours), and the minimum fatigue strength at  $10^6$  cycles is 265.282MPa and 281.881

MPa for Pack carburizing at temperature (925°C) and carbonitriding respectively with time (2 and 0.5 hours).

Thus, it can be observed that the fatigue strength of the selected material increasing with increasing in soaking time, due to the diffusion of more carbon atoms through the surface at a certain depth towards the core, where carbon with iron forms iron carbide  $\text{Fe}_3\text{C}$  (cementite) on the surface of the metal responsible for the high resistance of steel to stresses, and the nitrogen atom resulting from the carbonitrid process is characterized by its small size, which enables it to penetrate to greater distances Inside the surface of the mineral with deformation of the crystal structure. Thus, these atoms of carbon and nitrogen fill the voids and scratches and obstruct the initiation and growth of cracks.

Generally, the fatigue strength of a material is proportional to its tensile strength, so materials with a high tensile ultimate strength possess a high fatigue strength. The ratio of fatigue strength to tensile ultimate strength ( $\frac{\sigma_e}{\sigma_{ult}}$ ) (fatigue ratio) increased with an increase in time of surface hardening treatment (heat treatment chemical).

**Table (4.8):** Results S-N curve equation, and fatigue strength  $\sigma_e$  at  $10^6$  cycles function to (Pack carburizing) at temp 925°C.

Time(h)	S-N equation	Fatigue strength $\sigma_e(\text{MPa})$	$\frac{\sigma_e}{\sigma_{ult}}$	Correlation coefficient $R^2$
Un-treated	$\sigma_e = 2041.3 N^{-0.163}$	214.736	0.405	0.9264
2	$\sigma_e = 1335.7 N^{-0.117}$	265.282	0.5005	0.9776
4	$\sigma_e = 1634.1 N^{-0.123}$	298.729	0.553	0.9862
6	$\sigma_e = 1844.9 N^{-0.129}$	310.436	0.585	0.9641

**Table (4.9):** Results S-N curve equation and fatigue strength  $\sigma_e$  at  $10^6$  cycles function to (carbonitriding).

Time(h)	S-N equation	Fatigue strength $\sigma_e$ (MPa)	$\frac{\sigma_e}{\sigma_{ult}}$	Correlation coefficient $R^2$
Un-treated	$\sigma_e = 2041.3N^{-0.163}$	214.736	0.405	0.9264
0.5	$\sigma_e = 1399.8N^{-0.116}$	281.881	0.531	0.9789
1	$\sigma_e = 1765.2N^{-0.122}$	327.185	0.617	0.9706
1.5	$\sigma_e = 1824.2N^{-0.12}$	347.594	0.655	0.9368

Figures (4.6) and (4.7) show the relation between fatigue strength with time and depth of hardness after using Pack carburizing, and carbonitriding (cyaniding) for LCS. It can be observed that the fatigue strength increases with an increase in time, this is due to the diffusion of carbon or carbon and nitrogen together inside the metal surface, which leads to saturation of the steel surface because of the formation of carbides and nitrides ( $Fe_3C$ , and  $Fe_4N$ ). The surface hardness provides an improvement in the fatigue strength because the hard layer prevents plastic flow.

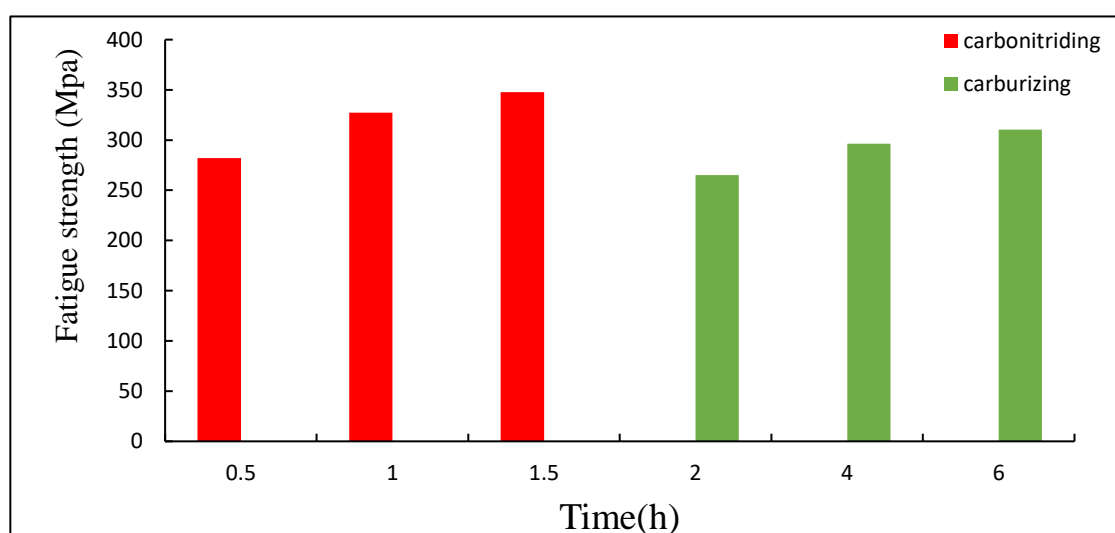


Figure (4.6): Variation in fatigue strength with time.

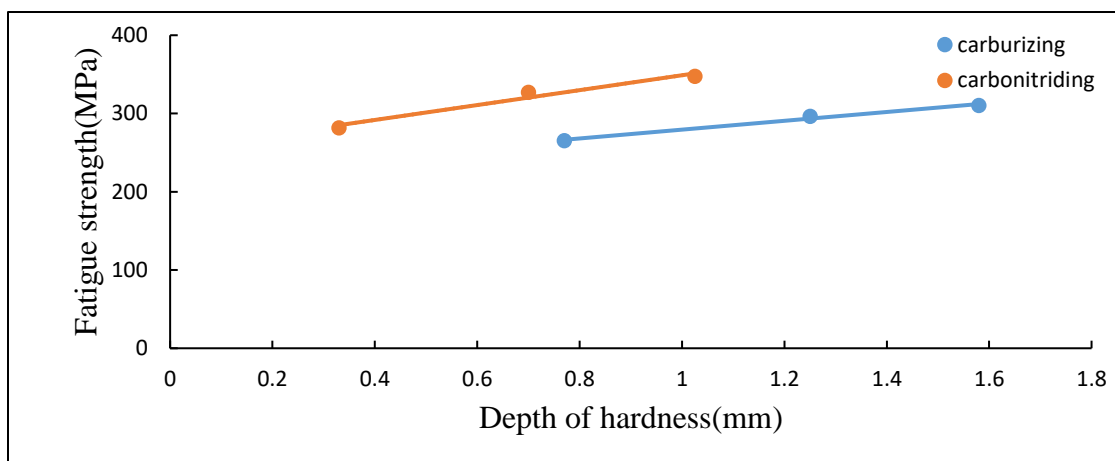


Figure (4.7): Variation in fatigue strength with Depth of hardness.

#### 4.4 Effect of Case Hardened on the Fatigue Properties for V-Notch Low Carbon Steel.

Surface treatments (pack carburizing (P.C) and carbonitriding (C.N)) significantly affect the mechanical properties of steel due to the increase of the hardness of the surface layer at different depths towards the core. This increase is created by adsorption of carbon or a mixture of nitrogen and carbon together, and through diffusion a concentration gradient is created. When the treatment is carried out by carbonization using 90% wood charcoal and 10% barium carbonate, a constant temperature of 925 °C and a variable time of 2, 4 and 6 hours, we notice an increase in the depth of carbonation from 0.7 mm to 1.58 mm, and the hardness increases with the increase in the time the sample is kept inside the furnace from 995.27 HV to 1082.68 HV due to the diffusion of carbon atoms towards the surface of the steel, forming solid  $\text{Fe}_3\text{C}$  cementite, where the concentration of carbon atoms diffusion decreases as it moves towards the core.

While, when performing carbonitriding (molten salt bath) with a chemical composition. At a temperature of 800 °C and with a variable time,

also observed an increase in the depth of the surface layer towards the core, and the hardness also increases with increasing time. Due to the diffusion of carbon and nitrogen atoms together towards the surface of the steel, forming iron carbide  $\text{Fe}_3\text{C}$  and iron nitride  $\text{Fe}_4\text{N}$  (at high temperatures), where the concentration of diffusion decreases when approaching towards the core. As a result of these treatments on the surface of the selected metal, the fatigue life and hardness are improved due to the formation of the surface layer the hard layer prevents plastic flow. It also improved the surface of the steel, giving it a smooth texture and resistance to fatigue due to the formation of martensite upon rapid cooling and reference.

Figures (4.8) to (4.10) show the S-N Curve curves for the surface heat treatments of the selected metal, where the results of carbonitride are compared with carbonization according to time. It is observed that the best improvement in the (S-N) curve is at a time of 1.5 hours during the cyanide process and also in the carbonation process at a time of 6 hours as shown in figure (4.11).

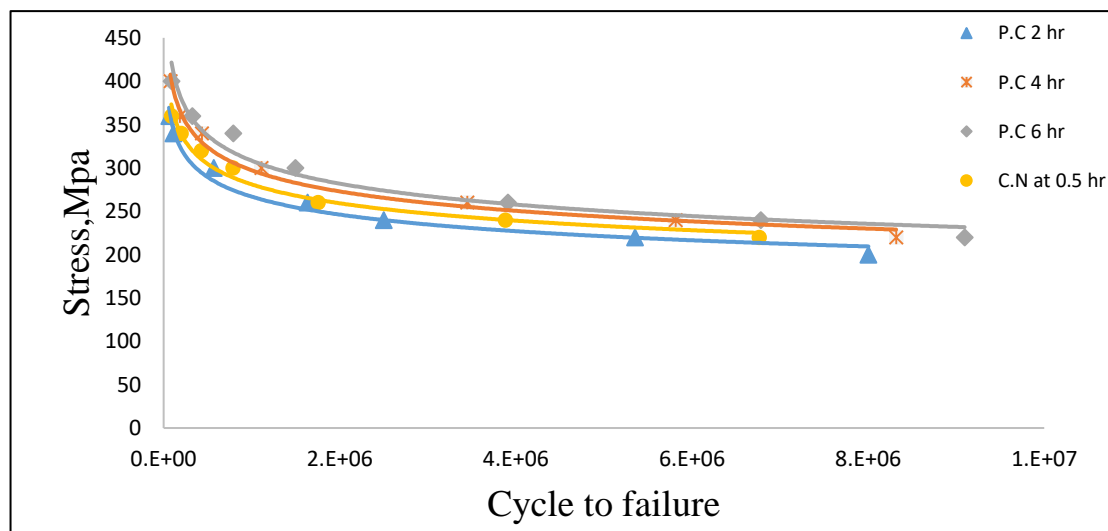
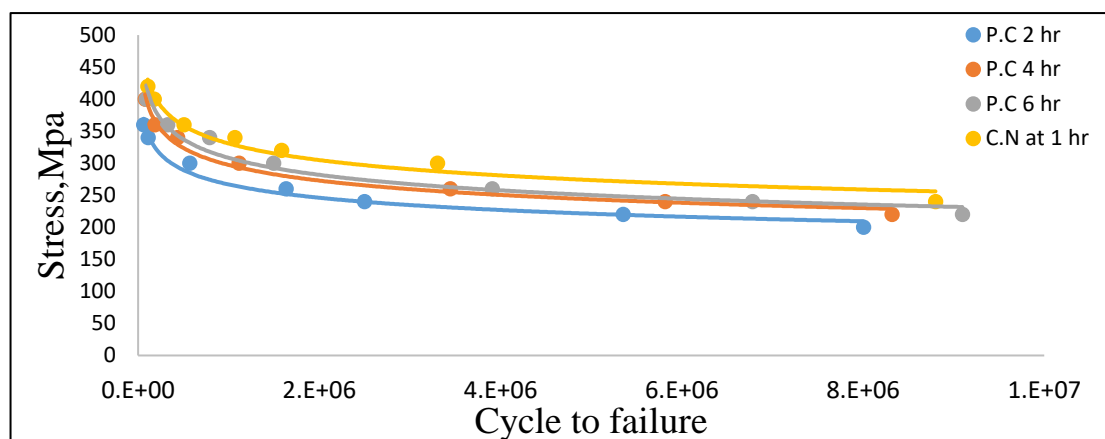
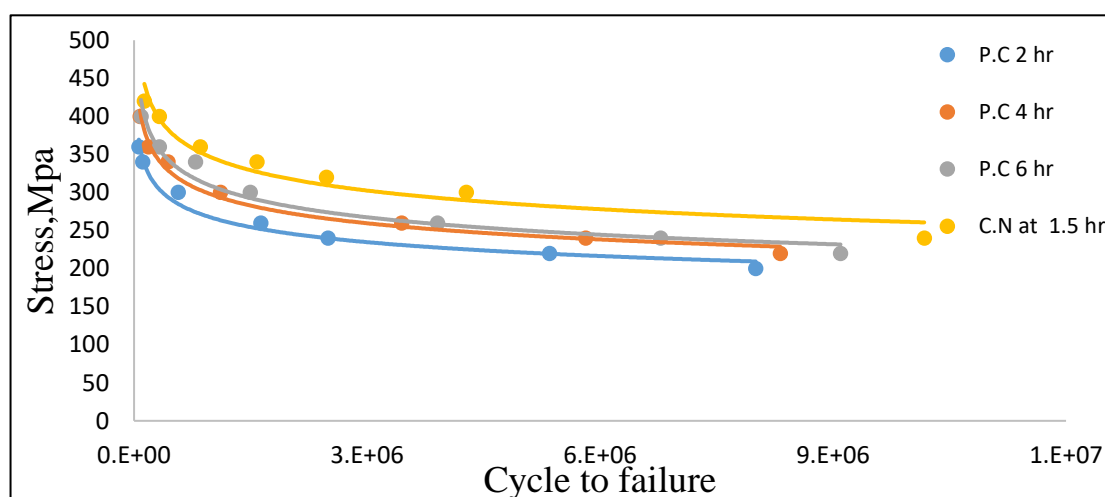


Figure (4.8): Comparison S-N curve of specimen on carbonitriding at temperature  $800^{\circ}\text{C}$  and soaking time 0.5 hour with pack carburizing at different time.



Figures (4.9): Comparison S-N curve of specimen on carbonitriding at temperature 800°C and soaking time 1 hour with pack carburizing at different time.



Figures (4.10): Comparison S-N curve of specimen on carbonitriding at temperature 800°C and soaking time 1.5 hour with pack carburizing at different time.

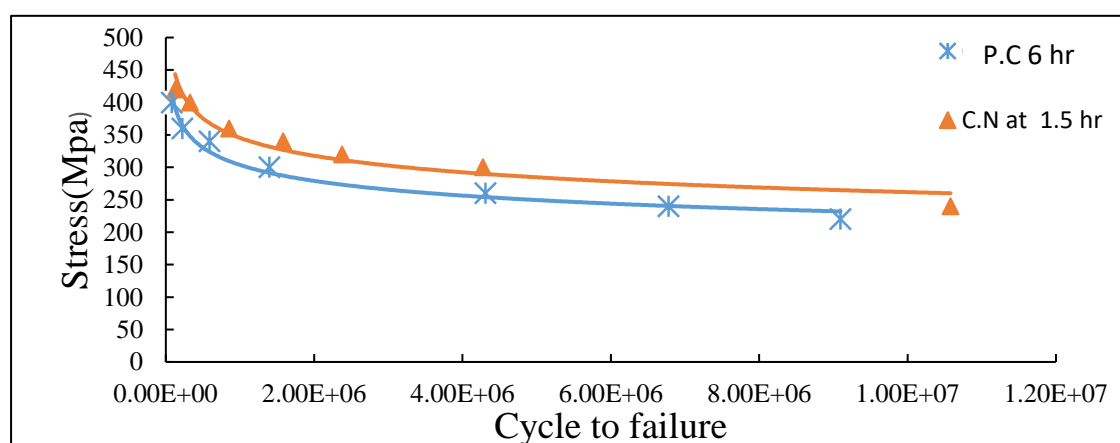


Figure (4.11): Comparison between carbonitrid (1.5h) with pack carburizing (6h).

#### 4.4.1 Fatigue Strength Improvement Factor (FSIF)

Surface hardness by pack (solid) carburizing and carbonitrid (cyaniding) process significantly alters the fatigue properties. So, increasing the soaking time (saturate the surface of the steel with carbon or carbon and nitrogen together) leads to an increase in Fatigue Strength. The fatigue strength improvement factor (FSIF) can be calculated from the flow equation 4.2 [65].

$$\text{FSIF}\% = \frac{\sigma_e - \sigma_{e \text{ ref}}}{\sigma_{e \text{ ref}}} \times 100 \% \quad \dots (4.2)$$

Where,  $\sigma_e$  is the fatigue strength at  $10^6$  cycles for surface hardened steel,  $\sigma_{e \text{ ref}}$  is the fatigue strength at  $10^6$  cycles of reference material which it un-treated specimen, has the smallest fatigue strength compared to the treated samples used. Table (4.10) shows the Percentage Fatigue Strength Improvement Factor for different surface hardening at different soaking time.

**Table (4.10):** Percentage of Fatigue Strength Improvement Factor (FSIF %) for pack carburizing and carbonitriding at different time.

Surface treatment	Time(h)	FSIF%
carburizing	2	23.53
	4	37.95
	6	44.56
Carbonitrid (cyaniding)	0.5	31.26
	1	52.36
	1.5	61.87

Figure (4.12) shows the effect of surface heat treatment on FSIF% by pack (solid) carburizing and carbonitrid at different soaking time. the Figure shows that the FSIF% increase with an increase in time, it is concluded that in pack carburizing process, FSIF% increases about 23.53%, 37.95% and

44.56% for 2h,4h and 6h respectively while in cyaniding process increases about 31.26%,52.36% and 61.87% with time 0.5 h,1h and 1.5h.

Also, it can be seen from the figure the increase of the time soaking pack carburizing and carbonitriding leads to an increase in the (FSIF%). It is concluded that the maximum improvement percentage of fatigue strength of (44.56%) for carburizing , (61.87%) for carbonitriding specimen.

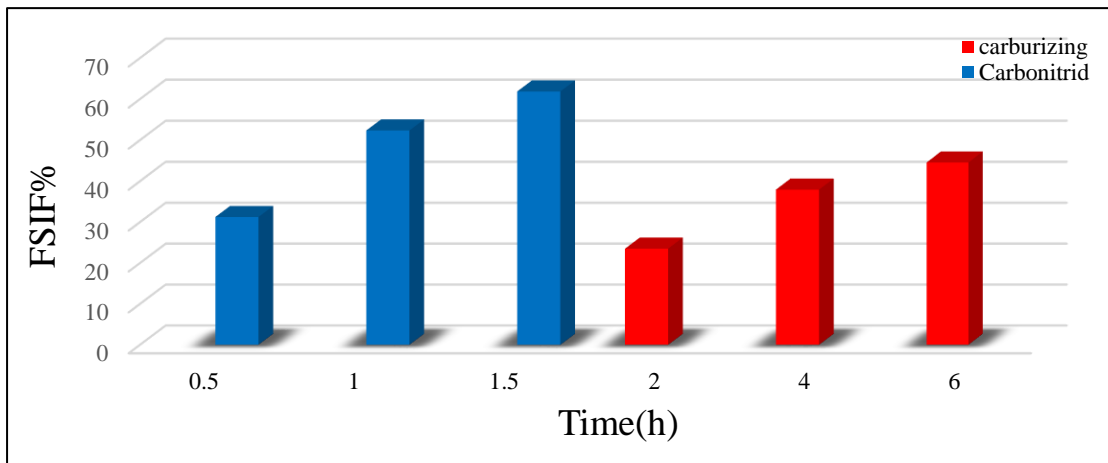


Figure (4.12): Fatigue Strength Improvement Factor for different time at carburizing and carbonitrid.

#### 4.4.2 Fatigue Life Improvement Factor (FLIF)

The Fatigue Life Improvement Factor (FLIF) can be calculated from the following equation

$$FLIF\% = \frac{\sum | \log N_f - \log N_{f ref} |}{\sum \log N_{f ref}} \quad \dots (4.3)$$

Where,  $N_f$  = number of failure cycles of the surface-hardened metal,  $N_{f ref}$  = number of failure cycles of the (un-treated) reference material that has the lowest number of cycles to failure compared to surface treated samples. Table (4.11) shows the Percentage Fatigue Life Improvement Factor for surface heat treatments at different time. It was concluded that the maximum improvement percentage of Fatigue Life of (20.2%) for

carbonitriding at time 1.5 hour, (15.9%) for pack carburizing specimen with time 6 hour, and the minimum fatigue life at time 2 hour is (8.2%) for pack carburizing.

**Table (4.11):** Percentage of Fatigue life Improvement Factor (FLIF %) for pack carburizing and carbonitriding at different time.

Surface treatments	Time(h)	FLIF%
carbonitriding	0.5	11.3
	1	18.6
	1.5	20.2
carburizing	2	8.20
	4	14.3
	6	15.9

Figure (4.13) shows a comparison between the Fatigue Life Improvement Factor (FLIF %) calculated from equation (5.4) for surface heat treatments (pack carburizing and carbonitriding) at different time. It can be shown that the FLIF% increasing with increase in time soaking, such as at carbonitriding, the FLIF % increases from 11.3% to 20.2% at time 0.5 to 1.5 hours. Also at carburizing, the FLIF % increases from 8.20% to 15.9% at time (2 to 6 hours).

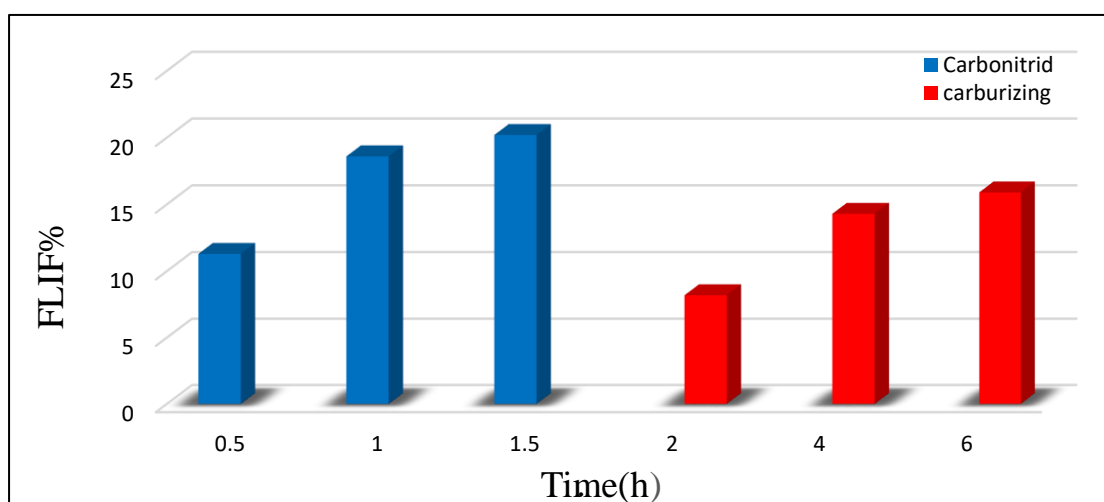


Figure (4.13): Fatigue life Improvement Factor for different time at carburizing and carbonitrid.

#### **4.5 Experimental Results for un-notched St44-DIN17100 before and after surface heat treatment**

Plain Low carbon steel has been treated by two surface heat treatment are pack carburizing at time soaking 2 hour and carbonitriding at time 0.5 hour.

Figure (4.14) represents the S-N curves of a surface heat treated metal in comparison with un-treated. This figure shows the behavior of fatigue for both carburizing and carbonitriding of plain specimen. It can be observed that a significant change in fatigue behavior after surface heat treatment.

It is observed that the best increase in fatigue behavior in the carbonitrided samples gives an increase in fatigue strength compared to the sample treated with carburizing. It is also noted that after treating the sample, there is an increase in fatigue behavior compared to the untreated sample with the same applied load.

The experimental results are correlated to obtain the equation (4-1) which can be used to predict the fatigue strength and presented in table (4.12).

The table presents that the maximum fatigue strength at  $10^6$  cycles is 348.07 MPa for carbonitriding, and the minimum fatigue strength at  $10^6$  cycles is 256.2 MPa for un-treated specimens.

Thus, it can be observed that the fatigue strength for St44-2 DIN 17100 selected improves with surface heat treatments. In general, a material's fatigue endurance strength is proportional to its tensile strength. So materials with high tensile ultimate strength possess a high fatigue strength. The ratio of fatigue strength to tensile ultimate strength ( $\frac{\sigma_e}{\sigma_{ult}}$ ) (fatigue ratio) is increased with surface hardening.

**Table (4.12):** Experimental S-N curve equation and fatigue strength  $\sigma_e$  at  $10^6$  cycles function for carburizing and carbonitriding.

Surface treatments	S-N Equation	Fatigue strength $\sigma_e$ (MPa)	$\frac{\sigma_e}{\sigma_{ult}}$	Correlation coefficient $R^2$
Un-treated	$\sigma_e = 5065N^{-0.216}$	256.2	0.483	0.984
carburizing	$\sigma_e = 2476.3N^{-0.144}$	338	0.637	0.9969
carbonitriding	$\sigma_e = 1761.7N^{-0.116}$	354.75	0.669	0.9598

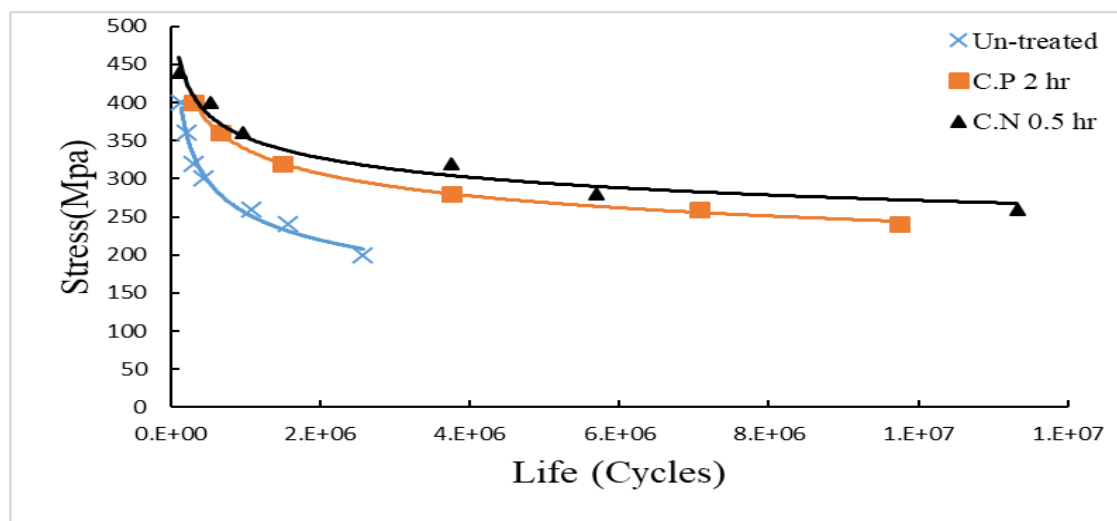


Figure (4.14): Comparison surface hardening by carburizing and carbonitriding with untreated for plain specimens.

#### 4.5.1 Fatigue Strength Improvement Factor (FSIF) for plain steel

Table (4.13) shows the Percentage Fatigue Strength Improvement Factor for pack carburizing and carbonitriding at time 2 and 0.5 hours respectively.

The Percentage Fatigue Strength Improvement Factor (FSIF) can be calculated as mentioned in equation (4.2).

**Table (4.13):** Percentage of Fatigue Strength Improvement Factor (FSIF %) For Carburizing and Carbonitriding at Time 2, 0.5 hr.

Surface treatment	FSIF %
Carburizing	31.92
Carbonitriding	38.466

From table (4.13) it is noticed that FSIF% increases after performance surface heat treatments. It is concluded that treatment by pack carburizing (P.C) for plain carbon steel, FSIF% increases about 31.92% compared with un-treated specimens. While treatment by carbonitriding (C.N), FSIF% increases about 38.466% compared with un-treated specimens. Because surface treatments give the surface of the metal smoothness in addition to forming a surface layer of different depths according to the soaking time. Heat treatments form strong carbides and nitrides that retard crack growth due to quenching in water and tempering at temperature 180°C for 2hours, so it improves the Fatigue Strength Improvement Factor.

#### 4.5.2 Fatigue Life Improvement Factor (FLIF) for plain steel

The Percentage Fatigue Strength Improvement Factor (FLIF) can be calculated as mentioned in equation (4.3).

Table (4.14) shows the Percentage Fatigue Life Improvement Factor for both surface hardening treatments.

**Table (4.14):** Percentage of Fatigue Life Improvement Factor (FLIF %) for Carburizing and Carbonitriding at Time 2, 0.5 hr.

Surface treatment	FLIF%
Carburizing	11
Carbonitriding	13

It is concluded from table (4.14) that treatment by pack carburizing (P.C) for plain carbon steel, FLIF% increases about 11% compared with un-treated specimens. While treatment by carbonitriding (C.N), FLIF% increases about 13% compared with un-treated specimens

## 4.6 Validation

The results of experimental work for the fatigue test can be compared with the experimental results obtained by the references [25, 38, and 68] for plain low carbon alloy steels at room temperature, in order to verify the results of this research, this comparison is shown in figure (4.15).

By fitting the curve to the results of the figure (4.18), the basquin's equations for the fatigue data expressed in table (4.15). Good agreement is obtained when comparing the current work with other expressions of Basquin's equations, where the error rate in fatigue strength not more than 2.92% and not less than 1%. The reason is due to the percentage of carbon in the alloying elements of the metal, the higher the carbon percentage in the steel metal lead to increase fatigue strength according to [66].

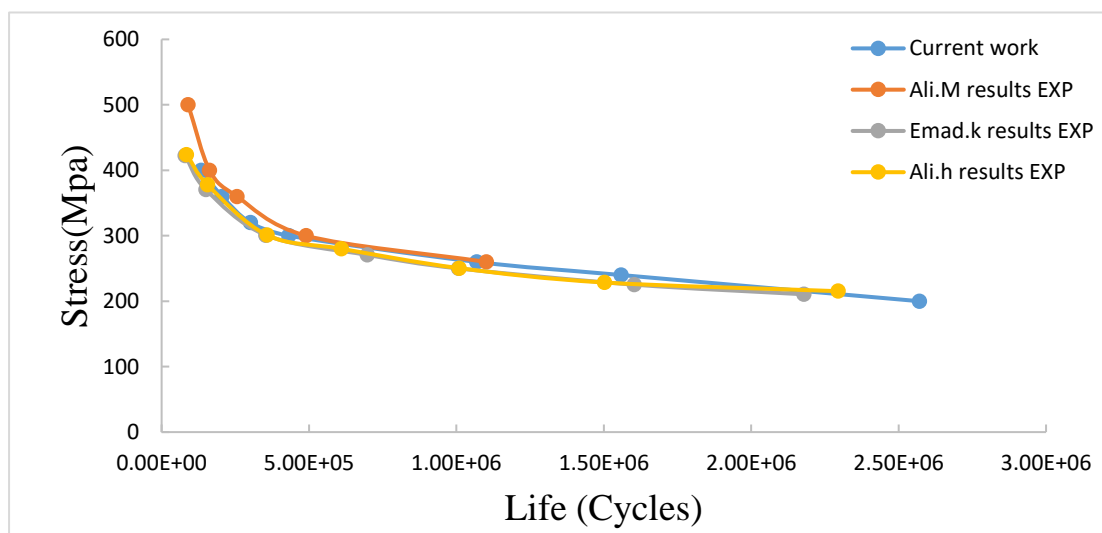


Figure (4.15): A comparison S.N curve between present results with researcher's results for plain low carbon steel without treated.

**Table (4.15):** Basquin's equations compared with available fatigue data at room temperature for the current study at  $10^6$  cycles .

Validation	S-N equation	Fatigue strength $\sigma_e$ (MPa)	Error %
Current result	$\sigma_e = 5065 N^{-0.216}$	256.20	---
Emad.k result [25]	$\sigma_e = 4111.1 N^{-0.203}$	248.86	2.86
Ali.M result [38]	$\sigma_e = 9010 N^{-0.257}$	258.65	1
Ali.H result [66]	$\sigma_e = 4463.3 N^{-0.209}$	248.7	2.92

## 4.7 Result of Microstructural

A microscopic study is conducted on samples of low -carbon steel that is purchased locally before and after heat treatment. The sample was polished using emery papers with different grades and finally polished by alumina powder in the grinding wheel. The polished samples are etched with 2 % nital (a mixture of 2 % nitric acid and 98 % alcohol). Then the microscopic structure is observed by the optical microscope.

Figure (4.16) shows microstructure for St44-2 DIN 17100 as received the light area is the ferrite, whereas the dark area is pearlite. The light area is dominant one since the carbon content is 0.22%. Figures (4. 17(a,b&c)) show the microstructure of low carbon steel whose surface has been treated with pack carburizing. It is seen that the pearlite increases along the penetration. The effect of introducing a carbon element to the material during the diffusion process of carbon interaction resulted in an increase amount of pearlite relative to the microstructure of the material as received. As an energizer, 10% barium carbonate is added to the steel to speed up the diffusion of carbon, resulting in the formation of additional pearlite structures. Figures (4.18(a,b&c )) shows the microstructure after carbonitrid. The white compound layer can be seen as a result of the

diffusion of nitrogen and carbon together, which formed  $\text{Fe}_3\text{C}$  and  $\text{Fe}_4\text{N}$  high hardness of the metal.

These results are micro photo of carbonitriding and pack carburizing process with temperature holding and time variation. The thickness of the layer shows a significant increase with the increase in time of the carbonitriding and pack carburizing. It can be seen that the microstructure carbonitriding and carburizing divided into two regions, the hardening region and the core region.

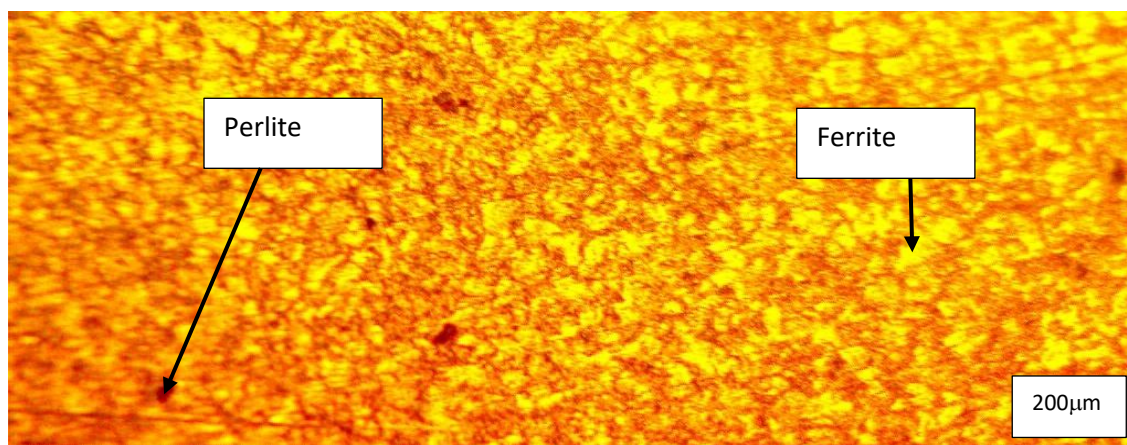
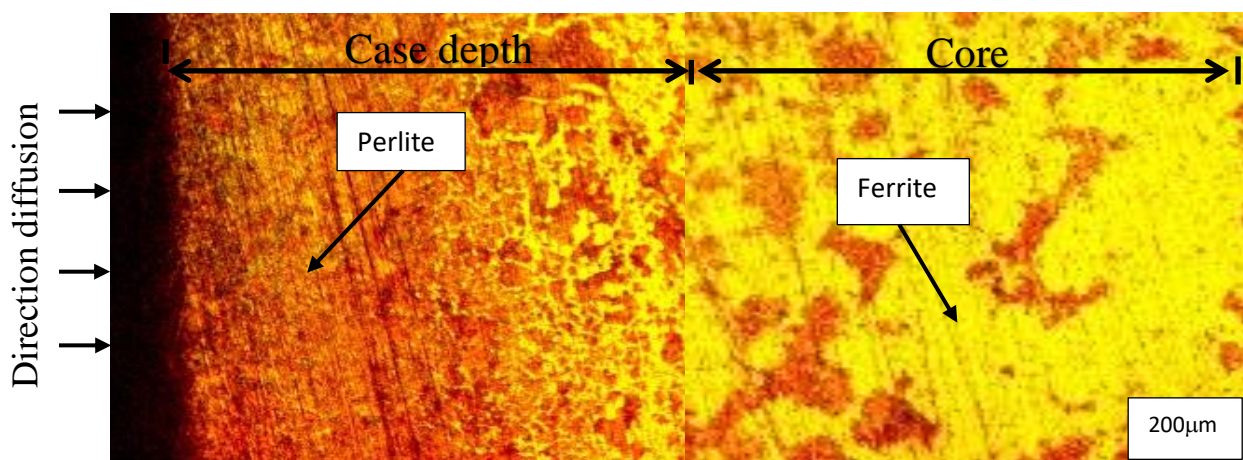
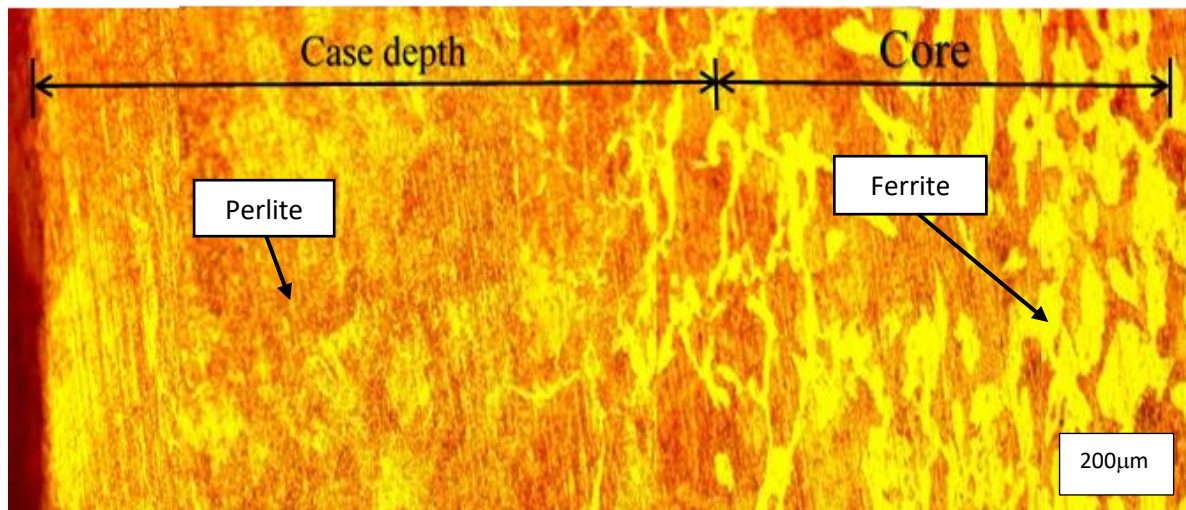


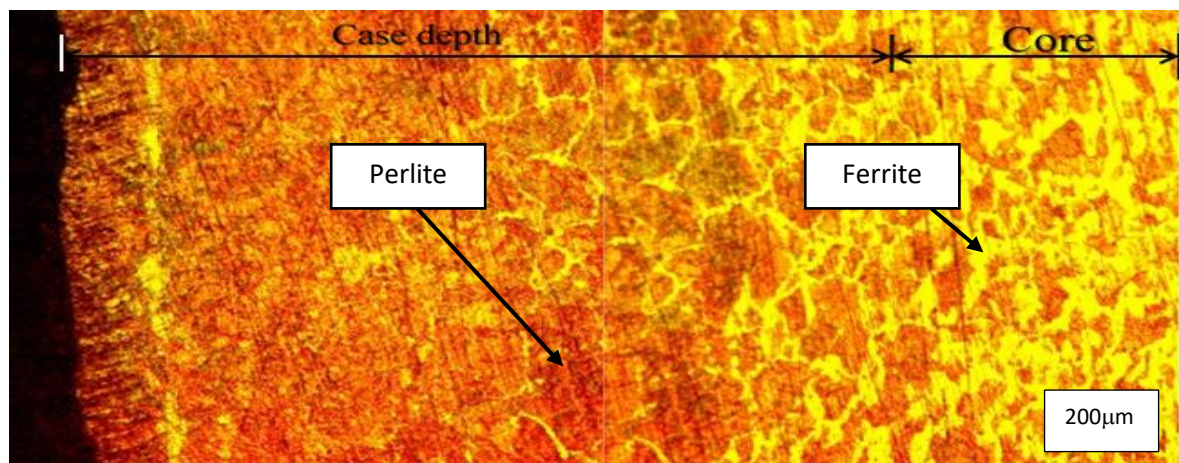
Figure (4.16): Microstructure of the raw material.



(a)

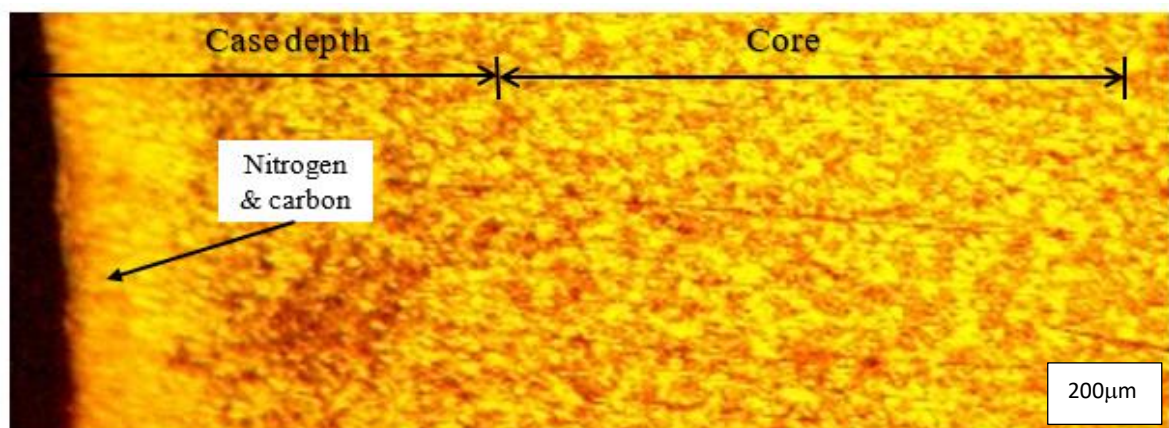


(b)

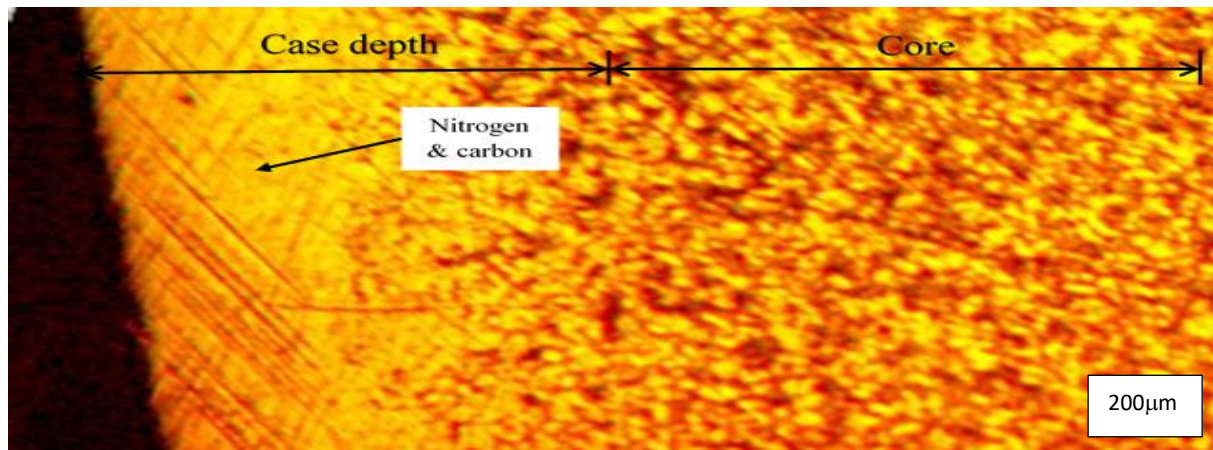


(c)

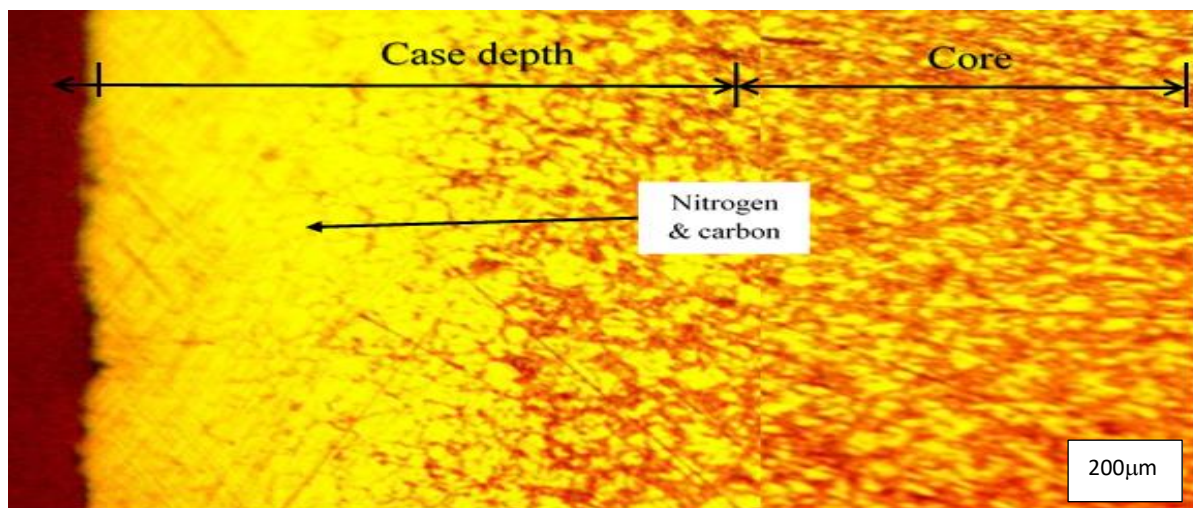
Figure (4.17): Microstructure of low carbon steel after carburizing. (a) Specimen at time 2 hour. (b) Specimen at time 4 hour. (c) Specimen at time 6hour. Magnification 100x)



(a)



(b)



(c)

Figure (4.18): Microstructure of low carbon steel after carbonitriding: (a) specimen at time 0.5 hour. (b) Specimen at time 1 hour. (c) Specimen at time 1.5 hour. Magnification 100x).

Figure (4.19) shows the macrostructure of specimens at fracture position when the notch depth is (1 mm with angle 45) and for different treatments (carburizing, carbonitriding) in addition the specimen untreated. The cross sectional area of the specimen divided into two regions. The first one is smooth region which refers to the slowly crack propagation, while the second one is the rough region which refers to the sudden fracture.

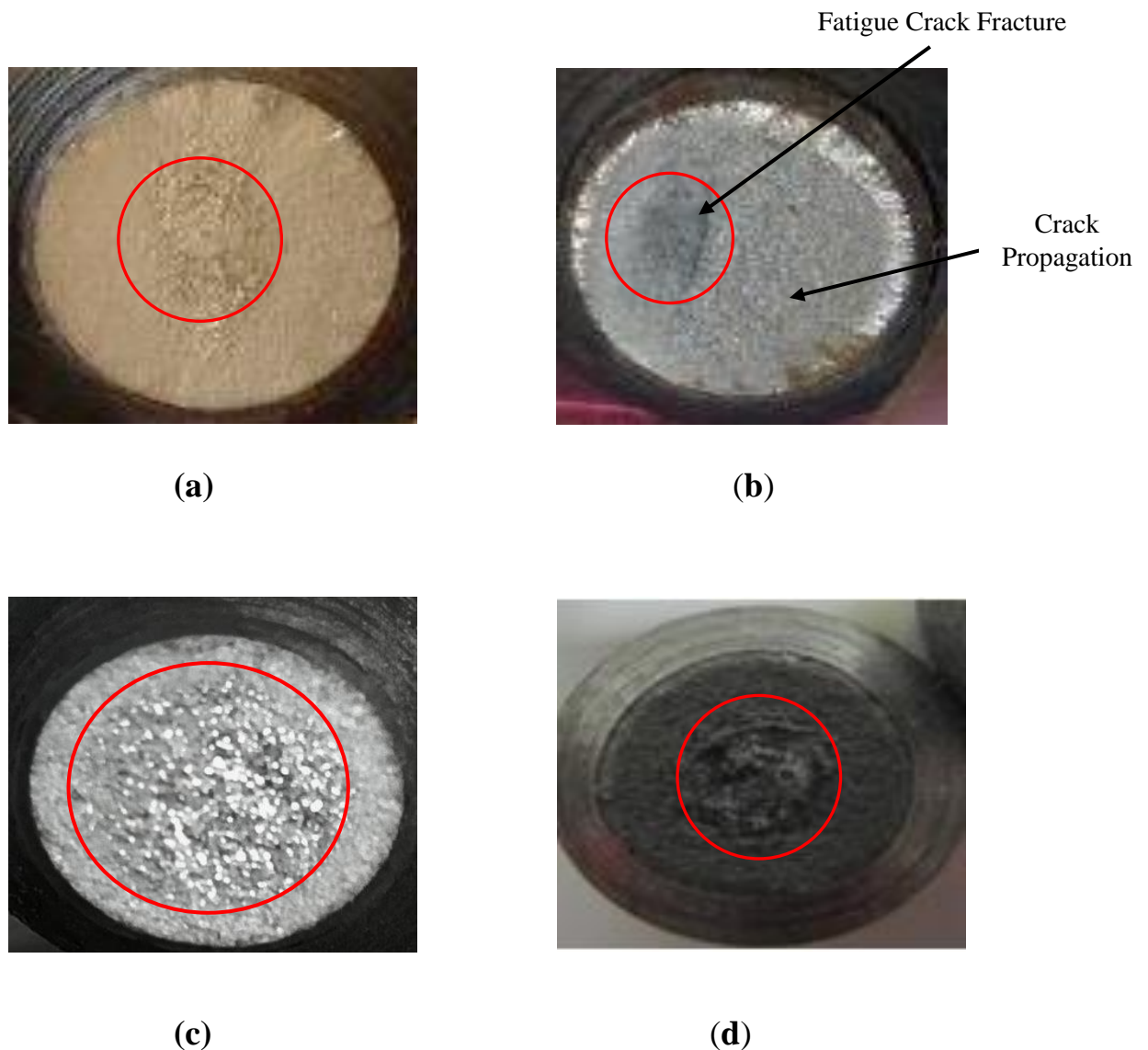


Figure (4.19): Fracture surface of a specimen: (a) with carbonitriding. (b) With pack carburizing followed by quenching. (c) With pack carburizing without quenching. (d) Specimen without treatment.

#### 4.8 Inspection of the sodium cyanide

Figure (4.20) shows the X-ray diffraction of NaCN powder. It was recorded in the range of  $2\theta$  ( $10^\circ$ - $90^\circ$ ). This pattern was compared with the standard diffraction spectrum, and it was found that all peaks were in good agreement with standard card **Monga et al.(2022)**.

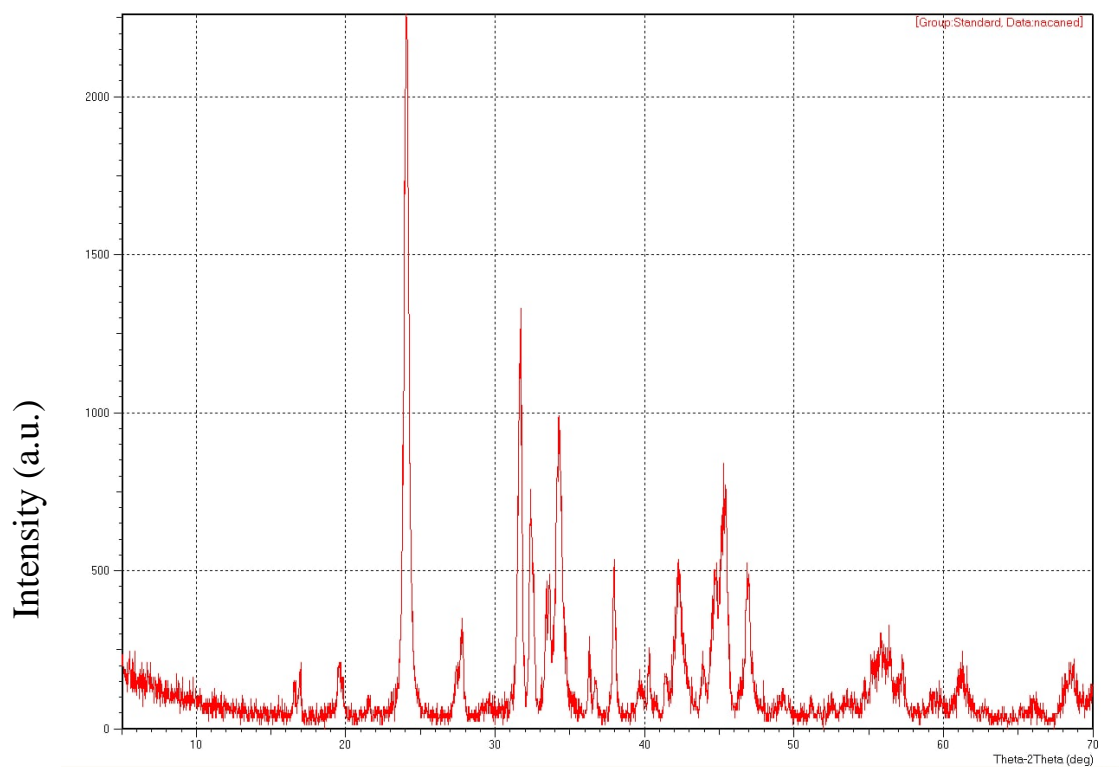


Figure (4.20) XRD pattern of sodium cyanide ball.

***Chapter Five***

***Conclusions and***

***Recommendation***

## CHAPTER FIVE

Chapter five includes the important conclusions and remarks that are obtained from the present study as well as some recommendations that may be useful for the future research work.

### 5.1 Conclusion

The results of obtained in the present work lead to the following conclusions.

1. The experimental fatigue test shows that the surface heat treatments using carburizing and carbonitriding improved the fatigue life of St44-2 DIN17100 by 11% for carburizing at time 2 hours and 13% for carbonitriding for un-notched samples.
2. The carbonitriding with soaking time of 1 hour and 1.5 hours a significant improvement in fatigue life by 18.6% and 20.2% respectively compared to the heat-treated samples using carburizing at a time of 2, 4 and 6 hours by 8.20% , 14.3% and 15.9% for V-notch St44-2.
3. The surface heat treatments increased the surface hardness of St44-2 DIN17100 by 270% and 461% for carburizing and carbonitriding comparison with the un-treated specimens.
4. The improvement percentage of fatigue strength in comparison with the un-treated specimens from two surface heat treatments process (carburizing and carbonitriding) is increased. The maximum improvement percentage of fatigue strength of (44.56%) for pack carburizing, (61.87%) for carbonitriding, for V-notch low carbon steel.
5. Due to using surface heat treatments (carburizing and carbonitriding), the energy absorbed have been improved by 36% 42% respectively.

## **5.2 Recommendations for the Future Works**

1. Investigating the effect laser powder bed fusion on fatigue performance of V- notch and un-notched specimens made of low carbon steel
2. Studying the effect surface heat treatments on different shape of notch on fatigue life behavior such as U-notch and compare the result with V-notch and plain specimen.
3. Studying experimental and numerical of carbonitriding effect on fatigue properties of low carbon steel with v-notch at different angles.
4. Investigating the effect thermal spray deposited on fatigue behavior of tungsten carbide-cobalt-chrome (WC-CoCr) coated beam.

# ***References***

## REFERENCES

- [1] Klotz, T., Delbergue, D., Bocher, P., Lévesque, M., & Brochu, M. "Surface characteristics and fatigue behavior of shot peened Inconel 718." *International Journal of Fatigue*, 110, pp.10-21,2018.
- [2] Angelova. D, R.Yordanova,S .Yankov" Influence of microstructure on fatigue process in a low carbon steel. Analysis and modelling." *Engineering Failure Analysis*, 82, pp.350-363, 2017.
- [3] Campbell , Flake C. "Elements of metallurgy and engineering alloys ". ASM International, 2008.
- [4] Hu . L , Peng . F , and Xiao – L. Zhao. "Fatigue design of CFRP Strengthened steel members." *Thin-Walled Structures*, 119, pp.482-498,2017.
- [5] Tokaji , K., and M . Akita."Effect of carburizing on fatigue Behavior in a type 316 austenitic stainless steel." *WIT Transactions on Engineering Sciences* 55, pp.53-62, 2007.
- [6] Amiri M . S . and Kashefi . M . " Application of eddy current nondestructive method for determination of surface carbon content in carburized steels." *NDT & E International* , Volume 42, Issue 7, pp. 618-621,October 2009.
- [7] Stone , R . " Fatigue life estimate using goodman diagrams ." Retrieved August 17 , 2012.
- [8] Richard . G , and Keith . J Nisbett . " Shigley's mechanical engineering design". *Eleventh edition, McGraw-Hill*, 2020.
- [9] Briottet. L. *et al* ,.Fatigue crack initiation and growth in a CrMo steel under hydrogen pressure,. *Int. J. Hydrogen Energy*, vol. 40, no. 47, pp. 17021–17030, 2015.
- [10] AIH Committee. "ASM handbook volume 19 fatigue and fracture ." (1996).
- [11] Klesnil and Lukaso .P," Fatigue of Metallic Materials", *Materials Science Monographs*, Vol.7, Elsevier (1980).
- [12] Schijve . J , " Fatigue of Structures and Materials ", *Dordrecht Kluwer Academic*, 2001.
- [13] Tarafder.S, "Mechanisms of fatigue failures," *Cofa-1997*, pp.147–168, 1997.
- [14] Jaypuria . S ." Heat treatment of low carbon steel ". Diss . 2009.
- [15] Britannica , The Editors of Encyclopaedia . "surface hardening". *Encyclopedia Britannica*, 1 Nov. 2016,

- [16] Davis . J. R. , " Surface hardening of steels " : understanding the basics. ASM international, 2002.
- [17] Lampman. S, Schneider. M, and Chatterjee. M. S, "introduction to Surface Hardening of Steels," *Asm Handbook, Steel Heat Treating Fundam. Process.* vol. 4, pp. 389–398, 2013.
- [18] Abdulrazzaq . M. A. " Investigation the mechanical properties of carburized low carbon steel." *Int. J. Eng. Res. Appl*, 6(9), pp.59-65, 2016.
- [19] Panda. R. R., A. M. Mohanty, and D. K. Mohanta, "Mechanical and Wear Properties of Carburized Low Carbon Steel Samples," pp. 109–112, 2014.
- [20] Miao . S ., “ Optimization Design of Carburizing and Quenching Process in Consideration of Transformation Plasticity Mechanism,” 2019.
- [21] Darmo . S, "Study on mechanical Properties of pack carburizing SS400 STEEL WITH Energizer pomacea Canaliculata," vol. 9, no. 5, pp. 14–23, 2018.
- [22] Cai, Zhihui , Jingwei Zhao , and Hua Ding . " Transformation - Induced Plasticity Steel and Their Hot Rolling Technologies." *Rolling of Advanced High Strength Steels: Theory, Simulation and Practice* ,pp.289-322,2017.
- [23] Digges, Thomas G., Samuel J. Rosenberg, and Glenn W. Geil. Heat treatment and properties of iron and steel. *National Bureau of Standards Gaithersburg Md*, 1966.
- [24] Smith W . F. and Hashemi J . " Foundations of Materials Science and Engineering", 4th Edition, McGraw's - Hill Book, 2006.
- [25] Emad K . Najm , "Notch Effect on Mechanical and Fatigue Behavior of Steel Alloys Beams", M.SC. Thesis, University of Babylon, Babylon, Iraq, 2015.
- [26] Al-Turaihi, Ali, Qasim Hasan Bader , and Ameen Basim. "Notch Effect on Aluminium Alloy Rod under Rotating Bend Fatigue Load." *IOP Conference Series: Materials Science and Engineering*. Vol. 1094. No. 1. IOP Publishing, 2021.
- [27] Hassani-Gangaraj, S. M., Moridi, A., Guagliano, M., Ghidini, A., & Boniardi, M. "The effect of nitriding, severe shot peening and their combination on the fatigue behavior and micro-structure of a low-alloy steel." *International Journal of Fatigue* ,vol, 62, pp. 67-76,

- 2013.
- [28] Xie, L., Palmer, D., Otto, F., Wang, Z., & Jane Wang, Q. "Effect of surface hardening technique and case depth on rolling contact fatigue behavior of alloy steels." *Tribology Transactions*, vol. 58, no. 2, pp. 215-224, 2014.
- [29] Fragoudakis, R., Karditsas, S., Savaidis, G., & Michailidis, N. "The effect of heat and surface treatment on the fatigue behavior of 56SiCr7 spring steel." *Procedia Engineering*, Vol.74, pp.309-312,2014.
- [30] Chang, S., and Young, S. Pyun. "Wear and Fatigue Properties of Surface-Hardened Rail Material." *Journal of the Korean Society of Manufacturing Technology Engineers* 25.5 (2016): 380-385.
- [31] Abdulrazzaq, Mohammed Abdulraoof. "Studying the fatigue properties of hardened for carbon steel." *Int. J. Comput. Eng. Res* 6 (2016): 9-13.
- [32] Poursaiedi, E., and A. Salarvand. "Effect of coating surface finishing on fatigue behavior of C450 steel CAPVD coated with (Ti, Cr) N." *Journal of Materials Engineering and Performance* 25.8 (2016): 3448-3455.
- [33] Maleki, E., and K. Reza Kashyzadeh. "Effects of the hardened nickel coating on the fatigue behavior of CK45 steel: experimental, finite element method, and artificial neural network modeling." *Iranian Journal of Materials Science and Engineering*, vol.14, no.4, pp. 81-99, 2017.
- [34] Guarino, S., M. Barletta, and Abdelkarim Afilal. "High Power Diode Laser (HPDL) surface hardening of low carbon steel: Fatigue life improvement analysis." *Journal of Manufacturing Processes*, vol.28, pp.266-271,2017.
- [35] Barkat, A., A. D. Hammou, and O. Allaoui. "Effect of boriding on the fatigue resistance of C20 carbon steel." *Acta Physica Polonica A*, vol. 132, no.3, pp. 813-815, 2017.
- [36] Zhang, S., Xie, J., Jiang, Q., Zhang, X., Sun, C., & Hong, Y.. "Fatigue crack growth behavior in gradient microstructure of hardened surface layer for an axle steel." *Materials Science and Engineering: A*, vol. 700, pp. 66-74,2017.

- [37] Vackel, Andrew, and Sanjay S. "Fatigue behavior of thermal sprayed WC-CoCr-steel systems: Role of process and deposition parameters." *Surface and Coatings Technology* 315 (2017): 408-416.
- [38] Ali, A. Mohamed . "Nano Surface Coating Effects on Fatigue behavior of Steel Beam". *Diss. M. Sc. Thesis, the University of Babylon, College of Engineering, Mechanical Engineering Department*, 2019
- [39] Dunchev, V., J. Čapek, and M. Atanasov. "Effect of ion nitriding on fatigue behavior of steel 35HGS." *Journal of the Technical University of Gabrovo* (2019).
- [40] Selva S. Prabhu, C., P. Ashoka Varthanan , and T. Ram Kumar. "Shot peening effects on fatigue life, corrosion behavior and surface roughness of low carbon alloy steel." *Bulletin of the Polish Academy of Sciences: Technical Sciences* (2021): e136214-e136214.
- [41] Ramesh, S., S. Natarajan, and V. J. Sivakumar. "Effect of Surface Condition on the Torsional Fatigue Behaviour of 20MnCr5 Steel." *Metals and Materials International* 27.9 (2021): 3132-3142.
- [42] S . Priyadarshin i, T. Sharma , and G . Arora, "Effect of Post Carburizing Treatment on Hardness of Low Carbon Steel," vol. 4, no. 7, pp. 763–766, 2014.
- [43] MD. abdul motalleb." Improvement of Mechanical Properties of Low Carbon Steel for Manufacturing OF Spindle OF jute Sinning mill"*Department of mechanical engineering Dhaka University of engineering and Technology, gazipur October – 2014.*
- [44] Negara, D. N. K. P., Muku, I. D. M. K., Sugita, I. K. G., Astika, I. M., Mustika, I. W., & Prasetya, D. G. R." Hardness distribution and effective case depth of low carbon steel after pack carburizing process under different carburizer." *Applied Mechanics and Materials. Vol. 776. Trans Tech Publications Ltd*, 2015.
- [45] Sujita, S. "Study on fatigue strength of pack carburizing steel ss400 with alternative carburizer media of pomacea canalikulata lamarck shell powder." *International Journal of Applied Engineering Research (IJAER)*, vol.13, no.11, pp.8844-8849, 2018.


- [46] Darmo, Sujita. "Fatigue Strength of Low Carbon Steel SS400 on Pack Carburizing Treatment with Pinctada Maxima Shell Powder Energizer." *Journal of Advances in Scientific Research and Engineering (IJASRE)* 5.12 (2019): 267-273.
- [47] Jabbar, D., Kadhim, Z. D., & Abdulrazzaq, M. A. "Wear and Hardness Properties of Carburized (Aisi 1011) Steel, ". *Eng. Sustain Dev.*, vol. 24, no. Special, pp. 402–408, 2020.
- [48] Qin, S., Zhang, C., Zhang, B., Ma, H., & Zhao, M. "Effect of carburizing process on high cycle fatigue behavior of 18CrNiMo7-6 steel." *Journal of Materials Research and Technology* 16 (2022): 1136-1149.
- [49] Ayodeji .S. P, Abioye .T. E, and S. O. Olanrewaju, " Investigation of surface hardness of steels in cyanide salt bath heat treatment process," *IMECS 2011 - Int. MultiConference Eng. Comput. Sci.* 2011, vol. 2, pp. 1244–1247, 2011.
- [50] Aziz. A. A. J, Khalid. E. A, and Alwan. A. S, " Influence of Nd:YAG Laser Energy on Mechanical properties of Nitriding Steel," *Al-Nahrain J. Eng. Sci.*, vol. 23, no. 2, pp. 187–193, 2020.
- [51] Alza .V. A, "Cyanide in salt bath Applied to ASTM A-517 Steel Effects on Hardness Wear and Microstructure," *Int. J. Recent Technol. Eng.*, vol. 9, no. 3, pp. 571–580, 2020.
- [52] Ghanem. A, and Mohamedali. T. "The influence of carbon potential after gas-carbonitriding on the microstructure and fatigue behavior of low alloyed steel." *Materials Research Express* 9.2 (2022): 026505.
- [53] Davis, Joseph R., . "Tensile testing". ASM international, 2004.
- [54] Alang .N, and Miskam .A, "Effect of surface roughness on fatigue life of notched carbon steel,"*International Journal of Engineering Technology IJET-IJENS*", vol. 11, pp. 160-163, 2011.
- [55] Geels, K., Fowler, D. B., Kopp, W. U., & Michael R. "Metallographic and materialographic specimen preparation, light microscopy, image analysis, and hardness testing". Vol. 46. West Conshohocken: ASTM international, 2007.

- [56] Mustapha Baqir H. Al-Khafaji, " Theoretical and Experimental Study of Composite Material Under Static and Dynamic Loadings with Different Temperature Conditions", Ph.D. Theses University of Technology / Mechanical Engineering Department, Baghdad / Iraq, 2014
- [57] Luay S. Al-Ansari, Al Najar Laith H, , and Mohammed W. Al-Jibory. "Effect of notch dimension and location on fatigue life and thermal behavior of low carbon steel (St37-2)." Kufa Journal of Engineering 8.3 (2017).
- [58] Mohammed A. Sadik." Effect o f the Surface Hardening on the Corrosion and Erosion Corrosion of Low Carbon Steel" Journal of the College of Engineering - Al-Nahrain University - Vol. 71 No.2, pp. 34 - 55, 2014.
- [59] Abdul . K Wahed. R. "principles and Metallurgical examination. "University of Babylon College of Materials Engineering,2016.
- [60] Panda, R. R., A. M. Mohanty, and D. K. Mohanta. "Mechanical and wear properties of carburized low carbon steel samples." Int. J. Multidiscip. Curr. Res 2 (2014): 1-2.
- [61] Dossett, J., and G. E. Totten. "ASM Handbook, Volume 4A : Steel Heat Treating Fundamentals and Processes, ASM Intern." (2013).
- [62] Essam Z. Fadhe." Effect of the Elevated Temperature on Fatigue Behavior of Aluminum Alloy AA 7075" Journal of University of Babylon for Engineering Sciences, Vol. (26), No. (8): 2018.
- [63] Sabri , Hazizi Azri Bin Ahmad. " Experimental study of pack carburizing of carbon Steel." Bachelor of engineering University malaysia pahang (2010).
- [64] Samborsky. D, J. Mandell, and P. Agastra, "Fatigue trends for wind blade infusion resins and fabrics," in 51st AIAA/ASME/ASCE/AHS/ASC Structures, Structural Dynamics, and Materials Conference 18th AIAA/ASME/AHS Adaptive Structures Conference 12th, 2010, p. 2820.
- [66] Qasim H. Bader and Ali Hussein Ali " effect of temperature variation on fatigue behaviour of steel alloys beams". Department of Mechanical Engineering, Babylon University, Hilla-Iraq.
- [67] Monga, I., Paul,V., Muniyasamy, S., & Zinyemba, O. (2022). Green Synthesis of Sodium Cyanide Using Hydrogen Cyanide Extracted under Vacuum from Cassava (*Manihot esculenta* Crantz) Leaves. *Sustainable Chemistry*, 3(3), 312-333.


# ***Appendices***


## APPINDIX-A

### CHEMICAL COMPOSITION ANALYSIS



**TUV**  
AUSTRIA  
EN ISO 9001:2015  
EN ISO 14001:2015





**Ministry of Industry and Minerals**  
**State Company for Inspection and Engineering Rehabilitation (SIER)**  
**Engineering Insp. & lab Department**

**Client:** الطالب سجاد حسن / جامعة بابل - كلية الهندسة

**Order No:** 1204/2021

**Tested Item:** shaft

**Address :** Iraq – Babylon

**Date of Test:** 6 / 12 / 2021

**Type of Test:** Chemical Composition

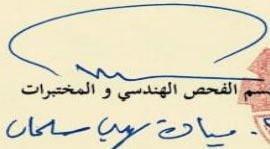
**Standard Specification:** ASTM E415:2017

**Test Report**

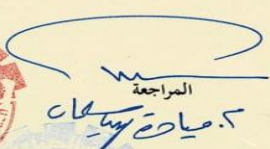
Sample	C%	Si%	Mn%	P%	S%	Cr%	Mo%	Ni%	Al%	Cu%	Fe%
Shaft Ø 16mm	0.221	0.136	0.499	0.0193	0.0727	0.138	0.023	0.147	0.0099	0.394	Bal.
U ex	±0.013	±0.007	±0.039	±0.002	±0.057	±0.002	±0.02	±0.008	±0.009	±0.005	---±

**NOTE:-**

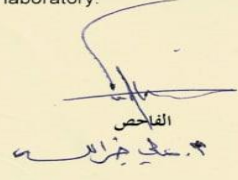
- Values were calculated through three tests.
- the results of uncertainty as they are shown in the table above. the report expanded uncertainty of standard uncertainty of measurement multiplied by the coverage measurement is stated as the factor K= 2 which for a normal distribution corresponds to confidence level of 95%.
- This test report is for the tested samples only.
- Test condition ( 22 ° C , 34% ).
- The test report shall not be reproduced except in full without written approval of the laboratory.



مدير قسم الفحص الهندسي و المختبرات



المراجعة



الفاحص

Head office: Baghdad –Iraq /Baghdad –Hilla Highway .E-mail: mahed@siei.gov.iq, lab.sier@sier.gov.iq  
DG Office:+9647810484016.Planning Dep.Head: +9647706084844IP: 91.106.34.21 – SIER@engineering Comp

DOCUMENT: ID:F/TC/7.8/MT/01	Issue No.:02	IssueDate:9/11/2021	Revision NO:00	Page NO:1 OF1
-----------------------------	--------------	---------------------	----------------	---------------

**Figure (A-1):** chemical elements of low carbon steel specimen

## APPENDIX-B

### TYPE OF MATERIAL



EN ISO 9001:2015  
EN ISO 14001:2015





SMARTCLOUDGROUP  
SYSTEM & SOLUTION

**Ministry of Industry and Minerals**  
**State Company for Inspection and Engineering Rehabilitation (SIER)**

1204      ISO 17025:2005   ISO 9001: 2015   ISO14001: 2015

Client:- **المجالس سجاد حسين ناصر / جامعة بابل - كلية الهندسة**      Address:- **Iraq - Babylon**  
Order No:- **1204/2021**      Date of Test: **6 / 12 / 2021**  
Tested Item: **Shaft**

**CERTIFICATE**

Sample	Type of Material
Shaft (Ø=16)mm	المعدن يقع ضمن المواصفة القياسية <b>DIN 17100</b> ضمن النوعية <b>St 44-2</b>

- المطابقة من حيث الخواص المفحوصة فقط .



مدير قسم البحث والتطوير  
نهلة الحسن أحمد



مسؤول شعبة المواصفات  
م. تمارة نوري عبد علي  
عروة ابادوقتي



اعداد  
صفا عبد الرحمن مجيد

Doc. No.: S.I.E.R/QWII/18/01

Issue No.: 02

Date: Oct. 2021

**Figure (B-1): Material specification**

## APPENDIX-C

### LIFE EVOLUTION DUE TO CONSTANT AMPLITUDE LOADING

The fatigue curve or S-N curve can be presented by the following equation based on Basquin's equation form:

$$\sigma a = a (Nf)^b \quad \dots (C-1)$$

Where:

$\sigma a$ , is an applied stress in Mpa

, is cycle's number of fatigue failure.

Equation (B-1) can be written as following:

$$Nf = \left( \frac{\sigma a}{a} \right)^{\frac{1}{b}} \quad \dots (C-2)$$

Where: a and b are material constants and may be determined by linearizing the curve using equation (C-1) in logarithmic form:

$$\log \sigma a = \log a + b \log Nf \quad \dots (C-3)$$

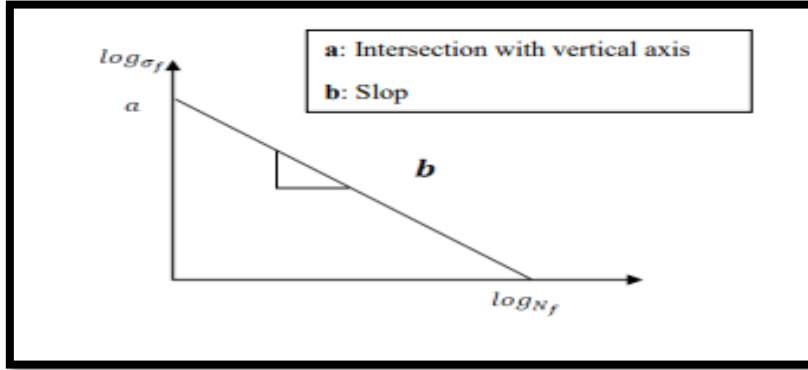


**Figure (C-1):** Logarithmic description of fatigue life equation [61]

$$b = \frac{\sum_{i=1}^h \log \sigma_{ai} \log N_{fi} - \sum_{i=1}^h \log \sigma_{ai} \sum_{i=1}^h \log N_{fi}}{h \sum_{i=1}^h (\log N_{fi})^2 - (\sum_{i=1}^h \log N_{fi})^2} \quad \dots (C-4)$$

$$\log a = \frac{\sum_{i=1}^h \log \sigma_{ai} - \sum_{i=1}^h \log N_{fi}}{h} \quad \dots (C-5)$$

Where, (i) is the number of tests (i=1, 2, 3, 4.....n) and (h) is a total number of test specimens in each S-N curve.

## APPENDIX-D

### THE COEFFICIENT OF DETERMINATION ( $R^2$ )

Coefficients of determination ( $R^2$ ) had been used, to measure the overall proportional differences for the response variables shown with the lowest squared regression lines. The coefficient of determination is a number with the range of (0 to 1), which is ( $0 \leq R^2 \leq 1$ ). The line has no explanatory value if  $R$  is equal to zero but, if equal to one, means the line variable explain 100% of the variation in the response variable [29].

In statistics, how well a set of data points fits a line or curve is indicated by the coefficient of determination ( $R^2$ ). It is a statistic used in the context of statistical models whose main objective is either to predict future results or to test hypotheses, on the basis of other relevant information. It provides a measure of how well observed outcomes are replicated by the model, as the proportion of total variation of outcomes explained by the mode

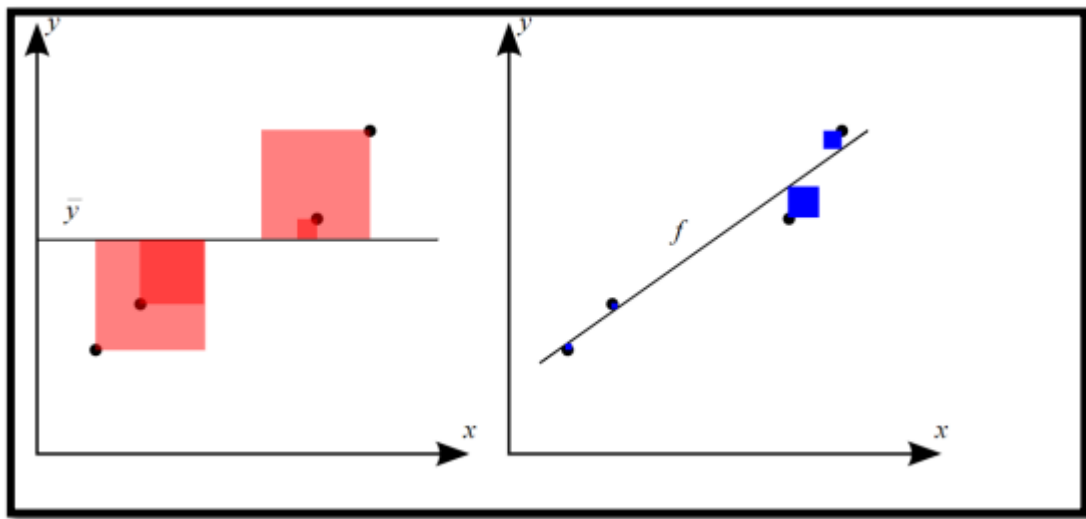


**Figure (D-1):** Relation between x and y

#### Definitions

$$R^2 = \frac{SS_{reg}}{SS_{tot}} \quad \dots (D-1)$$

The better of the linear regression (on the right) fits the data in comparison to the simple average (on the left graph) figure (D-1), the

closer the value of  $R^2$  is to one. The areas of the blue squares represent the squared residuals with respect to the linear regression. The areas of the red squares represent the squared residuals with respect to the average value.

A data set has values  $y_i$ , each of which has an associated modeled Value  $f_i$  (also sometimes referred to as  $\hat{y}_i$ ). Here, the values  $y_i$  are called the observed values and the modeled values  $f_i$  are sometimes called the predicted values.

In down  $\bar{y}_i$  is the obtained data:

$$\bar{y} = \frac{1}{n} \sum_{i=1}^n y_i \quad (D-2)$$

Where  $n$ ; is a number of observation.

The data variability set is determined as different squares sum:

$$SS_{tot} = \sum_{i=1}^n (y_i - \bar{y})^2 \quad (D-3)$$

The total squares sum is proportional to the specimens varies:

$$SS_{reg} = \sum_{i=1}^n (f_i - \bar{y})^2 \quad (D-4)$$

The regression sum of squares is named the explained sums of square.

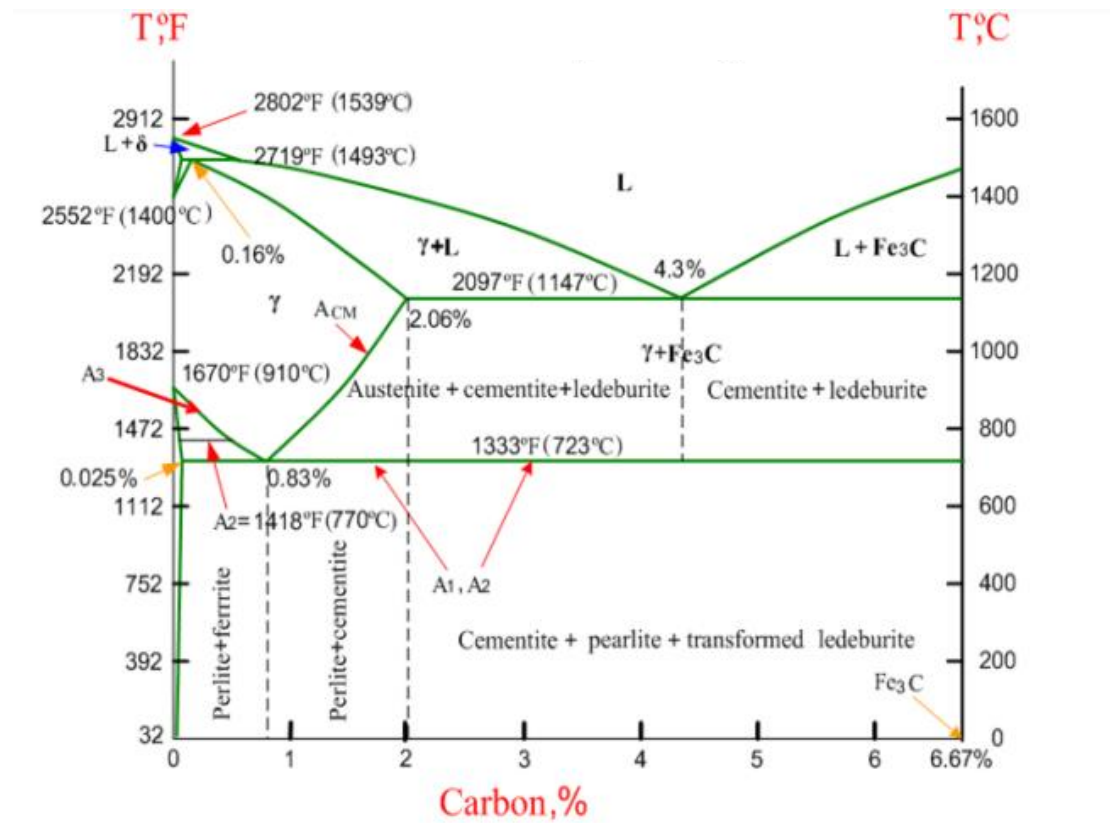
$SS_{res} = \sum_{i=1}^n (y_i - f_i)^2$  · The sums of residual squares of also can defined the residual sum of squares.

The notation  $SS_R$ , and  $SS_E$ , would be avoid because of some texts this meaning is represented to residual sum of square and explained sum of squares; respectively. Generally definitions of the coefficient of determination can be defined as:

$$R^2 = 1 - \frac{SS_{res}}{SS_{tot}}$$

## APPENDIX-E

### IRON –CARBON PHASE DIAGRAM



## APPENDIX-F

### PUBLISHED PAPER



DIAGNOSTYKA, Vol. 23, No. 3 (2022)

Article citation info: Nasser AH, Bader QH. Surface hardening effect on the fatigue behavior of isotropic beam. Diagnostyka. 2022;23(4):2022312.

<https://doi.org/10.29354/diag/154901>.



DIAGNOSTYKA, 2022, Vol. 23, No. 3

e-ISSN 2449-5220

DOI: 10.29354/diag/154901

### SURFACE HARDENING EFFECT ON THE FATIGUE BEHAVIOR OF ISOTROPIC BEAM

Sajad H. NASSER <sup>\*</sup>, Qasim H. BADER

University of Babylon, College of Engineering, Mechanical Engineering Department, Babylon, Iraq

<sup>\*</sup> Corresponding author, e-mail: [sajad.nasser.engh420@student.uobabylon.edu.iq](mailto:sajad.nasser.engh420@student.uobabylon.edu.iq)

#### Abstract

This paper is to present an experimental study of the impact of surface hardening on the high-cycle fatigue behavior of an isotropic beam. The beams made from low carbon steel (St 44-2). Surface treatments used are pack carburizing and carbonitriding. The experimental work included mechanical test, surface heat treatment, fatigue test and Microscopic inspection. The surface hardening was done by using pack-carburizing process at a temperature of 925°C holding time variation (2, 4, and 6hr) followed by quenching and tempering process, and using the carbonitriding process at a temperature of 800°C and for periods (0.5, 1 and 1.5hr) then quenching directly in water. The fatigue test



## ISAESC 2023

### Fourth International Scientific Conference of Agriculture, Environment and Sustainable Development

College of Agriculture , University of Al-Qadisiyah, IRAQ

Ref.: 38

Data: April 27,2023

**Subject: Acceptance Letter and Participation in A conference**

Dear Author (s) :

**Sajad H. Nasser, Qasim H. Bader, Ahmed J. Mohammad and Mohsin Abdullah Al-Shammari**

We are pleased to inform you that after hard review process your paper entitled as :

**Carbonitriding Effect on Fatigue Behaviour and Mechanical Properties of Steel Beam**

Has been accepted for participating in the“ Fourth International Scientific Conference of Agriculture, Environment and Sustainable Development (ISAESC 2023) “. The conference will be held by College of Agriculture, University of Al-Qadisiyah, Iraq. In cooperation with the Iraqi Ministry of Agriculture , The Food and Agriculture Organization (FAO) , The Arab Center for the Studies of Arid Zones and Dry Lands (ACSAD) , Center of Desert Studies (CDS), Badiya Studies Center and Sawa Lake and Sahara Majan Agricultural and Food Consultation Center (Qutoof), during the period 17-18 May 2023 .

**Note:** The paper will be published after accept from journal in “IOP Conference Series: Earth and Environmental Science” , Publisher :IOP Publishing Ltd. , Country: United Kingdom, Scopus Index , Cite Score: 0.6, E-ISSN (1755-1315 ), Volume 1189.

**Head of The Conference**

**Prof. Dr. HayyawiWewa Al-jutheri**

Iraq / University of Al-Qadisiyah / College of Agriculture  
+009647801212466  
Email : conference.agr@qu.edu.iq



## الخلاصة

يركز هذا العمل على الدراسة العملية لتأثير معالجات التصليد السطحي، وزمن التثبيت (Soaking time) وعمق التصلب على سلوك الكلال والخواص الميكانيكية للفولاذ منخفض الكربون DIN 17100، وقد أجريت هذه الدراسة على كل من العينات غير المحززة (un notched) والعينات المحززة (v-notch) بعمق 1 مم وزاوية 45°.

تتضمن الدراسة العملية على اختبارات ميكانيكية، وتصليد سطحي واختبار الكلال، وفحص كرات سيانيد الصوديوم باستخدام جهاز اكس ري X-Ray diffraction، كما تم فحص البنية المجهرية باستخدام مجهر ضوئي (optical microscope).

تم اجراء نوعين من طرق التصليد السطحي هي الكربنة الصلبة (pack carburizing) والنيترنة الكربونية (carbonitriding).

الطريقة الأولى، الوسط الكربوني يتم تحضيره من فحم الخشب وتحويله إلى مسحوق عن طريق الطحن وخلطها مع 10% من كربونات الباريوم لاستخدامه أثناء عملية الكربنة الصلبة. تم معالجة عينات الفولاذ بزمن نقع متغير (زمن التثبيت / soaking time) 2 و 4 و 6 ساعة عند درجة حرارة ثابتة 925 درجة مئوية متبوعة بعملية التبريد بالماء والتلطيف بدرجة حرارة 180 درجة مئوية لمدة 2 ساعة.

الطريقة الثانية، تم تحضير المنصهر الملحي بإذابة كرات سيانيد الصوديوم بالتسخين. كان وقت غمر العينات (زمن التثبيت / soaking time) خلال عملية النيترنة الكربونية 0.5 و 1 و 1.5 ساعة عند درجة حرارة ثابتة 800 درجة مئوية ثم التبريد مباشرة في الماء متبوعاً بالتلطيف.

اختبار التعب قد تم اجراءه بواسطة نظام ثني ناتئ. تشير نتائج الاختبار ان التحسن في حياة الكلال تعتمد على طريقة التصليد ووقت التصليد (soaking time).

تشير النتائج إلى ان (carbonitriding) له تأثير أكبر على قوة وحياة الكلال Fatigue Strength مقارنة بالعينة المعالجة بالكربنة الصلبة. بالإضافة إلى ذلك، أن زيادة وقت التثبيت soaking time، يؤدي الى زيادة عمر الكلال بنسبة 20.2% و 15.9% للنيترنة الكربونية والكربنة الصلبة.

اظهرت النتائج أن العينات التي تم تصليدها باستخدام طريقة النيترنة الكربونية (carbonitriding) حققت صلادة أعلى للسطح بمقدار 1644.28HV. حيث ازدادت الصلادة السطحية بنسبة 461% نسبتاً الى النيترنة الكربونية في حين الصلادة السطحية ازدادت بنسبة 270% للكربنة الصلبة.

وجد ان منطقة اختبار المقطع العرضي للعينه المكسورة والتي كانت تصلد بواسطة الكربنة الصلبة والنيترة الكربونية مقسمة إلى جزأين، طبقة سطحية وقلب المعدن. نلاحظ أن الطبقة السطحية يتركز فيها الكربون، أو الكربون والنيتروجين معاً، بينما منطقة اللب لا يتغير فيها. كلما طالت مدة بقاء العينات في وسط التصلب (زمن التثبيت/soaking time) زاد عمق الطبقة المتصلبة باتجاه القلب.

بينت نتائج الفحص ان لتأثير المعالجات الحرارية السطحية على مقاومة الكلال Fatigue Strength عند القيمة القياسية لعدد الدورات  $10^6$  بالمقارنة مع العينات الغير معالجة الى تحسين جيد في كلا من الطريقتين المستخدمتين.

تم الحصول على أعلى نسبة تحسين في مقاومة الكلال (Strength Fatigue) (44.56%) و (61.87%) لكل من الكربنة الصلبة و النيترة الكربونية على التوالي ، لعينات محززة v-(notch).

بينما نسبة تحسن مقاومة الكلال (strength fatigue) للعينات الغير محززة (un notched) هي 31.92 % و 38.46 % على التوالي عند زمن تثبيت (soaking time) 2 و 0.5 ساعة.



جمهورية العراق

وزارة التعليم العالي والبحث العلمي

جامعة بابل

كلية الهندسة / قسم الهندسة الميكانيكية

## تحسين أداء الكلال والخواص الميكانيكية للفولاذ واطئ الكربون 17100

رسالة مقدمة الى جامعة بابل / كلية الهندسة / قسم الهندسة الميكانيكية  
وهي جزء من متطلبات دراسة ماجستير في الهندسة الميكانيكية  
(ميكانيك تطبيقي)

من قبل الطالب

سجاد حسن ناصر عيدان

بكالوريوس (2018)

بإشراف

الأستاذ الدكتور قاسم حسن بدر